Three Dimensional Numerical modelling Of Coal Mine Roadways Under High Horizontal Stress Fields

CSM Project Dissertation

Submitted by Arun Sarathchandran to the University of Exeter as a dissertation towards the degree of Master of Science by advanced study in Mining Resource Engineering, May, 2014

“I certify that all material in this dissertation which is not my own work has been identified and that no material is included for which a degree has previously been conferred on me.”

Abstract

The detrimental effects of high horizontal stresses on mine roadway stability is a well-known fact among the rock mechanics community. The orientation of the horizontal stresses plays a significant role in defining the amount of damage; Field observations confirm that high horizontal stresses parallel to the tunnel excavation result in significantly less damage compared with tunnels driven perpendicular to high horizontal stresses. The three dimensional effects cannot be modelled using two dimensional programs. Full three dimensional analysis is needed to capture the details of these damaging effects.

An investigation was undertaken on the detrimental effects of high horizontal stresses for a coal mine roadway. The analysis is carried out using Rocscience's new three dimensional FEM program RS^3. The model parameters were obtained from two mine fields from UK and India. Initially a simple model of a coal mine roadway was created, and analysed for varying high horizontal stresses. The results shows that the stresses at an angle to the tunnel shows asymmetrical distribution of yield zones and displacements at the tunnel face. The analysis also showed a sharper and longer stress damaged zone for stress parallel case and skewed stress distribution for tunnels driven at an angle to the stress field.

A sequential three dimensional bolted model of a coal mine tunnel was created using RS^3, for a more realistic representation of the field situation. The observed tunnel roof displacements at field and model results exhibited reasonable similarity. The model was able to predict the larger stress damaged yield zones for the stress perpendicular case than for stress parallel case. The analysis was extended by varying the thickness of weak mudstone layer on immediate roof top. Results indicated that a thicker weak mudstone strata on rooftop creates more damage than a relatively thinner layer, proving that strata on the immediate roof layer plays a critical on the stress damage. Examination of bolt loads confirms that for the stress parallel case the loads acting on the bolts are lower than that of the stress perpendicular case.

Successful modelling results of the coal mine roadways gave more confidence in building a more complicated tunnel junction model in RS^3. The modelled results displayed a similar trend as before with its inner corner experiencing significant yield damage on the stress perpendicular case, and stress orientations at an angle to the junction showed an asymmetrical distribution of stresses and plastic zones at corners.

A full three dimensional model of a room and pillar mine was then developed. The case example was taken from an Indian mine. The mine adopted a diagonal depillaring method. This pillar extraction method was implemented in RS^3 to model the stress amplification due to an advancing goaf towards the observation point. The modelled results were validated against the field measurements obtained for the case example

A single sequential coal mine roadway model consumed 2.6GB of space and took 18hours to compute. This suggests that the applicability of three dimensional programs for day to day modelling will be limited due to computation capability. But in near future, due to rapid advance in computing capabilities, 3D modelling will be a major tool for geotechnical engineers for routine calculations.

Table of Contents

List of tables

List of figures

Acknowledgements

The author would like to thank his supervisor Professor John Coggan, for his encouragement and support throughout the thesis.

The author would like to thank Federation of European Minerals Program Board and European Union for the scholarship provided for the completion of studies.

The author would like to thank the Rocscience team for generously providing the RS^3 software for the thesis. The author would also like to thank the technical support team for their prompt responses to the queries regarding the software.

Finally the author would like to acknowledge the support of his parents and friends for their motivation and encouragement.

Definitions

The following list of terminology is included to explain the terms that are used in the thesis.

Advancing Panel	Production panel where access roadways are mined as the panel advances
Extensometer	An instrument which measures the deformation and strain of the rock mass with height into the roof or depth into the entries ribside, from a borehole in by means of reference
Goaf/Gob	The caved ground left following longwall extraction
Longwall Mining	A method of mining where all of the coal within an area is extracted without leaving pillars of installing permanent support, causing the ground caves/subsides.
Panel	A region of coal either extracted or to be extracted whose boundary is defined by the serving gateroads and the expected face start and end position
Rib	The side of a roadway beyond which there is no existing excavations or tunnels
Roadway	A mine tunnel usually driven in seam for access to areas of coal reserves, with typically rectangular cross-section. (Known as development tunnels in metal mines)
Roadway Drivage Direction	The direction that the roadway was constructed described as a whole circle bearing.
Roadway Orientation	The angle between the roadway drivage direction and the maximum in-situ horizontal principal stress direction expressed as an angle between 0 and 90 degrees.
Seam	Payable material to be mined in a tabular orebody.

Notations used in the thesis

ϑ	Poisson's ratio
σ_{ci}	Intact compressive strength
σ_1	Maximum principal stress
γ	Density
m_i & m_r	Hoek Brown peak and residual material
S_i & S_r	Hoek Brown peak and residual material
P	load applied,
K	Nonlinear stiffness of the spring
U	displacement
[D]	Incremental Stiffness matrix
$\Delta\sigma$	Incremental stress
$\Delta\varepsilon$	Incremental strains

1 Introduction

1.1 Research Description

The thesis investigates the effects of high horizontal stresses on excavations in Coal Measures. Initially a relatively simple single stage model of a coal mine roadway is modelled for varying high horizontal stress orientations and progressively the model is made more and more complex by introducing multiple stage excavation simulating a continuous miner, roof bolting, modelling of a coal measure junction and finally developed into a full scale room and pillar mine.

For validating the model two case examples are used in this thesis. The first one is from North Selby Complex UK for validating the displacements of bolted coal mine roadways. The second one is from an Indian mine known as VK-7 incline for validating the stress effects due to an advancing goaf. The study shows the detrimental effects of high horizontal stresses on excavations, and concludes that stress acting perpendicular to the tunnel axis results in more damage than stress parallel situation. Horizontal stresses acting at an angle causes asymmetrical distribution of yield zones. It also shows that the weak layers immediately above the roof have a significant role in governing the extent of damage induced.

The investigation into the pillar extraction process of room and pillar mine demonstrates the high stresses in the observation point with approaching goaf. The stresses obtained from the model was in good agreement with the field measurements.

1.2 Structure of the thesis report

Chapter 1 gives a short description of the research problem and a brief overview on the forthcoming chapters.

Chapter 2 mainly deals with the various numerical modelling procedures adopted for modelling underground excavations. Its capabilities, benefits and limitations are discussed. The chapter also provides a flow chart of activities involved for successful modelling.

Chapter 3 introduces the constitutive models that are commonly used for rock mechanics applications. It also describes the importance of selecting representative parameters and introduces various methods available to convert laboratory test data to representative field values.

Chapter 4 describes the commonly practiced mining methods for coal mining. A brief review of the previous application of three dimensional modelling for coal mining is also explained.

Chapter 5 introduces RS^3 software; it mainly focuses on the pitfalls while using Finite Element Model (FEM) programs as a modelling tool. A short description regarding the working of a FEM program is also given.

Chapter 6 introduces the North Selby case study in detail, a sensitivity analysis is carried out to illustrate the impact of parameter variation on the modelled results. A preliminary study is undertaken to examine the effect of stress orientation on yield points and maximum principal stress distribution.

Chapter 7 shows the inability of a single stage excavation to realistically simulate a continuous miner coal mine roadway. A multistage excavation is more reasonable and it creates more stress induced damage than deletion/creation of the whole excavation in single step.

In chapter 8 simulation of a multistage bolted coal mine roadway is modelled for different stress orientations and for varying thickness of mudstone. The modelled results are validated against field data.

All the investigations so far dealt with linear excavations, in chapter 9 a junction is modelled for varying stress orientations and the effects of stress induced damage is compared.

Chapter 10 deals with the modelling of a full scale room and pillar mine. The mine roadways are initially excavated, followed by a pillar extraction procedure with diagonal depillaring. The model used a case example from India and the methodology adopted in the field was replicated in the model. The modelled stress damage is validated using field data.

Finally, chapter 11 provides a summary of the conclusion from the modelling undertaken as part of this investigation. A DVD having all the RS^3 models used for the analysis is attached along with the report.

2 Numerical modelling procedures for underground excavations

Analytical solutions for practical problems are difficult to obtain, hence the governing equations are solved numerically in an approximate approach. Its flexibility to apply in a variety of fields make numerical methods very popular. Nowadays, it is widely used in all fields of engineering, but application to geotechnical problems were limited due to complex unpredictable fuzzy behaviour of soil and rocks. Also in olden days, engineers gave little attention on design of structures on rock, (Pande et al. (1990)), simply because rocks were believed to be competent enough. This proved to be wrong and a few catastrophic failures like Malpasset dam in 1960's and the challenges in mining deeper deposits turned attention of engineers towards rock mechanics.

2.1 Modelling methods

Broadly, modelling methods for rock engineering problems can be classified into the following categories (Jing and Hudson (2002), Coggan et al. (2012), Jing (2003))

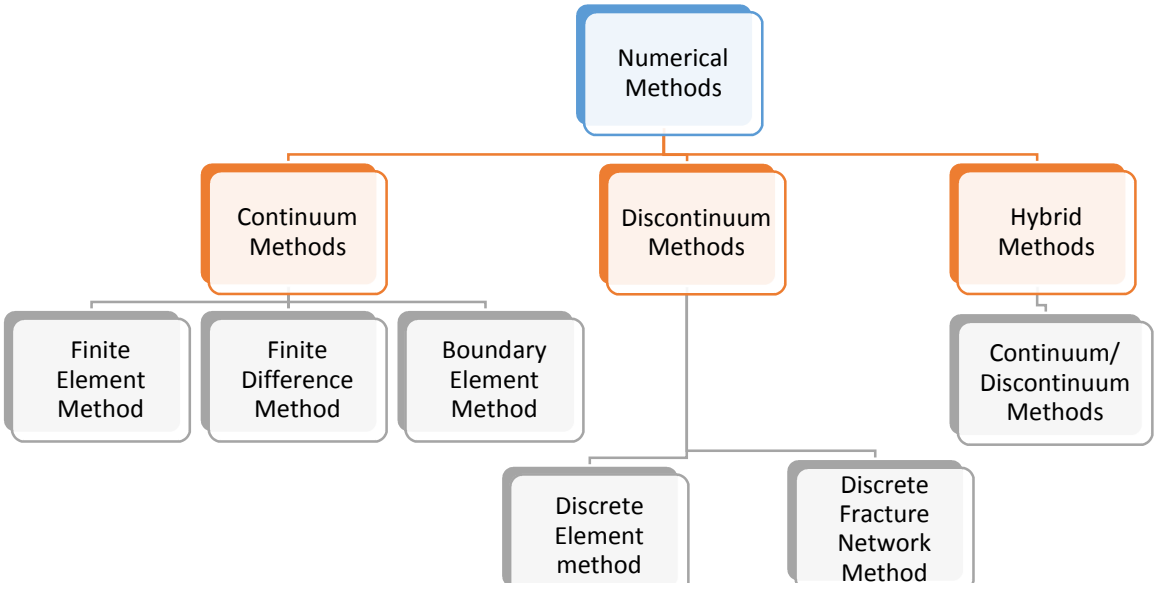

Figure 1: Popular modelling methods for rock mechanics problems

2.1.1 Continuum methods

2.1.1.1 Finite Element Method

With the FE method the whole problem domain is, divided into non-overlapping regions connected to each other through points called nodes. The behaviour of each element satisfying equilibrium conditions, compatibility, material constitutive behaviour and boundary conditions is described and the elements are assembled together. This is the most popular method for engineering problems, but the method needs extensive computing power. A large set of simultaneous equations (several thousands) have to be stored and solved to obtain the solutions.

2.1.1.2 Finite difference method

Here the solid body is divided into finite difference mesh consisting of quadrilateral elements, but the solution scheme adopted is different. The solution of solid body problems using FDM invokes Newton's laws of motion, constitutive relations and boundary conditions. In a calculation cycle new velocities and displacements are obtained from stresses and strains using equations of motion, strain rates are obtained from new velocities and new stresses from strain rates. Unlike implicit FEM's no iterative procedure is adopted (Itasca (2005).Highly non-linear models are best handled by explicit solution schemes. Computer memory requirements are lower, it need not store large matrixes but the solution time might be larger due to smaller time steps to ensure numerical stability.

2.1.1.3 Boundary element method

In BEM the discretizations are only done at the boundaries of the model. The method is suitable for problems having low ratio of boundary surface to volume. The whole concept of BEM method can be described as follows; the excavation is assumed to be a series of negative tractions applied to the boundary Figure 2 , the boundary surface of the excavation is discretized and for each element a fictitious traction force is applied which is assumed to be equal and opposite to the in-situ stress prior to the excavation. A mathematical iterative procedure is adopted to match the fictitious

forces in such a way that external shear and normal components is equal to internal negative shear and tractions (Hoek and Brown (1980))

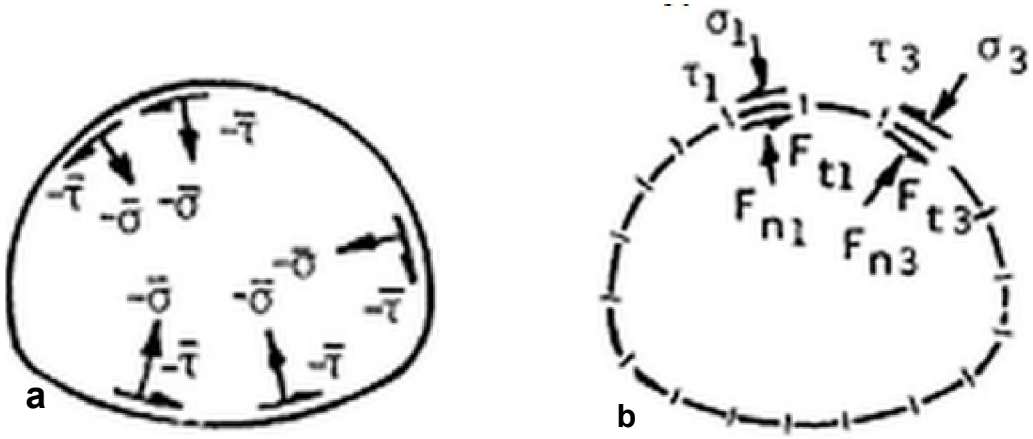

Figure 2: (a) Assumed negative tractions representing the effects of excavation (b) fictitious forces applied to discretized elements to represent the unknown negative tractions, after Hoek and Brown (1980)

2.1.2 Dis-continuum methods

2.1.2.1 Discrete Element Method (DEM)

In DEM each body is composed of independent element which communicates with the surrounding elements via boundary contacts which may change as a function of time. In contrast to FEM/FDM no nodes are common to more than one element. In typical rock mechanics applications elements would represent intact rock while the spaces between the elements can be represented as joints. It can treat nonlinearities which may arise from large displacement, rotation, slip, and separation. The methods is particularly suitable for jointed rock masses where large displacements are expected. In other words if the rock fractures are comparable to size of excavation DEM methods are most suitable (Pan and Reed (1991)).

2.1.2.2 Discrete Fracture Network (DFN)

This method is most suitable for the study of fluid flow and mass transport in fractured rocks for which an equivalent continuum model is difficult to model or establish (Jing and Stephansson (2007)). This is a special discrete model that considers fluid flow

and transport processes in fractured rock masses through a system of connected fractures (Jing and Hudson (2002)).

2.1.2.3 Discontinuous Deformation Analysis (DDA)

DDA is a fully discontinuous analysis that resembles and follows the procedures developed for FEM with an implicit solution scheme. DEM has an explicit solution method while DDA is implicit, in DEM stresses and forces are unknowns while in DDA displacements are unknowns similar to displacement based FEM programs (Bobet (2010)).

2.1.3 Hybrid models

Hybrid models are combination of the methods mentioned above to optimize the results and computing power. Different modelling combinations are mentioned in the literature such as FEM/BEM, DEM/FEM as well as DEM-BEM (Jing (2003)). Pan and Reed (1991) mention that in a practical coal mining environment the combination of DEM/FEM can give more realistic results. Each of these softwares are having steep learning curves

2.1.4 Commercial packages used for numerical modelling in mining

The following table shows the list of popular commercial packages that are used for modelling underground excavations.

Table 1: Popular commercial packages for excavation modelling

Package Name	Company	Modelling method
FLAC 2D and 3D	Itasca Inc. http://www.itascacg.com/	2D and 3D FDM
RS^3	Rocscience Inc. http://www.rocscience.com/	3D FEM
Plaxis 2D and 3D	Plaxis bv http://www.plaxis.nl/	2D and 3D FEM
DIANA	TNO DIANA BV www.tnodiana.com/	2D and 3D FEM
3DEC	Itasca Inc.	3D DEM
UDEC	Itasca Inc.	2D FEM
PFC 2D and 3D	Itasca Inc.	2D and 3D DEM
ABAQUES	Dassault Systèmes http://www.3ds.com/	2D and 3D FEM
$Phase^2$	Rocscience Inc.	2D FEM
Examine 2D and 3D	Rocscience Inc.	2D and 3D BEM
Map3D	Mine Modelling Pty Ltd http://www.map3d.com/	3D BEM
BESOL	Mining Stress systems	2D and 3D BEM
ELFEN	Rockfield Software Ltd http://www.rockfield.co.uk/	2D and 3D FEM/DEM

2.2 Selection of suitable methods

There are no guidelines to decide when a particular model has to be used, in general it can be said that when the size of the model is same order as the characteristic dimension of the design a dis-continuum model seems to be more suitable. If very few or no discontinuities are present continuum models seems to be more suitable (Bobet et al. (2009)). If the size of the block determined by the discontinuities are much smaller than that of the opening it still can be modelled as pseudo continuum model. All these modelling methods have steep learning curve, successful application of these models depends on the expertise of the modeller. According to Coggan et al. (2012) knowing the limitations and capabilities of a software is essential for successful results.

Table 2: Methods available for underground excavation analysis Coggan et al. (2012),Cai (2008)

Analysis method		Advantages	Limitations
Continuum methods	BEM	• Need only limited amount of parameters • Lower computer run times • Rapid assessment of stress concentrations • Allows to model sequential 3D excavations	• Normally limited to elastic analysis (nonlinear options are not very popular) • Not ideal for modelling thin multiple layers of strata.
	FEM	• Large pool of constitutive models available to simulate a range of soil/rock behaviour. • Possibility of plastic analysis • Modelling of complex geometry and multiple strata. • Realistic simulation of post peak behaviour and failure • Ability to follow true stress path with explicit solution schemes.	• Memory requirements are quite high and running 3D models is expensive in terms of computing time • Quality of results depends upon the mesh size, solution schemes, tolerances, boundary effects • Need to be validated with field data. • Expertise of the modeller is critical for usage and interpretation. • Not suitable to simulate large displacements on discontinuous rock masses.
	FDM	• Same as above • Memory requirements are lower since stiffness matrices are not formed and solved but uses dynamic equations of motion in solution schemes • Can handle any solution algorithm without any modifications • Can handle highly nonlinear problems.	• Time consuming than implicit FEM solution schemes, since numerical stability requires increment smaller than critical time step. • Has a steep learning curve
Dis-continuum methods	DEM	• Can simulate fracture propagation large rotations and displacements easily. • Highly dynamic effects can be simulated • Can incorporate synthetic rock masses to represent fracture network	• Predominantly used for jointed rock. • Scale effects • Validation through instrumentation essential
Hybrid Methods		• Combination of best features of FEM/BEM/DEM models	• Require in-depth experience • Limited capability to simulate effects of ground water • Longer run times • Little data available for contact properties and fracture mechanics properties

A model is a simplification of reality rather than imitation of reality (Starfield and Cundall (1988)).Purpose of modelling data limited problem as often is the case in rock mechanics is to exploit potential trade off rather than precise answers. Figure 3 is an illustration given by Wiles (2007) which explains pictorially that simple models such as tributary area method can give solutions at significantly lower cost but at very high standard deviation. At the other end a 3D plasticity model can give solutions at a much lower standard deviation, point B but at a higher cost, since investments are needed in terms of computation cost as well as for the calibration of results for large number of parameters. If sufficient budget and time investment is not allotted, a 3D plasticity model could end up point C which gives the only the same accuracy of simple tributary area method.

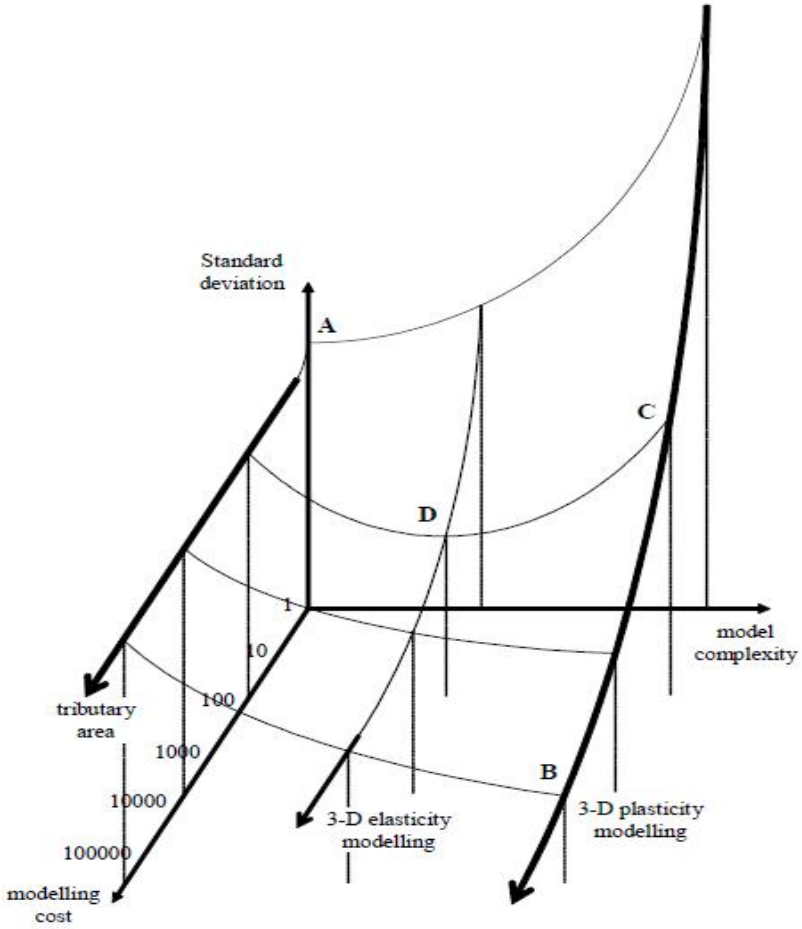

Figure 3: Cost benefit analysis of modelling methods, Wiles (2007)

2.3 Benefits of using numerical modelling techniques

Numerical methods provides viable alternatives instead of using complex, expensive time consuming physical models. They gained more popularity with development of affordable computing power.

- It offers fast and systematic methods for solving complex problems
- Possibility of using wide range of constitutive models available.
- Easier to rerun and optimize the results, if done with the help of a computer.

2.4 Need of three dimensional modelling in Rock mechanics

Mining or tunnelling problems in rock in most cases cannot be approximated to a two dimensional plane strain analysis. The reasons can be summarized as follows

- In many cases, the orientation of principal stresses will be in such a way that a two dimensional approximation is impossible.
- The normal to the joint planes do not lie on the two dimensional analysis plane (Pande et al. (1990)).
- In case of complicated underground excavation the stresses can no longer be analysed reasonably with at 2D model, since 3D effects are significant, for example the case of a mine pillar (Hoek and Brown (1980)
- Obtaining a longitudinal displacement profile for convergence confinement analysis for complex geometries is only possible with a full 3D analysis,(Vlachopoulos and Diederichs (2009))

2.5 Problem solving approach using a Numerical model

In general the methodology adopted for a numerical model can be summarized as follows.

a) Define the objective of the analysis: - The modeller needs to have a clear idea on what should be the outcome of the analysis.
b) Preparation of model: - It should a simplistic representation of the actual geology, at the same time it should be ensured that all the essential details are included.

c) Verification using available closed form solutions: - to build confidence in the tool used for modelling, run and compare simpler models for which analytical solutions are available.

d) Assign input parameters and boundary conditions:- Representative input parameters are given and boundary conditions are assigned

e) Meshing: - A suitable meshing to capture the subtle details.

f) Run and verify the model: - Results are compared with field measurements and recalibrate the model if required to match the field measurements.

g) Result interpretation: - Proper interpretation of the results depends on the experience and knowledge of the modeller.

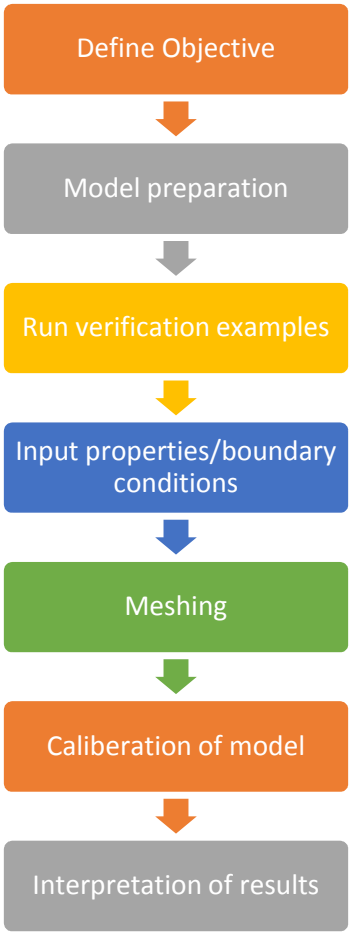

Figure 4: Numerical modelling procedure

3 Constitutive models and parameter selection.

Stress strain relations of the rock masses is the most critical parameter that determines the accuracy of the solution; the more realistic the relations are the more accurate will be the solution. But there is no constitutive model exists which accommodates all the aspects of rock behaviour defined by a realistic number of parameters that can be obtained from laboratory results. There are a number of commercially available models but the discussion here is limited to models which are commonly applied to rock mechanics problems and which are available in RS^3. A stress strain graph is also provided at the end, showing the implications of different constitutive models on material behaviour.

3.1 Constitutive models

Constitutive models widely applied for rock mechanics problems are as follows

3.1.1 Elastic model

Elastic model is based on Hooke's law of elasticity. It is simplest model involving two basic parameters Young's modulus and Poisson's ratio. It doesn't have a failure plane, it implies that the stresses and strains will increase infinitely with increase in load. In Rocscience packages, it does allow to calculate the degree of overstress (strength factor), if failure parameters are given. Even though it is simple, the method is quite popular for rock engineering applications, since the hard rocks behave elastically for stresses that are dealt with in Civil engineering and mining applications (Hajiabdolmajid and Kaiser (2003); Meyer (2002)). It gives a preliminary idea for the engineer whether to go for more complex models or not. This model forms a part of elastic behaviour, for more advanced elastoplastic models (Brinkgreve (2005))

3.1.2 Mohr Coulomb model Linear Elastic Perfectly plastic model

This model is formulated by combining the linear elastic Hooke's law and adopting Mohr Coulomb as failure criterion in plasticity framework (Smith and Griffiths (2004)). This model gives a first order approximation of rock and soil behaviour. Failure behaviour is reasonable but the deformations before the failure is not reliable since it is using Hooke's law to predict deformations in the elastic region. For non-associated

flow rule phi angle replaced by dilation angle in the equation. If LEPP model is assumed with associated flow rule then the model parameters reduced to 4 with (phi = dilation angle) which is unrealistic. Always it is recommended that, MC model should be used with non-associated flow rule with a specified dilation angle (Zdravkovic (2001a)). Another drawback is the infinite increase of volumetric strains with increase in axial strains, which is unrealistic.

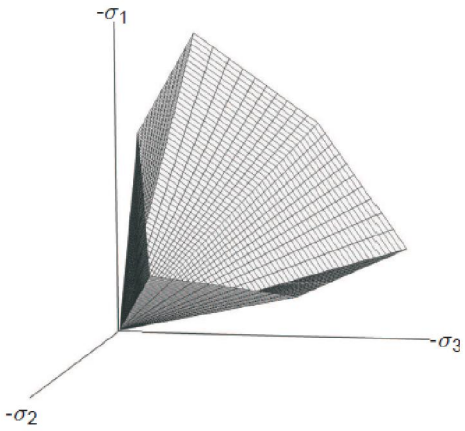

Figure 5: Shape of Yield surface in Principal stress space for cohesion less material - Mohr Coulomb model (Plaxis (2011))

3.1.3 Drucker Prager model

This model is just a simplification of Mohr coulomb model, dealing with sharp corner of Mohr coulomb model involves elaborate computer code and extensive use of computing power (Plastic potential functions and yield functions are not uniquely

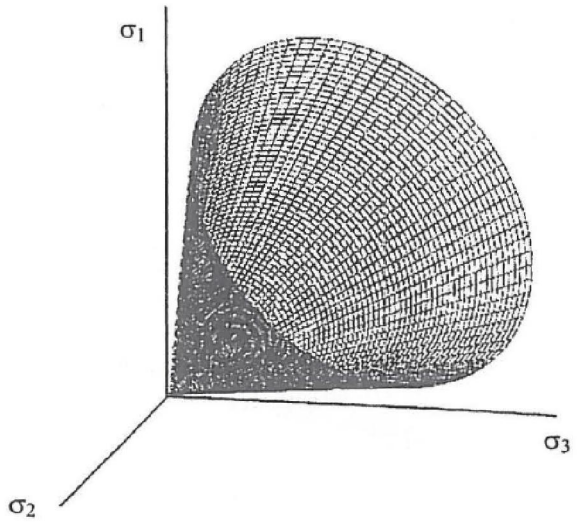

Figure 6: Shape of Yield surface in Principal stress space for cohesionless material-- Drucker Prager model Brinkgreve (2005)

defined at the corners). This means that the analysis using Drucker Prager is independent of sigma2 which can have significant impacts on the analysis.Zdravkovic (2001a).

3.1.4 Hoek Brown model

Like Mohr Coulomb criterion Hoek Brown also uses Hooke's law to predict the stresses in the elastic region but uses Hoek Brown as failure criterion, which is empirical and suitable for rocks (Hoek et al. (2002)). For rocks dependency of shear strength on stiffness is higher (Plaxis (2011)), hence a linear failure curve proposed by Mohr Coulomb model is not suitable for modelling rocks. Furthermore the rocks will show significant tensile strength which is better predicted by Hoek Brown failure criterion, but this shortcoming of Mohr Coulomb model is overcome by introducing a tensile cutoff.

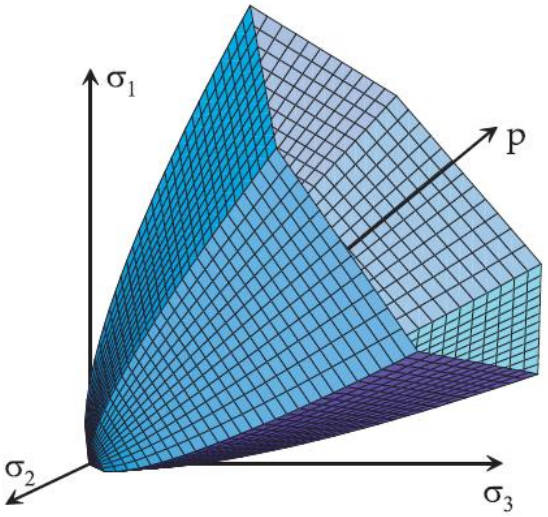

Figure 7: Shape of Yield surface in Principal stress space for cohesionless material- Hoek Brown model (Plaxis (2011))

3.2 Post Yield behaviour

The models mentioned above can well capture the failure and pre-yield behaviour of rock but in order to capture the post yield behaviour of rock, modifications are required for the above said constitutive models.

3.2.1 Elastic brittle plastic model

Failure of shallow rock structures and foundation are governed by the discontinuities, but at deeper levels it is primarily governed by in-situ stresses. Hoek et al. (1995) suggested that the brittle failure of rock can be simulated by assigning very low residual (m_r & S_r) coefficients. This approach was giving reasonable results when compared to field measurements (Hoek et al. (1995)).The model can either be implemented in Mohr coulomb model or in Hoek brown model by assigning very low values for the residual cohesion and frictional parameters.

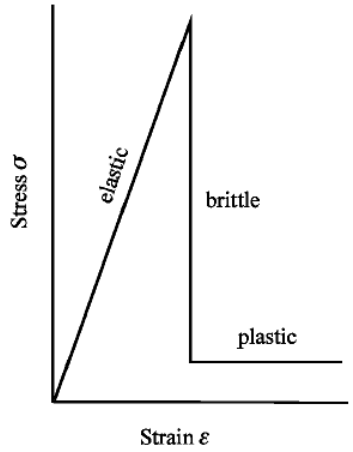

Figure 8: Assumed elastic brittle plastic behaviour of massive brittle rock, (after Hoek et al. (1995))

3.2.2 Cohesion weakening model

Studies by Hajiabdolmajid et al. (2002) have shown that for brittle rocks mobilization of cohesion and frictional strength of rocks are not happening at the same time and a significant amount of cohesive strength is lost at post peak behaviour. Similarly studies conducted by Wilson (1980) also implies the necessity of keeping low residual cohesive strengths while keeping the residual frictional value the same. It can be implemented in Mohr coulomb model by setting residual cohesive strength to low values and keeping the friction value same as peak friction. It is normally adopted model for predicting the post yield behaviour of coal measures strata (Coggan et al.

(2012)). As mentioned before, a model is a simplification of reality rather than imitation, there is no need of capturing all the details of rock behaviour in one model. For example even simple elastic constitutive law may be well enough to predict the behaviour accurately for a deep underground excavation. Several authors have highlighted the importance of starting from simplified models then build on it to make it more and more complicated if it is required (Wiles (2007);Coggan et al. (2012);Hammah and Curran (2009)).The following graph, Figure 9 shows the Triaxial simulation done with RS^3 using Mohr Coulomb model, to show the potential consequences of each model used on the resulting stress strain behaviour. The residual parameters used for elastic brittle plastic is half of peak of peak strength values and for cohesion weakening model the friction value is kept intact with cohesive strength reduced to very low values.

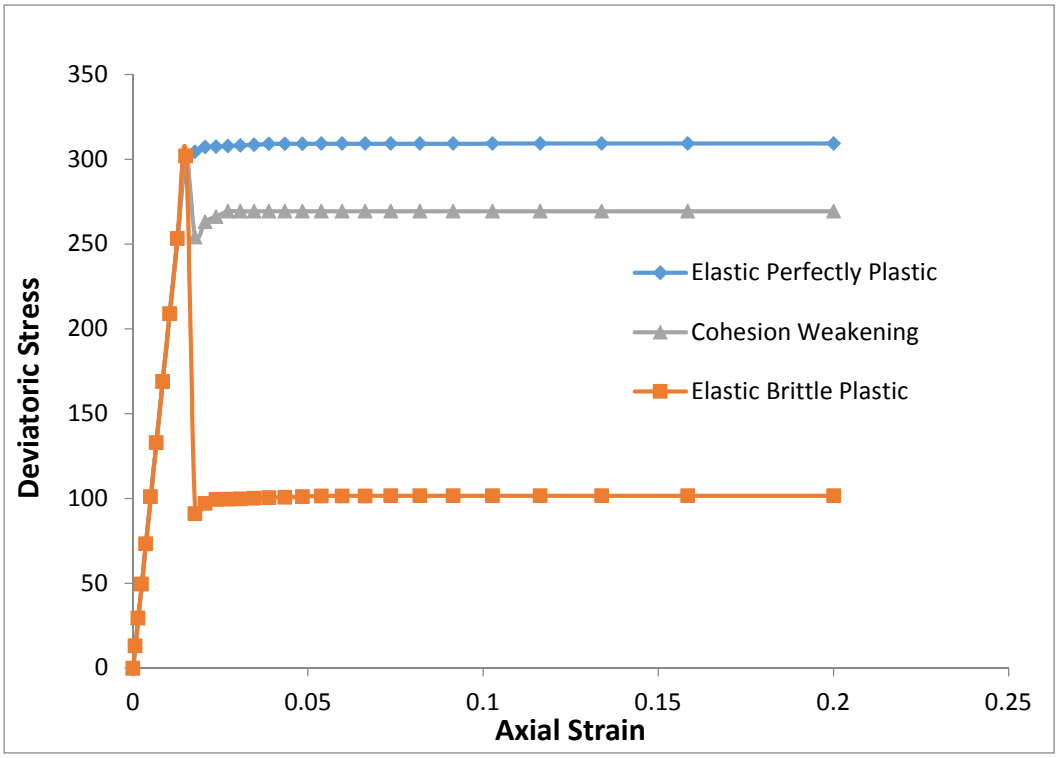

Figure 9: Triaxial simulation done with RS^3 to show the differences between Elastic perfectly plastic, Cohesion weakening and Elastic brittle plastic modelling using Mohr Coulomb

The next stage was to investigate how the longitudinal displacement profile varies for a cohesion weakening model and perfectly plastic model, when it is applied to a real tunnel problem. The parameters are taken from Table 3 page 47, the longitudinal

displacement profile is drawn for the tunnel roof passing through the centre of the tunnel. The results are as shown in Figure 10. Displacement profiles obtained from the perfectly plastic model is much lower than that obtained from a cohesion weakening model, which is said to be a more realistic representation of the coal mine road way behaviour (Pan and Hudson (1988); Coggan et al. (2012); Meyer (2002)).

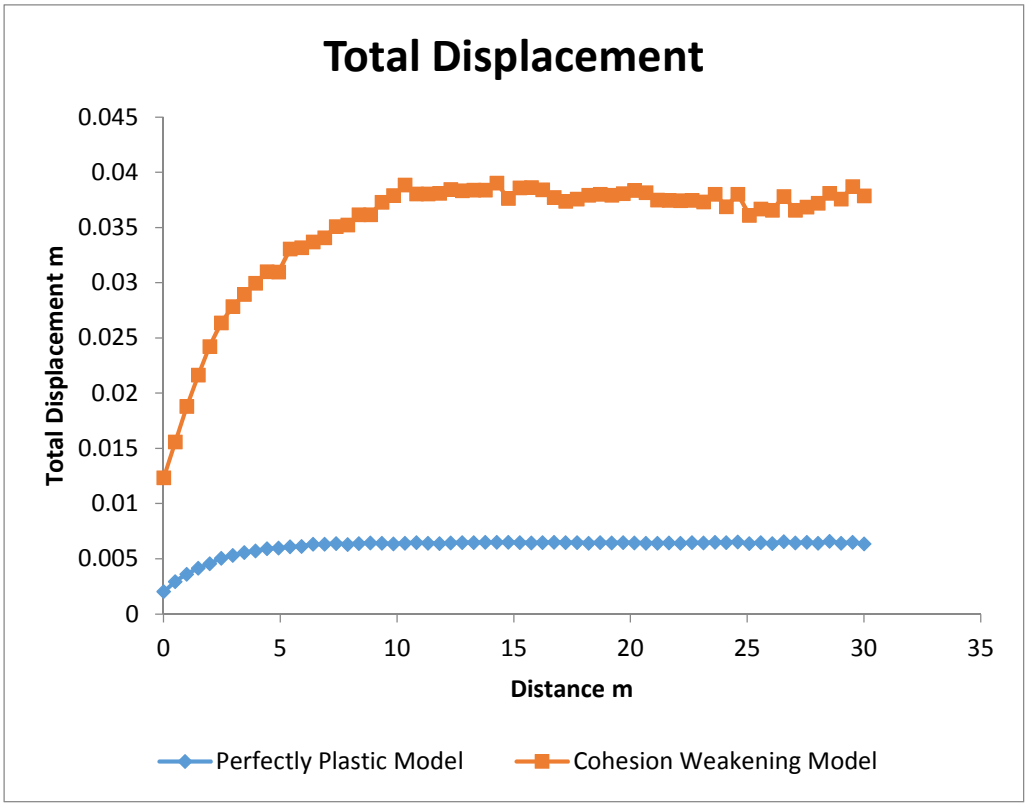

Figure 10: Comparison Longitudinal displacement profile of a tunnel modelled by Linear Elastic Perfectly Plastic Model and a Cohesion Weakening model

3.3 Parameter selection

The solution given by a computer program is as good as the input parameters used. The usage of laboratory data as such to the model will often give unrealistic results since they represent intact rock specimens. An alternative is to perform in-situ tests which are often time consuming and expensive. Often a wide range of variation in properties of materials can be expected and it is impossible to do in-situ tests for

every change in geology. In order to select the representative parameters for rock mass models, a number of methods are available, these include;

3.4 Scaling of laboratory test data

The stress required to cause failure of a laboratory sample depends on the length to width ratio (Wilson (1983)). Bigger the sample chances are higher that, the plane of weakness will be encountered thus causing premature failure. Based on his observations in UK coal mine environment Wilson (1983) suggested scaling factors to determine the representative values based on laboratory data. Typical parameters that are applied for UK coal mine model can be found in Meyer (2002).

3.4.1 GSI based Hoek Brown formulation

Hoek Brown criterion is the most popular failure criterion to describe the behaviour of rocks (Hoek et al. (2002)). This empirical criterion starts with intact rock properties and subsequently introducing factors to reduce these properties to describe a jointed rock mass. Marinos and Hoek (2000), describes how the most important components of Hoek Brown criterion m_i (material constant) and σ_{ci} (intact compressive strength) could be reduced from laboratory values to field values. It is an empirical system that has evolved over years combining the collective experience of geologists. RocLab is a freely available program based on Hoek Brown formulations (Hoek et al. (2002)), which can readily give the field parameters based on four input values: intact rock strength, material constant, GSI and Disturbance factor. Figure 11 can be used to get a first order approximation of Uniaxial Compressive Strength based on RMR, GSI or Q rating (Hoek (2004)).

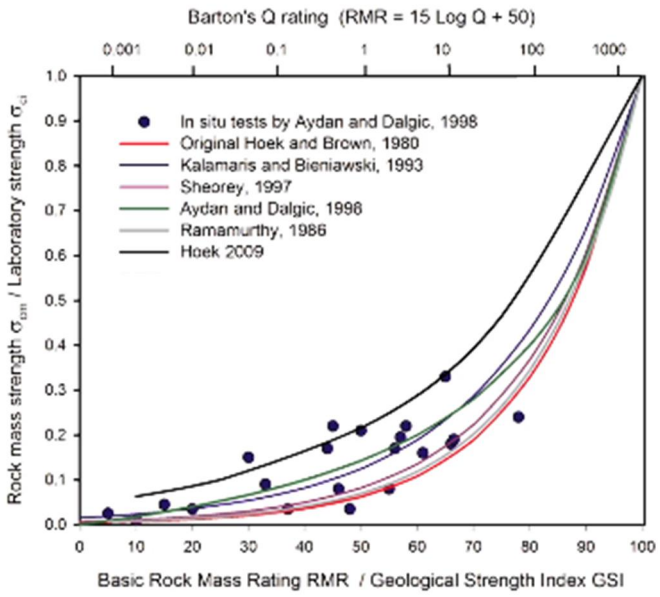

Figure 11: Rock mass strength estimates compared to laboratory strength results, after Hoek (2004)

3.4.2 Back Analysis of Stress Strain Relationships

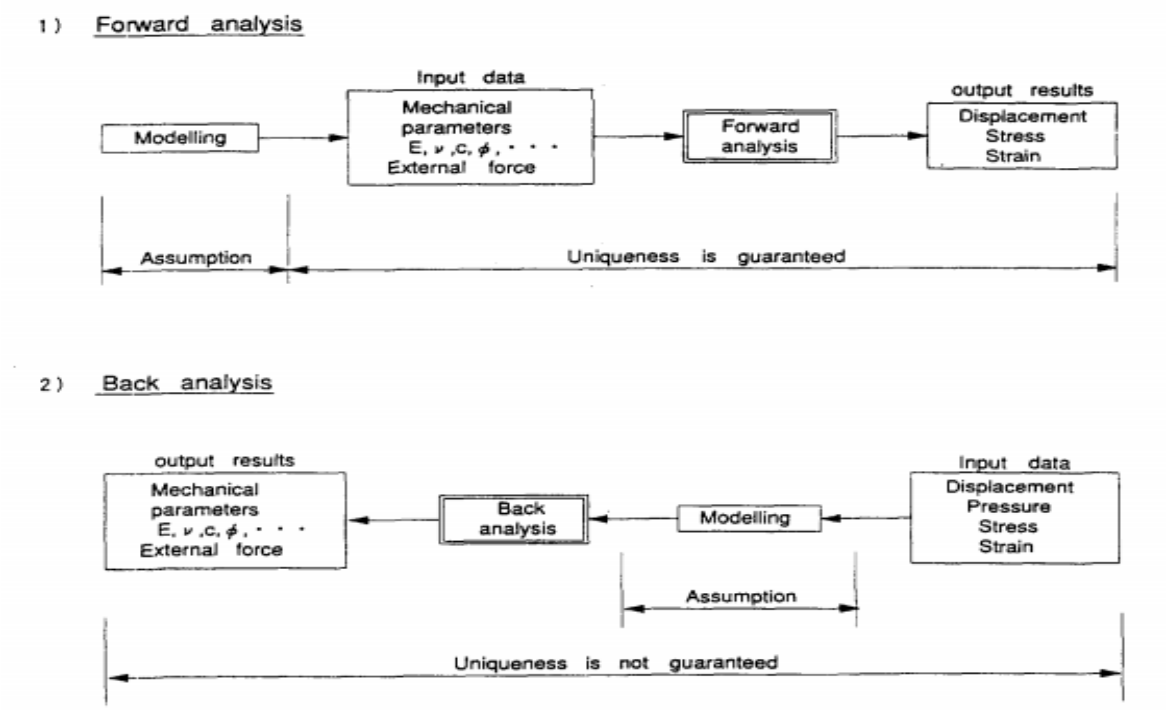

Figure 12: Forward and backward analysis (after Sakurai (1997))

As explained before, parameter determination for geotechnical problems is not a trivial task, often the estimated parameters will not be an actual representation of field conditions. Back analysis is a procedure to analyse the field measurements to estimate the model parameters which could be used for further calculations. This concept is explained in Figure 12 (Sakurai (1997)), it also emphases the idea that the output results of back analysis is dependent on the modelling assumptions and stresses the importance of selection of right model for parameter determination. The procedure is widely used in mine modelling, to calibrate the results obtained from modelling and optimize the design. This observational approach of modelling was first mentioned by Terzaghi et al. (1948).

3.5 Summary

Numerous constitutive models which are frequently used for rock mechanics problems have been introduced. It is important to understand the constitutive behaviour being used, since it is a key aspect in determining the accuracy of the solution. This is illustrated by Figure 10 which shows the difference in displacements modelled when using a perfectly plastic model and a cohesion weakening model. The chapter also highlights the importance of selecting representative parameters for the model and introduces methods for scaling down the parameters from laboratory data to rock mass parameters for the model.

4 Mining Methods and application of numerical modelling for underground coal mines

This chapter reviews the mining methods adopted for underground coal mines and a brief review is made regarding the application of modelling techniques for mine design. Coal is relatively low value material, so the focus of coal mining is to maximize the yield on minimal unit cost. Also the output of the coal must be continuous if it is intended for electricity production, since substantial amount of space is required for storage. Predominantly two mining methods are adopted for coal mines, room and pillar and longwall mining method. The later calls for extensive capital investment costs before beginning of the operation but guarantees high production rates. Whereas the room and pillar method allows for initiating the production with minimal initial capital investment costs. The two methods are explained in the following sections

4.1 Room and pillar mining

Coal seams are normally horizontal. Room and pillar, also called as bord and pillar, mining are best suited for extracting tabular and flat lying deposits such as coal. In this system the coal is extracted in horizontal directions at intervals connected by cross cuts, leaving coal seams in between to act as pillars for supporting the overlying strata and preventing the subsidence of surface. Hence it is the preferred method when subsidence has to be avoided, for example below the railway lines, important buildings etc. Recovery rates can be low since the coal is left behind as support pillars. Worldwide approximately 60% of coal is extracted adopting room and pillar mining. Weak layers and plastic zones induced are stabilized by rock bolts.

Coal seams are extracted by either using a conventional drill and blast method or by using a continuous miner. Increased efficiency and safety and ability to mine multiple locations at the same time made continuous miner a favourable option, Most of the room and pillar mining nowadays is utilizing a continuous miner. (Darling (2011)). The layout of a typical room and pillar mine is illustrated in Figure 13.

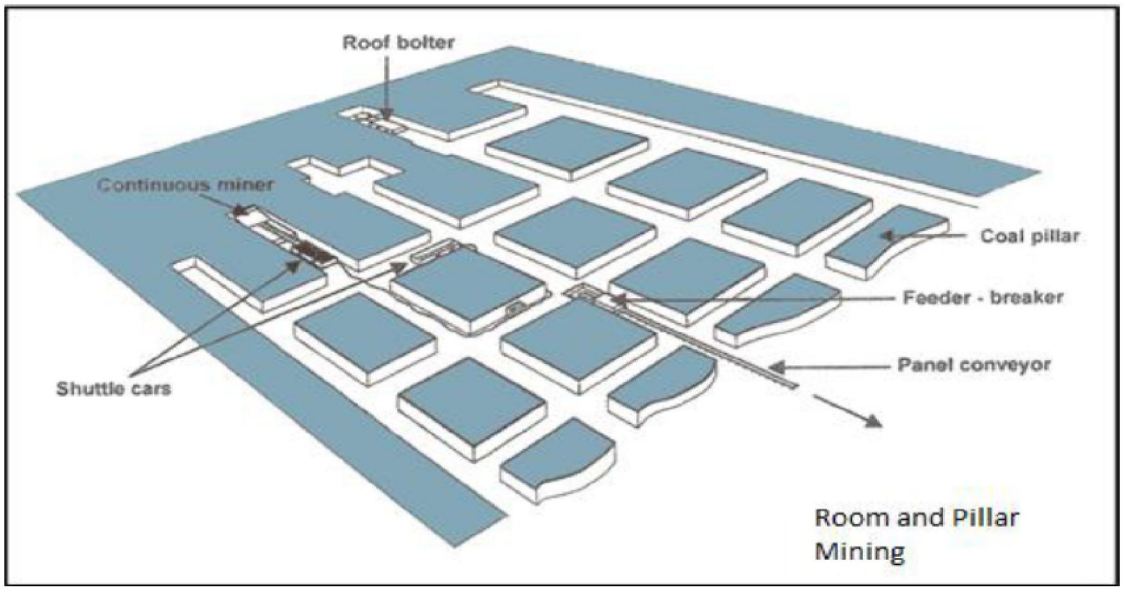

Figure 13: Layout of a room and pillar mine after Altounyan (1999)

4.2 Long wall mining

The method is best suited for horizontal coal seams of 1.5 to 2m thick. Seams are removed in single slice using a mechanical shearer. The longwall panel can be of several kilometres in length and 300 to 400m across the width.

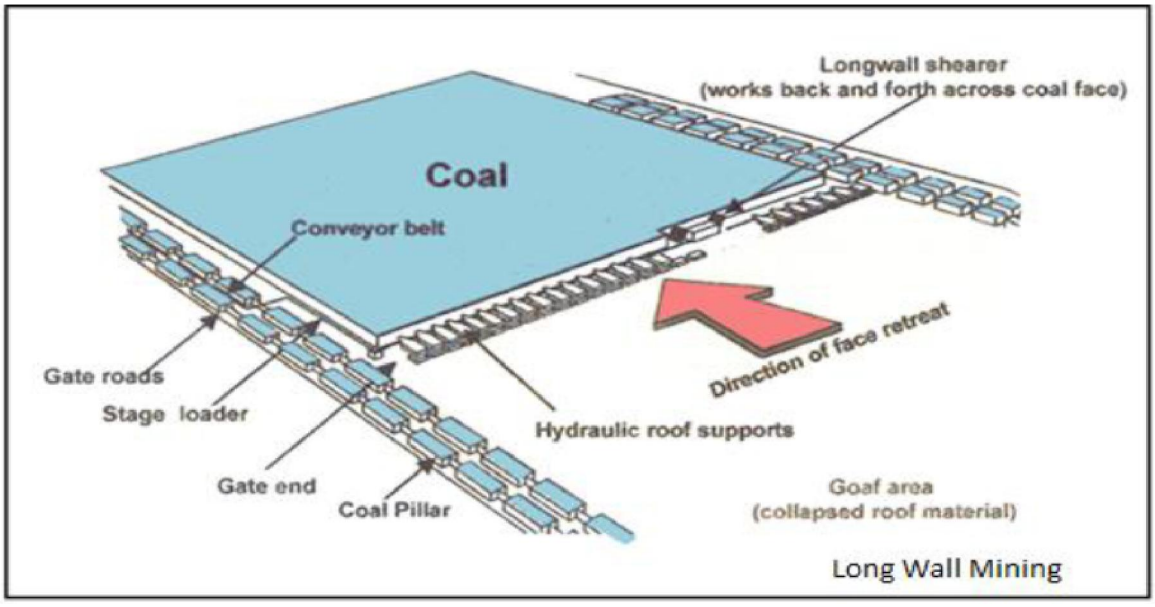

Figure 14: Mine layout of a typical long wall mine, after Altounyan (1999)

The overlying strata collapses into the mined out area creating a caved zone which may induce surface subsidence, the magnitude of which varies on depth of extraction. The face of the shearer is supported by a hydraulic jacking system. High percentage of extraction is guaranteed but initial investment costs are higher. Typical layout of a long wall mine is as shown in Figure 14.

4.3 Reinforcement systems

Reinforcement systems are primarily used for reducing the severity of deformations and collapse during the early stages of coal mine development. The support systems are incapable of taking the entire load induced due to deformation. It helps the loose rock around the excavation to create a self-supporting rock structure and thus preventing collapse or further deformation (Hoek and Brown (1980)). Rock bolting have become a normal practice in UK coal mine industry (Wilson (1983)). The UK Deep Coal Mines Industry Advisory Committee recommends a minimum rock bolt density of 1bolt/square metre. The length should be a minimum of 1.8m, but should be increased with the depth of weak strata.

4.4 Previous applications of three dimensional mine modelling

Extensive literature is available for the two dimensional modelling of coal mine excavations. In reality, rock failures often occur at the mine face where the assumption of plain strain condition is not valid and thus cannot be modelled in two dimensions. Limitations in computing power restricted earlier three dimensional modelling of mines to elastic analysis.

Gale and Blackwood (1987) made a three dimensional analysis of coal mines to determine 1) the principal stresses at the face 2) factor of safety against shear failure and 3). Displacement characteristics of excavation. It demonstrated the need of three dimensional analysis impact of in-situ stress field orientation on stability. The analysis showed good correlations with field observation.

Reed (1988) illustrated the usefulness of elastic brittle plastic models to predict the damage for tunnel excavations in soft rock. Su and Peng (1987) used three dimensional modelling to simulate the cutter roof failure mechanisms in West Virginia

coal mines. Meyer (2002) used a three dimensional finite difference models to predict the damage due to high horizontal stress orientation using elastic as well as elasto-plastic models. An extension of this modelling of North Selby Complex using finite element code is discussed in detail in the following chapters.

4.5 Pillar Extraction

To maximize production coal pillars are systematically removed after the primary extraction is completed. Pillar extraction methods should be properly designed some of the commonly used methods are Christmas tree or Split and fender method. Christmas treeing is most favoured by operators since it does not require place changes and bolting (Chase et al. (2002)). Another method that can be used is pocket and wing procedure. Pillar extraction is accomplished by continuous miner according to predetermined extraction plans.

Chapter 9 discussed a case example of an Indian mine which practiced diagonal depillaring during retreat mining. The case is replicated using RS^3 following the field procedure.

4.6 Summary

This chapter gave a brief introduction of popular mining methods available for coal seam extraction. Selection of a method largely depends upon the initial investment costs, extent of reserve and land use patterns. Systematic roof bolting practices are normally adopted for UK coal mines and proved to be successful in controlling the deformation and rood falls. There were only a limited amount of published literature available on the use of three dimensional models for modelling of mines. Mainly elastic models were used to model due to lack of powerful computing. Pillar extraction in bord and pillar mines are adopted to maximize the production. The use of finite element codes for prediction of damage on coal mine roadways and diagonal pillar extraction are analysed in the following chapters.

5 RS^3 as a modelling tool and Pitfalls in using numerical analysis for modelling

RS^3 (R stands for Rock and S for Soil 3 for three dimensional analysis) is a new 3D FEM tool from Rocscience for analysis of geotechnical structures for civil and mining applications. It can be used for a wide range of applications from tunnelling and support design, surface excavation, embankments, and foundation design and seepage analysis. First customer release of the software RS^3 1.005 was on October 09 2013. The version used for the analysis is RS^3 1.007 (December 04 2013). Since it's new, only a limited help files, literature and tutorials were available for the software. In order to be familiar with the software validation examples where done on RS^3 to compare the results. The analysis were compared with Phase^2 2D FEM program from Rocscience and the results were found to be satisfactory as shown in Appendix A. Several email communications were made with Rocscience support team for clarifications regarding the working of the software and their incessant support helped to increase the understanding of the software.

To perform a useful numerical analysis a geotechnical engineer requires a knowledge in a broad range of subject; one should be conversant with finite element procedure, concepts of rock mechanics and more importantly the knowledge of constitutive models and solution algorithms used to implement it. This chapter gives an overview of the general working scheme of a numerical model and the factors affecting accuracy of the results particular to RS^3. Focus is given to the advanced features of stress analysis settings in RS^3, Some of the critical aspects which influence the results are discussed in the next sections

5.1 Influence of Meshing and discretization

The finer the mesh, more refined the results will be, but there is a cost in terms of computing time and hardware requirements of the system used. It is recommended to adopt a progressively finer mesh till the results between two consecutive analyses is not significantly different (Rocscience (2013)). The following Figure 15 shows an example carried out in RS^3 to show the effects of meshing on the development of a

plastic zone of a simple single stage tunnel. It is shown that with a coarser mesh the damage is contained within the weak mudstone layer immediate above the tunnel but while adopting a finer mesh, the spread of yield zone is much larger. Figure 15 shows the layers of rock material along with the yielded elements. This was not directly possible in RS^3. Email correspondence with the Rocscience support team requested the possibility to present the results as shown in the figure.

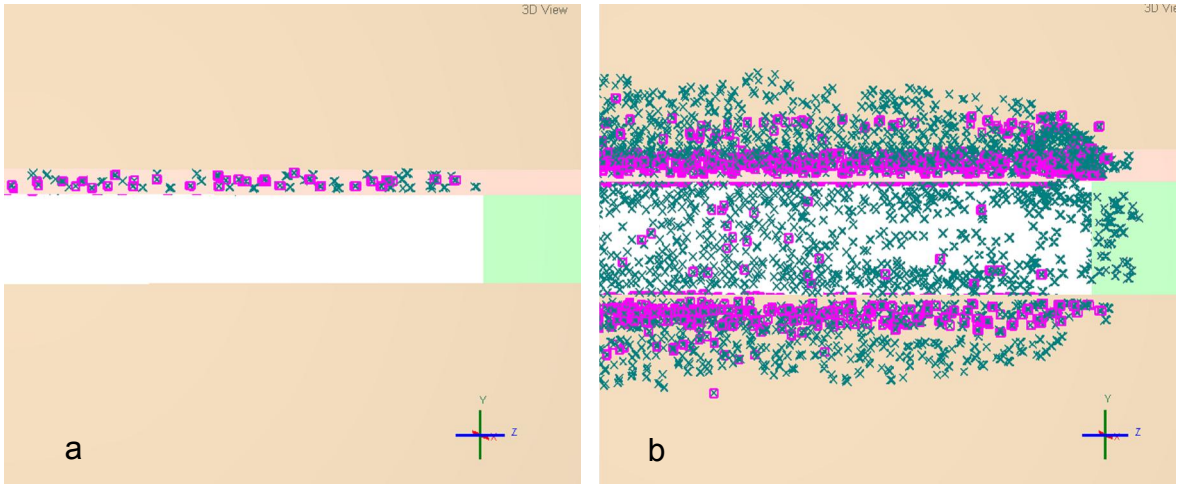

Figure 15: Yielded elements (a) by adopting a coarse mesh (b) by adopting a fine mesh

The experience and expertise of the modeller will also play an important role in finding a realistic solution. The modeller needs to know where abrupt changes in stress could occur and accordingly fine tune the mesh to obtain reasonable results. This concept is well explained by Zdravkovic (2001b) when using an example of a footing. It is shown that, a 35 element well-graded mesh is better in predicting the results than a 110 element ill-conditioned mesh.

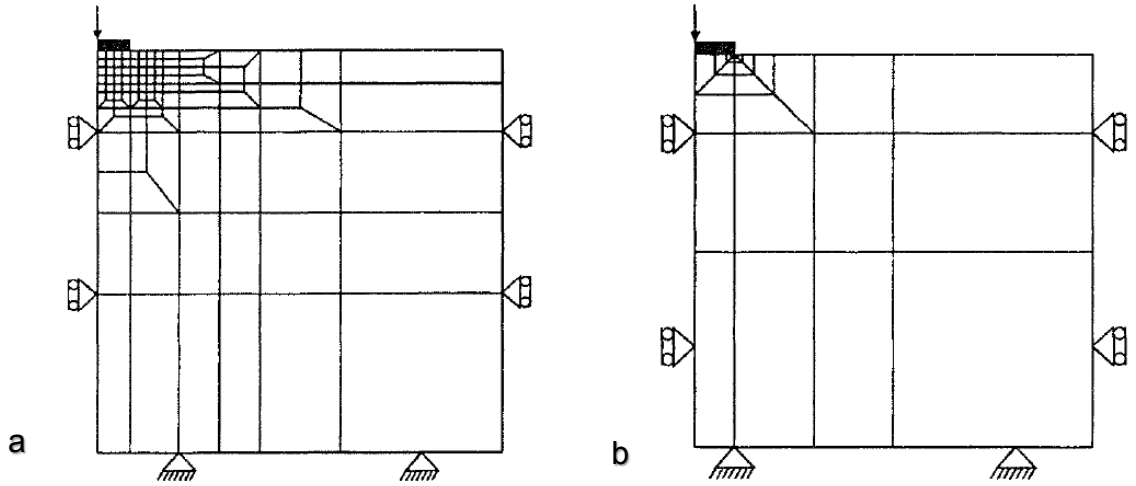

Figure 16: Meshing done for a strip footing (a)Graded 110 element mesh (b) Graded 35 element mesh with element length smaller at the corner where the stress strain gradients are large, predictions with figure b proved to be more realistic, (after Zdravkovic (2001b))

5.2 Solution Schemes and convergence criteria

There are number of commercially available FE softwares on the market, most of them have very user-friendly interfaces. They allow to model and run the analysis in minutes and give colourful graphs and contours as outputs, regardless of input parameters and modelling strategies adopted in underlying analysis (Cai (2008)). It is important to know the underlying solution scheme adopted by the developers to interpret the results correctly and to realize the possible limitations.

For a nonlinear finite element analysis the constitutive matrix [D] equation 1 is not a constant but varies with stress/ strain. Solution schemes are techniques used in FEM packages to implement this nonlinear behaviour to calculations as accurately as possible. Programs tackle this issue by implementing the governing finite element equations incrementally.

$$\Delta\sigma = [D]\,\Delta\varepsilon \quad \text{--- (1)}$$

Where $\Delta\sigma$ is the incremental stresses, [D] the constitutive matrix and $\Delta\varepsilon$ the incremental strains. In other words due to nonlinear behaviour of stress strain graph, the load increments are done in small steps to match it as close as possible.

Different solution schemes available which are widely used, like Tangent stiffness method, Visco-plastic method, and Newton Raphson. The review is limited to the solution scheme adopted by softwares RS^3 and Phase2; both of them use Newton-Raphson schemes (Rocscience (2014b)). This is an iterative procedure and is shown to be most robust and most economical in terms of computing time (Zdravkovic (2001a)). The philosophy behind newton Raphson is explained with an example of force applied to a non-linear spring (Potts and Ganendra (1994), Rocscience (2014b)). The force displacement relation spring can be written as

$$P = KU \text{ ------- (2)}$$

P is the load applied, U the displacement and K is the non-linear stiffness of the spring which is held as a constant for each load step. The initial force is known, final force is also known from the load increment given, and current displacement is calculated with known stiffness and the difference between initial and final forces. This iterative procedure is continued untill the difference between the forces are negligible and reduced to a set tolerance limit. The concept can be mathematically explained with following equations and Figure 17. The final displacement is cumulative displacement that occurred in all the iterations.

$$K_0 \Delta U_1 = P_{(n+1)} - F_0 \text{ ------- (3)}$$

$$\Delta U_1 = K_{(0)}^{-1}(P_{(n+1)} - F_0) \text{ ------- (4)}$$

$$U_{(n+1)} = U_n - \Delta U_{(1)} \quad \text{--------(5)}$$

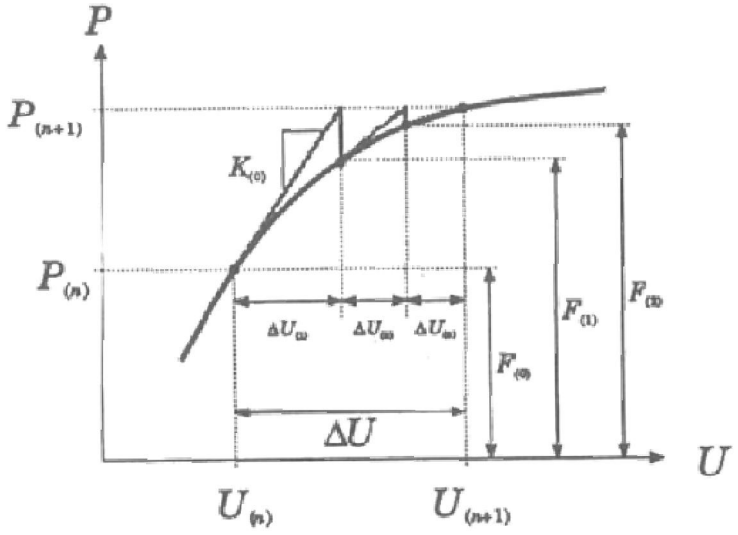

Figure 17: Iterative scheme adopted in Newton Raphson method in a single load step , the final solution scheme consists of multiple load steps which can be user controlled Rocscience (2014b),Potts and Ganendra (1994)

5.2.1 Explicit and implicit solution schemes

RS^3 and Phase^2 are implicit finite element methods (Rocscience (2014a)), For plasticity analysis it tackles the problem by first obtaining an elastic solution, the stresses are checked against the yield criteria, if the yield criterion is violated plastic deformation takes place (Cai (2008)). This principle is illustrated in Figure 18.

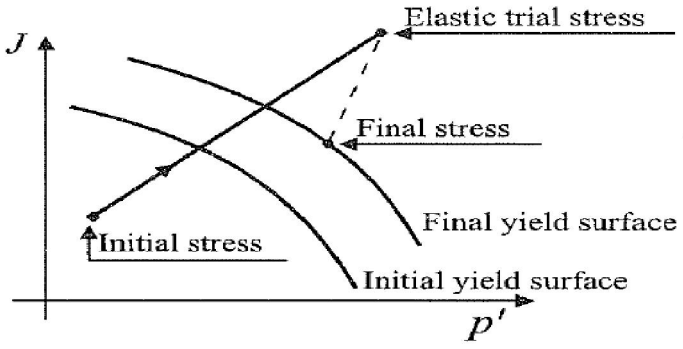

Figure 18: Return implicit algorithm approach (after Zdravkovic (2001a))

The implications of this approach is that the stress paths followed by the elements can be different from the true stress path and if the true stress path is not followed differences in results from reality can be expected But it allows faster computation than explicit algorithms (Cai (2008); Reed (1988)).

Whereas in explicit solution schemes for plasticity analysis stresses are checked against yield criterion for each cycle, and if the corresponding stresses violate plastic deformation takes place. The concept is best explained in the following Figure 19. Explicit schemes, are able to follow the true stress path and more realistic in terms of modelling results (Cai (2008)).

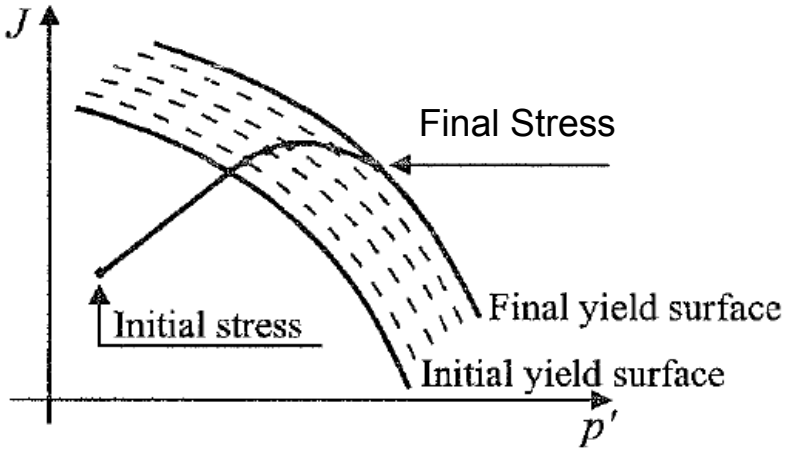

Figure 19: Explicit algorithm approach (Zdravkovic (2001a)), stress state is never allowed to cross the yield surface

5.3 Effects of boundary conditions

An important feature influencing the results is the nearness of the boundary to the excavation field. In general the movements of the mesh near to the boundary should be very small or negligible so that the boundary restraints given will not influence the results. It depends of the materials, shape of excavation, loads acting on it and the nature of boundary conditions. The problem can be avoided safely by keeping the boundaries far away from the excavation, but at the same time the computing time will increase sharply due to increase in number of elements. It is always advisable to run the model for different expansion factors and observe the results to select the right choice of boundary location.

Figure 21 shows the same tunnel model run by varying the expansion factors and its effects on the longitudinal displacement profile. For uniformity number of elements

immediately surrounding the excavation and the gradation after that is kept the same for all the models.

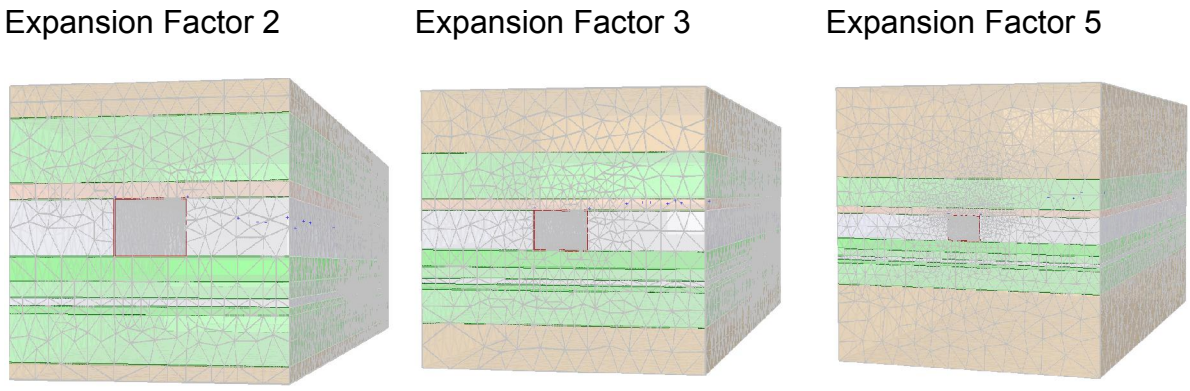

Figure 20: Tunnel modelled with expansion factor 2, 3 and 5 respectively

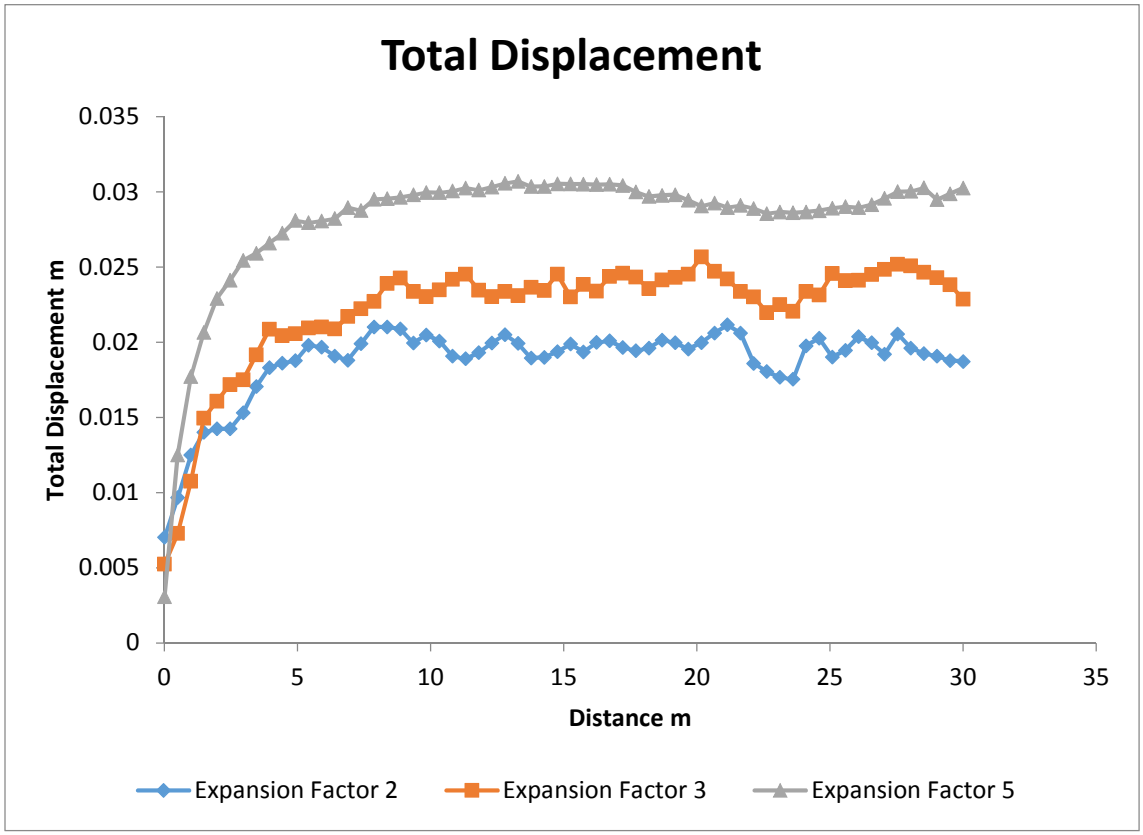

Figure 21: Effects on longitudinal displacement profile for the tunnel model run on various expansion factors.

5.4 Load stepping

This is a control parameter in RS^3 which allows how many steps the maximum load should be applied to the model in each load step an iterative procedure as mentioned in the previous section is adopted for convergence. The reduction in the number of load steps will result in lower accuracy of the solution but computation times will be short. In general it is set in automatic mode. Analysis conducted with higher number of load steps than from the default automatic mode didn't show too much variation in the results. Hence all the analysis carried out in this dissertation is performed with load stepping set to automatic mode.

5.5 Tolerances

The tolerance value determines the maximum load imbalance allowed between subsequent load stepping. For example if the convergence criterion is set to absolute force, and tolerance value is set to 1%, the solution will converge between 99 and 101 for an analytical answer of 100 (Rocscience (2014a)). Normally a tolerance value of 0.1% is set, if the model is showing convergence problems the tolerance value can be increased to 1%. (Rocscience (2014a)). Since cohesion weakening model with multiple materials and bolts was showing convergence issues all the analyses adopting cohesion weakening model was carried out with a tolerance value set to 1%.

Wherever comparisons are made between difference models in this dissertation, sufficient care is taken to set similar parameters for meshing, tolerances and load stepping.

5.6 Summary

This chapter gave an introduction to the RS^3 software package. A brief insight into working of the program was given. The chapter focused on the pitfalls that could occur while using a general purpose FE program for modelling. The impact of meshing, expansion factor, load stepping and tolerance was also discussed.

6 Applicability of numerical modelling for prediction of damage around coal mine roadways using RS^3

A review of previous numerical modelling work for coal mine roadway behaviour is made on Chapter 4. Chapter 5 considers the precautions and care to be taken while doing the analysis and consequences of using modelling softwares as a black box.

This chapter presents the initial modelling undertaken to predict the impact of stress orientation on a coal mine roadway. All the analyses are carried out using the software RS^3 (Rocscience 2014). In order to get familiar with the software a number of examples are done in the check if the results are matching with the closed form solutions or numerical solution done with other software. The results were found to be reasonable and are discussed in Appendix A.

6.1 Description of model

The multilayer model is a simplified representation of the North Selby coal mine geology and field stress conditions (Meyer (2002)). The generalized lithology of the North Selby Complex is described in Figure 22. The modelled lithology captures almost all the essential details of North Selby Complex. Figure 28 shows the modified lithological sequence used for modelling. The lithology is modelled in detail only around the zone of influence of excavation; and outside that area a competent strata is assumed. The advantage of axis symmetry can be made use of in case of stress parallel and stress perpendicular excavation. But for other stress orientations it is not possible.

In order to minimize the effects due to end restraints the excavation is carried out for a length of 50m and with an expansion factor of 3 and a free length of 25m is given ahead of tunnel face. Modelling done is chapter 5 shows that with an expansion factor of 5 the results are more refined but at the expense of computing time.

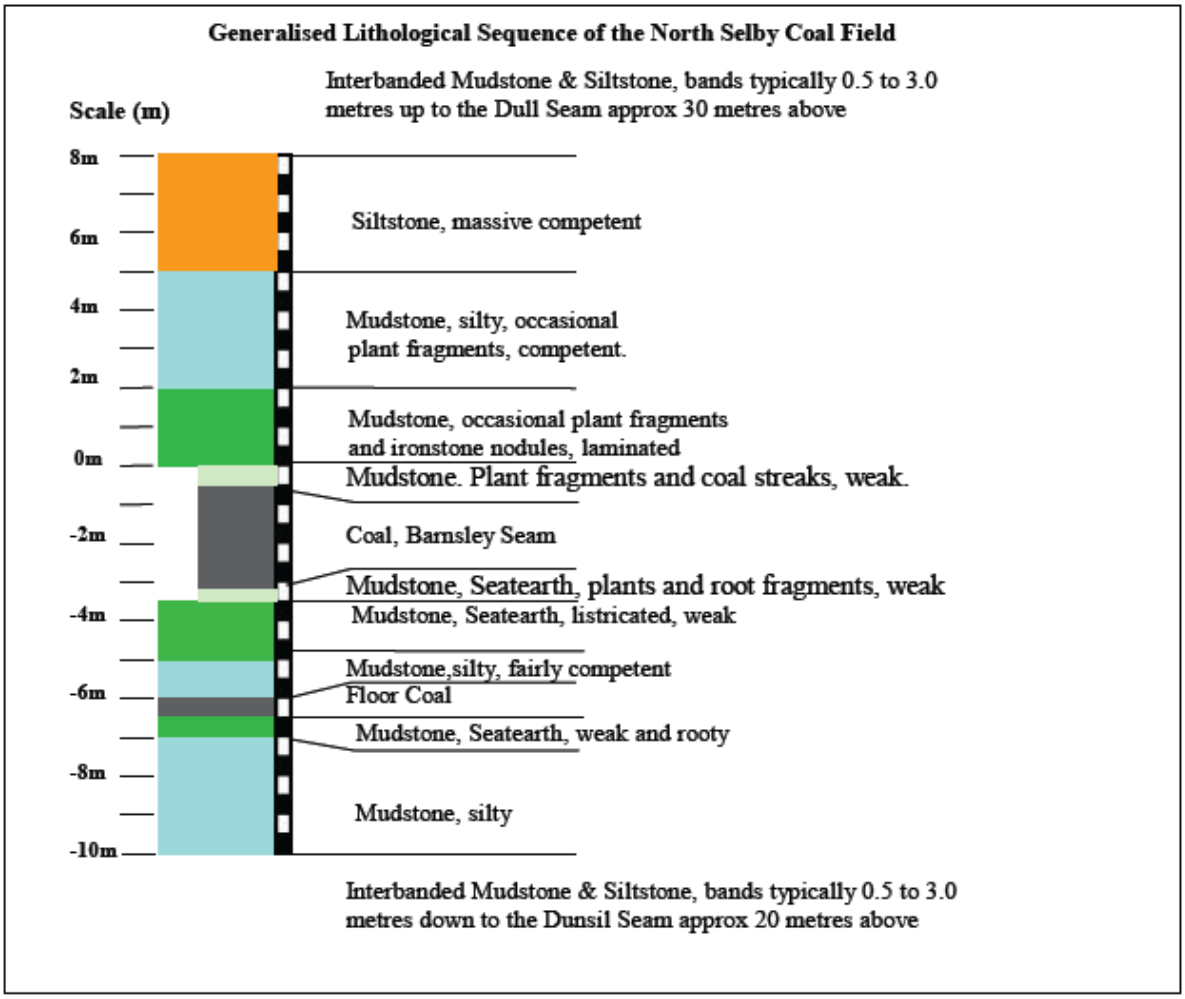

Figure 22: Generalized lithological sequence of North Selby Coal Field (after Meyer (2002))

6.2 Meshing and discretization

In Chapter 5 the influence of meshing on final results is explained, since the area of interest for the excavation is only at the tunnel face. A dense mesh is used in and around the tunnel face and for the rest of the area a coarser mesh is used. Meshing and expansion factor was selected so that it does not have significant influence on the modelled results.

6.3 Selection of constitutive model

Constitutive models that are available in RS^3 which could be used for describing the rock behaviour is explained in Chapter 3. All constitutive models are having its

advantages and limitations. For all the models described in Chapter 3, Hooke's law describes the elastic part of the rock and failure criterion is different for different models. If the stress levels are expected only in the elastic region no difference in calculated stresses can be observed in the results obtained with different models, but variation in the strength factor can be observed.

Since the deep seated rocks are strong enough to withstand the stresses induced by civil or mining application little damage due to stress redistribution is expected. It is generally an acceptable method to use an elastic modelling with a peak strength envelope (McCreath and Diederichs (1994)). Hard rock behaves in brittle plastic manner (Hoek et al. (1995)), hence all the analysis is carried out using an elastic brittle plastic with a cohesion weakening model which best describes the coal measures behaviour (Coggan et al. (2012)).

6.4 Modelling Parameters

The parameters from North Selby complex used for single stage model for different rock types are summarized in the table below

Table 3: Material properties used for modelling (after Coggan et al. (2012); Meyer (2002))

Material type	Young's Modulus (MPa)	Cohesion (MPa)	Friction Angle	Tensile Strength (MPa)	Poisson's Ratio	Residual Cohesion (MPa)
Siltstone	20000	7	34	4	0.25	0.7
Mudstone	17900	6	32	8	0.3	0.6
Weak Mudstone	14800	4	30	2	0.3	0.4
Coal	2600	1.6	35	0.8	0.3	0.2
Seat earth	15100	4	30	2	0.18	0.4

In-situ stresses adopted in the model represents a horizontal stress ratio (K) of approximately 1.6. The orientation and maximum horizontal stress is consistent with typical values measured in UK coal mines (Coggan et al. (2012)). Typical stress values used for modelling Major Principal Stress of 25MPa, Intermediate principal stress of 16MPa, and Minor (vertical) principal stress of 15MPa.

6.5 Sensitivity Analysis

The parameter determination is not an easy task in case of rock engineering problems. It is a common practice to do a sensitivity analysis to know the parameters which affects the results most. Analysis is carried out by varying the cohesion, friction angle and stiffness of weak immediate roof layer mudstone 20% below and above the representative values for the tunnel problem. Results are presented in Figure 23, it shows that variation of friction angle has a larger impact on the modelled results than other parameters like cohesion or stiffness.

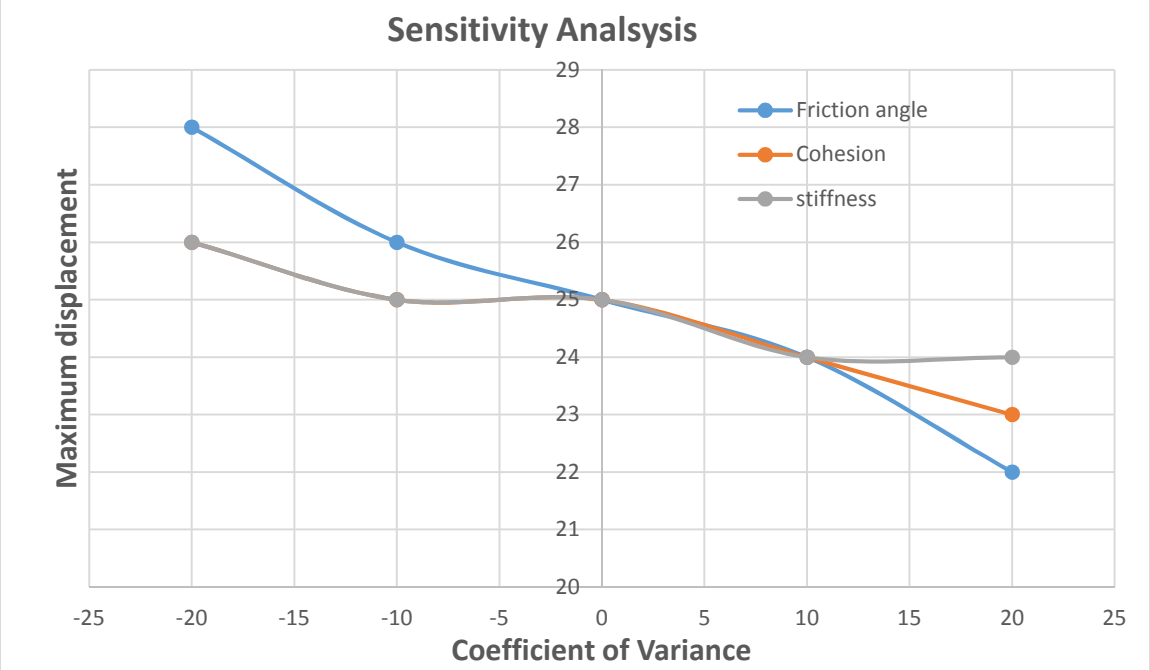

Figure 23: Results of sensitivity analysis showing the magnitude of displacements with change in parameters

6.6 Modelled results

Previous elastic and plastic modelling carried out by Meyer (2002) shows the damage due to high horizontal stresses on coal mine roadways in three dimensions in front of tunnel. The present analysis carried out with same parameters shows extent and spread of damage due to variation in stress orientation. For comparison five different models are setup with maximum principal stress orientations of 90,65,45,25 and 0 degree to the tunnel, 90 degree and 0 degree will be referred as stress perpendicular and stress parallel cases respectively.

Figure 24 depicts the maximum principal stress variation on roof top of the tunnel due to varying stress orientation. For clarity a three dimensional drawing is shown in Figure 24 highlights the stress orientation with respect to the tunnel and the point of observation. It can inferred that for maximum stress perpendicular to the tunnel the influence area of the stress damaged zone is much more wider than that of 0 degree orientation. Another important aspect to notice is the skewing of stress damaged zone when the stress orientation is changed from 65 to 25 degree with the degree of skewing much sharper for 25 degree before it becomes symmetrical for 0 degree. The extent of stress damaged zone is longer in case of 0 degree, but the spread width wise is comparatively less. The trend is reversed in stress perpendicular case with a wider spread of damage across the tunnel width.

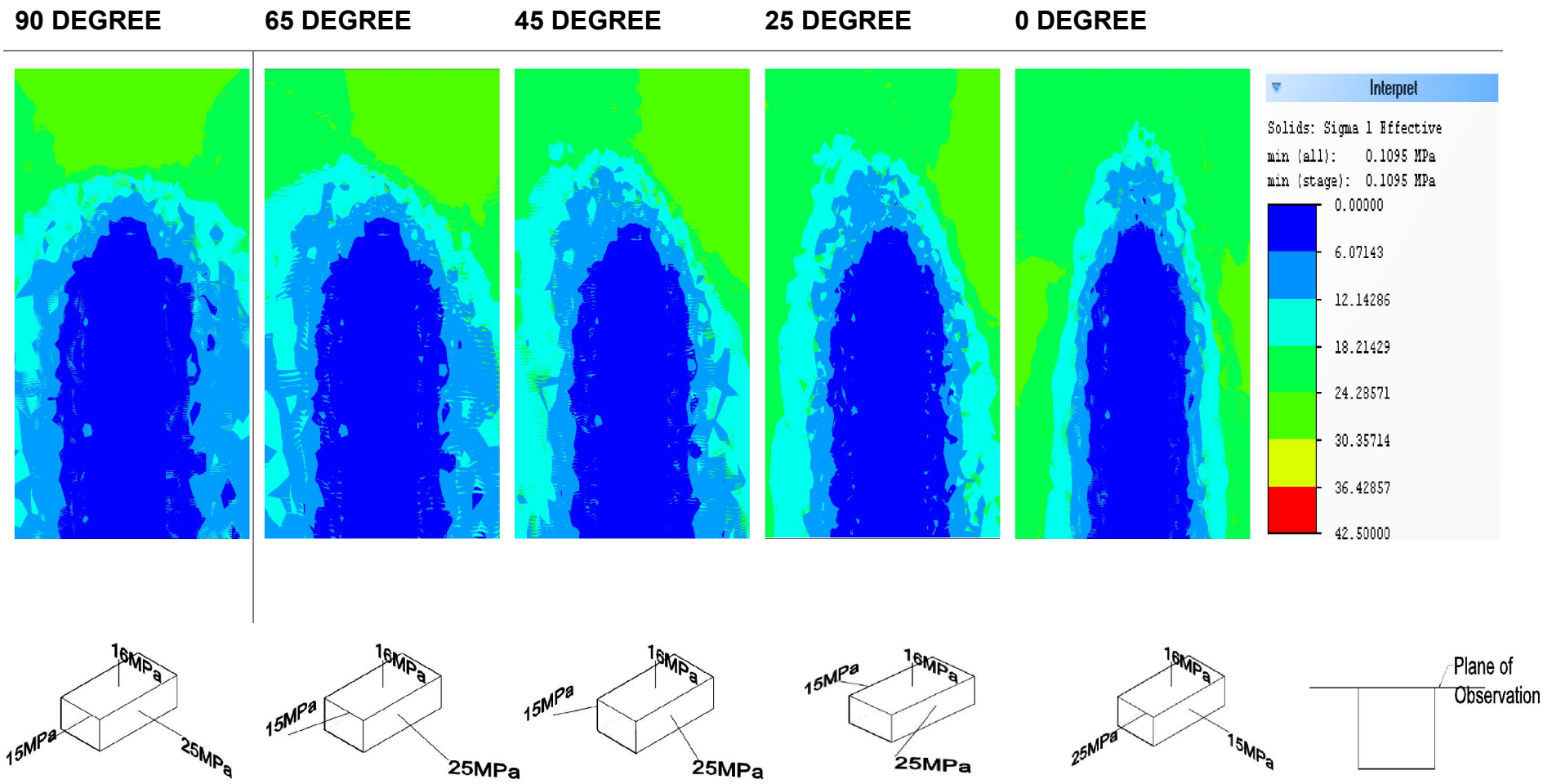

Figure 24: Effect of maximum principal stress orientation due to varying stress orientation

The spatial distribution of yielded elements near the tunnel face is discussed in Figure 25.The modelling is carried out for maximum principal stress orientations varying from 90 degrees to 0 degree to the tunnel axis. Cross sections are made at 2m behind the face, at the tunnel face, 1m, 2m, 3m and 4m ahead of face, in-order to easily understand the differences, all the results are presented in one single diagram.

The first row of figures from left hand side to right hand side shows the results for stress parallel condition. It can be observed that the zone of yielding is extended as far as 4m ahead of tunnel face. It is interesting to note that, the zone of yielding is much more significant on the periphery which is more competent than on the coal strata which is less competent. The reason could be well explained by streamline analogy (Hoek and Brown (1980)). When the stress orientation is changed from stress parallel to perpendicular condition, a change in yield pattern is evident. A non-symmetrical distribution of yield zone is evident, for 25, 45 and 65 degree orientation. Also the size of yield zone is much bigger with maximum spread for the stress perpendicular case. Figure 24 and Figure 25 show the extent of plastic zone ahead of tunnel face for stress perpendicular case is not as long as that of stress parallel situation. The yield elements is visible only till 3m ahead of face. Observation of yield patterns for various stress orientation also shows that there is gradual increase in yielded element when the stress is rotated from 0 degree to 90degree. This observation is consistent with the observation in field and reported by Kent et al. (1998) at the North Selby complex, in which the maximum damage and displacement is reported for the stress perpendicular case and comparatively minimal damage on the stress parallel case.

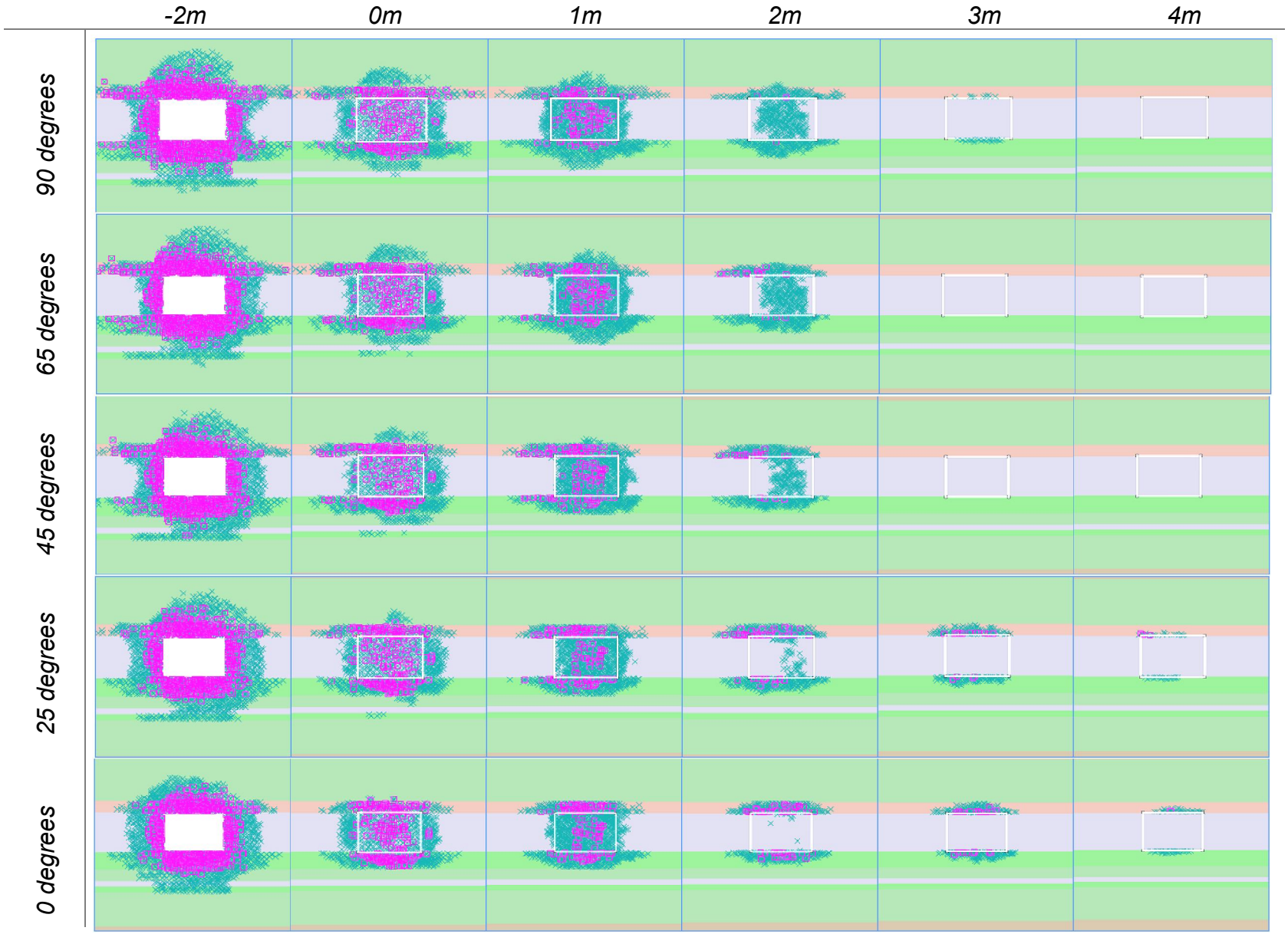

Figure 25: Plastic yielding observed in-front of the tunnel face for 90, 65, 45, 25 and 0 degree with respect to tunnel axis

6.7 Conclusion

The Chapter introduced the case example of North Selby mine, a simplified lithological model was recreated in RS^3, and the effects of varying high horizontal fields were studied. Sensitivity analysis were carried out to examine the impact of the parameter variation on the resultant displacement. Scaled representative values of the parameters were used for modelling. The modelling results show a wider and higher spread of plastic zone for the stress perpendicular case and shallower spread of plastic zones for the stress parallel case. The results of analysis with stress at an angle to the tunnel showed asymmetrical distribution of stresses and subsequent plastic zone development.

7 Single stage vs. multistage excavation

Chapter 6, explained the change in pattern of yield zone due to varying stress fields. As explained in chapter 4, several authors have detailed the importance of following the actual stress path in modelling to achieve realistic results (Pan and Hudson (1988);Meyer (2002); Cai (2008); Vlachopoulos and Diederichs (2014); Vlachopoulos and Diederichs (2009)). It is a well-documented fact in the literature that the tunnel advance has to be modelled in a similar fashion as it is undertaken in-situ. If the model is trying to replicate the continuous road header excavation then modelling has to be done in very small steps to predict the damages realistically. Vlachopoulos and Diederichs (2009) and Vlachopoulos and Diederichs (2014) showed that for continuous excavation the tunnel advance has to be modelled with an advance rate equal to 0.2 times the tunnel diameter or less.

A comparison is made between longitudinal displacements graphs modelled with varying advance rates using the parameters given by Vlachopoulos and Diederichs (2014). The modelling is done is Phase^2, as well as in RS^3, and the results are compared in Appendix B. It is found that the results from RS^3 are in good agreement with the results given by Vlachopoulos and Diederichs (2014),Vlachopoulos and Diederichs (2009) and phase^2 modelling undertaken.

Continuous road header excavation is a common extraction practice employed in coal mine road way excavation. In this chapter a comparison is being made between a single stage excavation model and a multistage excavation model. In the single stage excavation model the whole tunnel in modelled by simply deleting the material in one stage, which is totally unrealistic but modelling is much easier. For simplicity, roof bolting is not adopted for both models. For the multistage example, the modelling is done for very small advance stages of 1m which is 0.2times the width of the coal mine roadway.

7.1 Modelling Results

The modelling is done for stress perpendicular situation and representative geometry is same as explained in chapter 6 with an expansion factor of 3.Figure 26 explains

the difference in yield zone modelled for a single stage model and a multistage model. Pink squares indicate tensile failures and dark green colour indicates shear failure. It is very evident that for a multistage model, zone of yield covers a larger area and completely engulfs the tunnel face, which is not evident for a single stage model. It does mean that single stage model is not able to capture the progressive failure which is happening in reality. The multistage modelling shows that tunnel could have stability problems, not only in the roof but also on the tunnel front since the bullet shaped plastic zone completely engulfs the tunnel face. The reason for this difference in yield zone is, in a multistage model the tunnel advance happens in an already yielded zone which causes further damage to the strata.

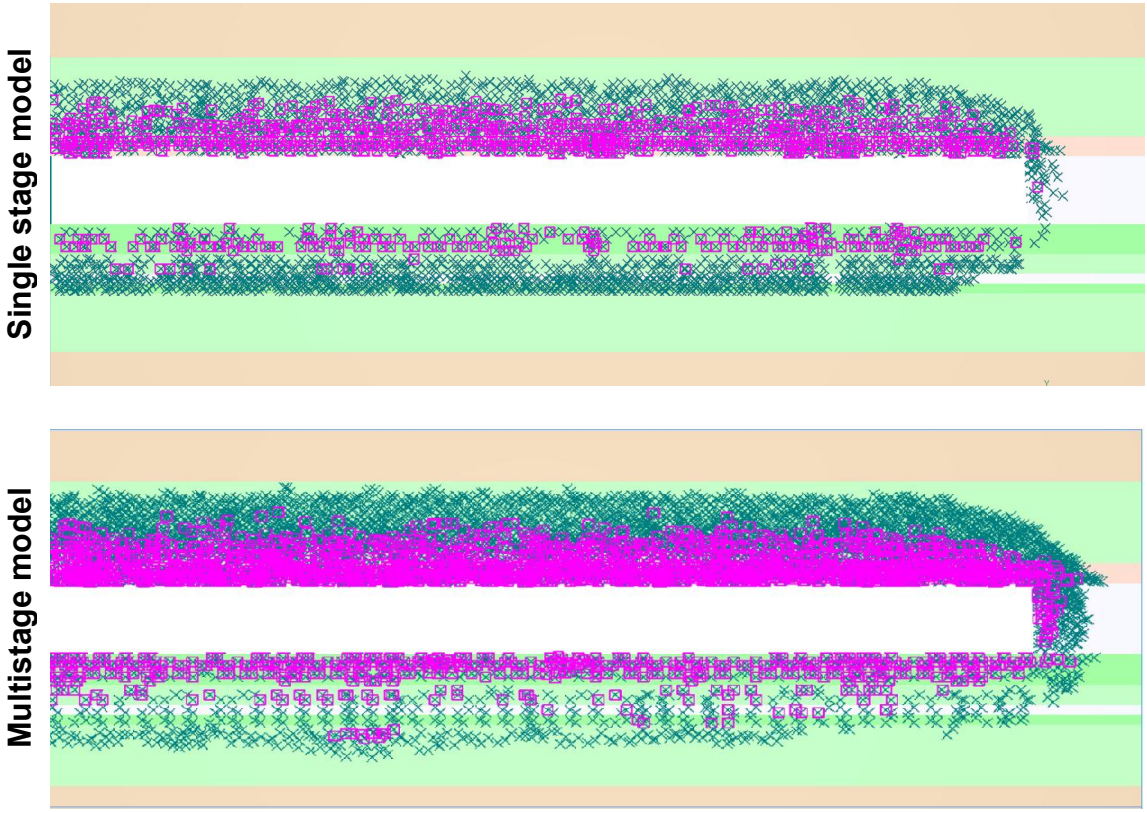

Figure 26: comparison of single stage and multistage analysis

Having discussed about the benefits of a conducting a multistage analysis to predict the yield zone realistically, it is important to look at the longitudinal displacement profile (LDP) given by both single and multistage models. Figure 27 clearly demonstrates that the magnitude of LDP given by a single stage model is much lower

than the LPP from a multistage model. This is in accordance with the predictions of Pan and Hudson (1988), in which it is proved that displacement profile from a 3D analysis will show relatively larger displacements. Engineering community is well aware of this drawback while using a 2D analysis for a three dimensional problem and it is circumvented, by using core softening method (Vlachopoulos and Diederichs (2009)). Chapter 7 demonstrates the usefulness of full 3D analysis to predict the field displacements in North Selby Complex. It is a well-known fact in the rock mechanics community that around 1/3rd of the total displacements will occur before the tunnel is excavated, which we could observe in the model. For both the single and multistage models some displacements have already occurred at the tunnel face itself.

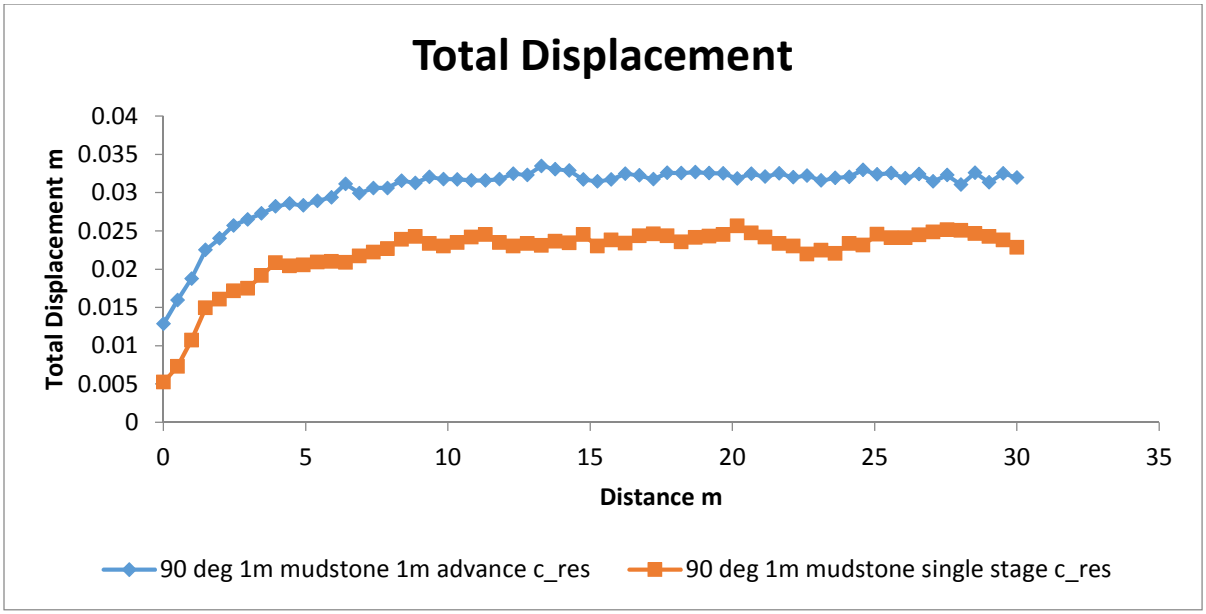

Figure 27: Displacement profile for single stage vs. multistage excavation

7.2 Conclusion

The modelling confirms that a multistage 3D analysis provides a more realistic field representation of yield zone and longitudinal displacement profile. It shows the importance of following the true stress path represented during actual excavation. Results will be drastically different if a comparison is made between a single stage excavation and a multistage excavation. This confirms the research done in the past (Meyer (2002); (Vlachopoulos and Diederichs, 2009); Cai (2008); Vlachopoulos and Diederichs (2014)).

8 Excavation of continuous coal mine roadway

Chapter 7 explained the importance of sequential numerical modelling for realistic prediction of the damage for a coal mine road way. In this chapter, detailed sequential modelling is done for coal mine roadways on varying high horizontal stress conditions. The analysis is then extended for varying the thickness of weak mudstone layer in the immediate roof. The model also incorporates typical roof bolting practice which is normally adopted for UK coal mine roadways.

The parameters used for modelling were the same as used in previous chapters. The models are made more realistic by adopting a typical roof bolting pattern which is used in UK coal mines. Typical bolt parameters adopted for the model can be found on Table 4. Installing the bolt very close to the tunnel face will induce significant amount of loading on the bolt and causes failure, installing it too far from the face will not serve the purpose since, most of the displacements would have happened and the bolt will not take any load. Two dimensional programs cannot model this phenomenon explicitly and simple 2D models will show unrealistic substantial loading on the bolt installations.

8.1 Bolted sequential model

For the model the bolt is installed 3m behind the tunnel face, which is a reasonable assumption for an underground excavation. A customized denser mesh is adopted around the excavation to capture the essential details.

Table 4: Bolt parameters adopted for modelling (after Meyer (2002))

Property	Parameter
Bolt model	Fully Bonded
Bolt diameter (mm)	22
Young's modulus (MPa)	205000
Tensile Capacity (MPa)	0.254
Residual Tensile Capacity(MPa)	0.254
Length of bolt(m)	2.4
Out of plane spacing (m)	1
In plane spacing (m)	0.833

A half symmetrical model could be used for stress parallel and stress perpendicular situations but for uniformity, all the five variants adopted the full scale model.

8.2 Results of analysis

Analysis is carried out for three different lithological formations. First one in the series consists of immediate roof layer having 3m of weak mudstone, second one with a 2m thick layer of weak mudstone and the third one having only 1m thick mudstone. For all the lithological formations a competent strata is assumed 5m above the roof and gap between weak mudstone layer and competent strata consists of a competent mudstone layer. For each lithological formation maximum horizontal stress orientation is varied from 90 to 0 degree.

8.2.1 Lithology with 3m thick weak mudstone layer

As explained in the previous paragraph the modelled lithology consists of 3m thick band of weak mudstone layer on tunnel roof. For more clarity the modelled lithology is illustrated in Figure 28

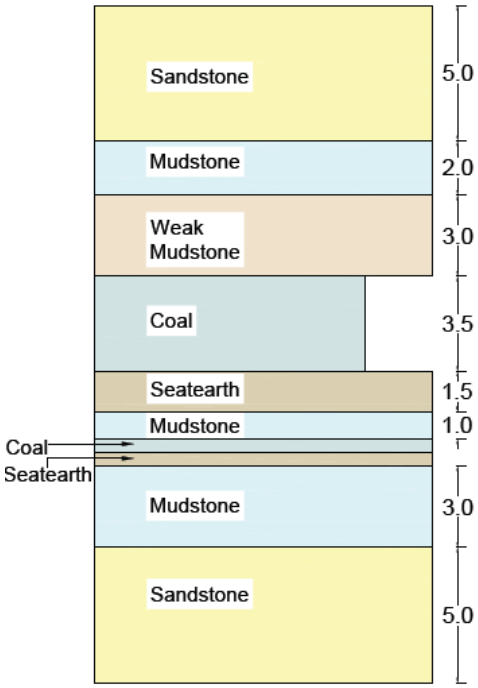

Figure 28: Modelled Lithology 3m thick mudstone on tunnel roof

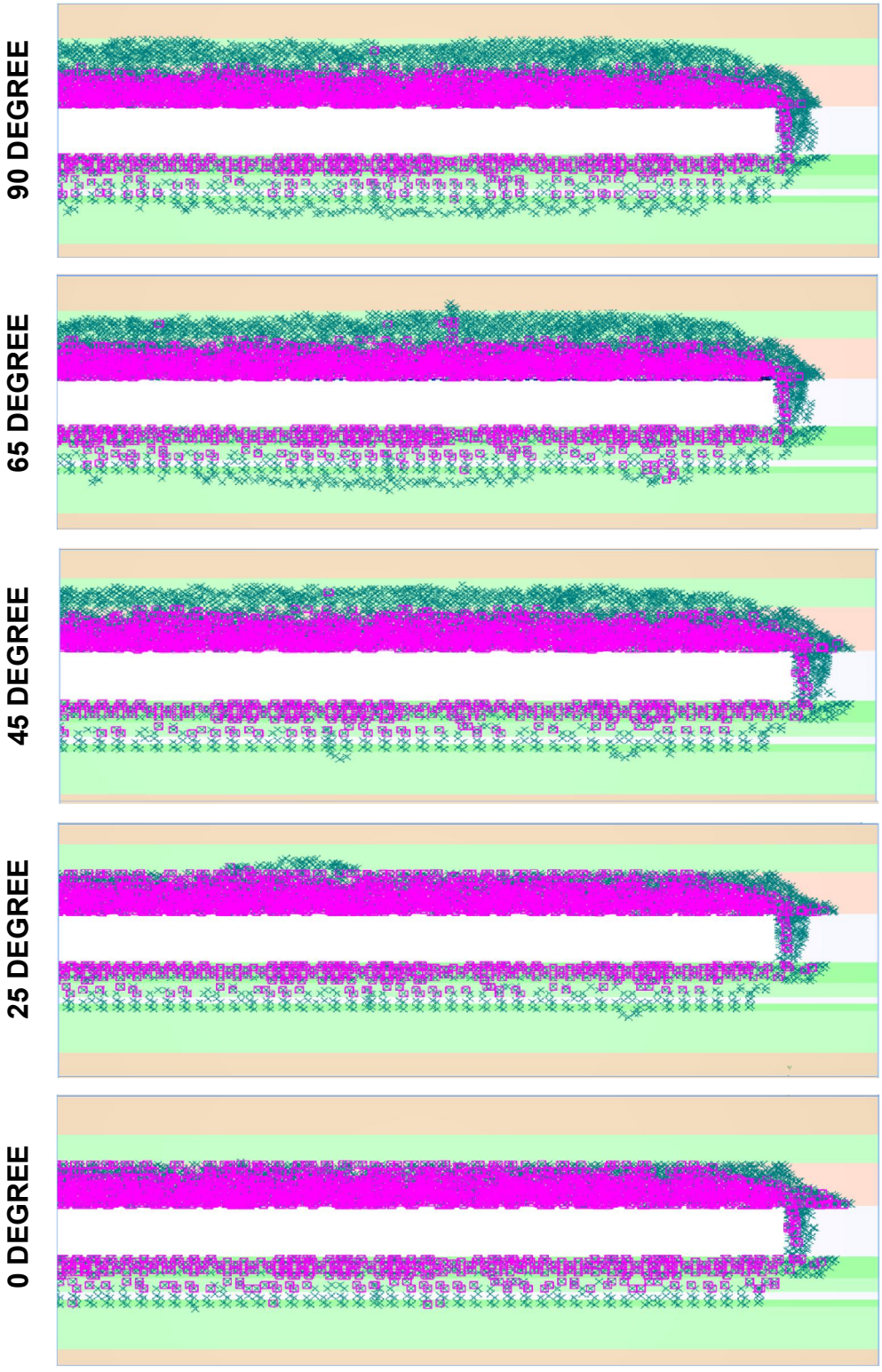

Figure 29: Yield pattern for stress orientation varying from 90 to 0 degree for 3m thick weak mudstone layer on roof

For illustrating the change in yield zone due to varying horizontal stress orientation, a longitudinal section is cut along the axis of the tunnel along the center line. From Figure 29 it can be clearly established that, stress perpendicular case is causing much more damage to the strata when compared to stress parallel case, increasing the angle from 0 to 90 degree shows a gradual increase of zone of distress with maximum damage occuring at stress perpendicular case. For stress parallel case the plastic zone is not able to break the relatively competent mudstone strata, where as for the stress perpendicular case, the yield zone extends upto 5m above the roof strata and further spread is restricted by a competent siltstone layer.

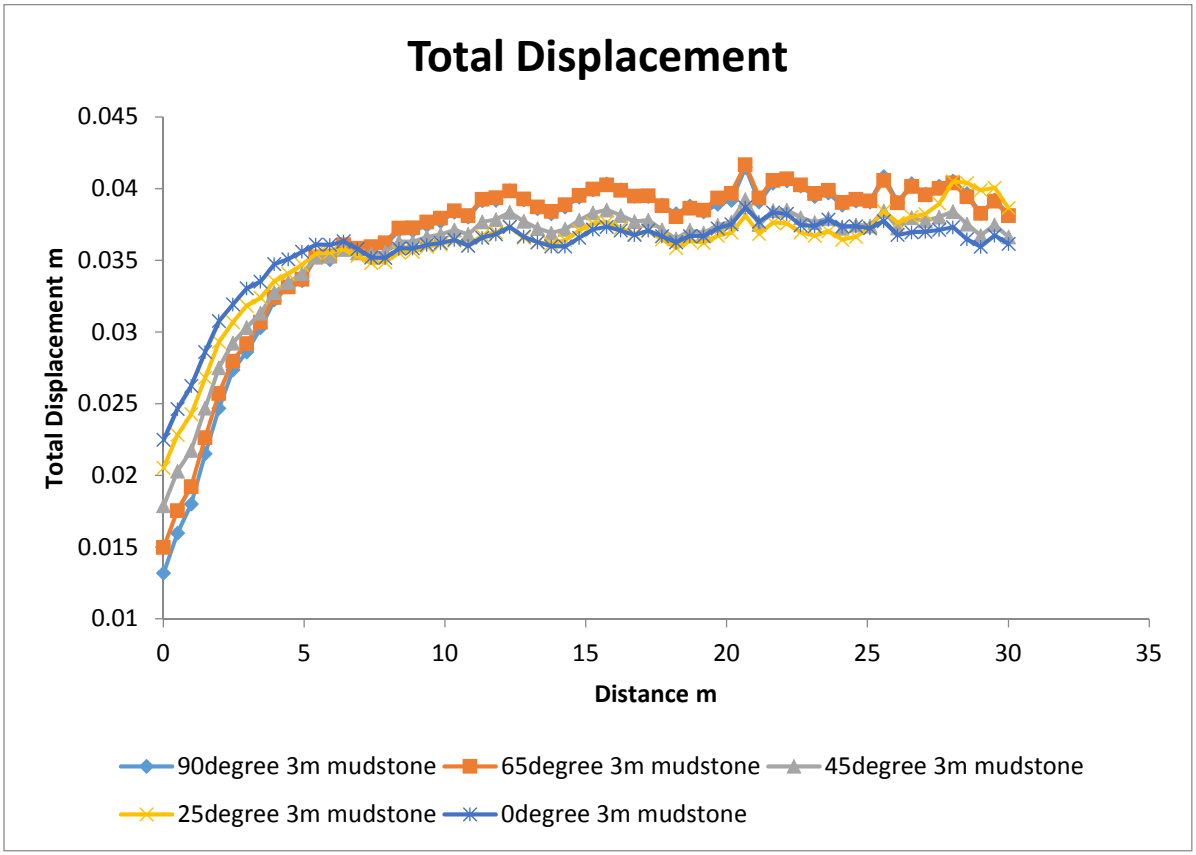

Figure 30: Longitudinal displacement profile for 3m mudstone layer on tunnel roof

Figure 30 highlights the longitudinal displacement profile(LDP) for varying stress orientations, LDP is drawn starting from the tunnel face and extending to atleast 5times the tunnel width where it can be safely assumed that all the displacements might have occured and the conditions are plane strain.

From the graph one may tend to jump into the conclusion that, there is no significant change in displacement for various stress orientations. But it has to be noted that magnitude of initial displacements at the tunnel face is varying for different stress orientations. The initial displacements at the tunnel face is significantly less for stress perpendicular condition than stress parallel condition. Field observations at site clearly shows an increase in magnitude when orientation is changed from stress parallel to stress perpendicular condition (Kent et al. (1998)).

The extensometers installed at site could measure only the relative displacement, it depends on the location at which it is installed from the tunnel face and the distance at which the measurements are read and it cannot give the absolute displacements as what is shown in the Figure 30. If one need to get an absolute displacement profile as shown in the graph, the only possibility is to install borehole extensometers ahead of tunnel face to measure the displacements from absolute zero which is not

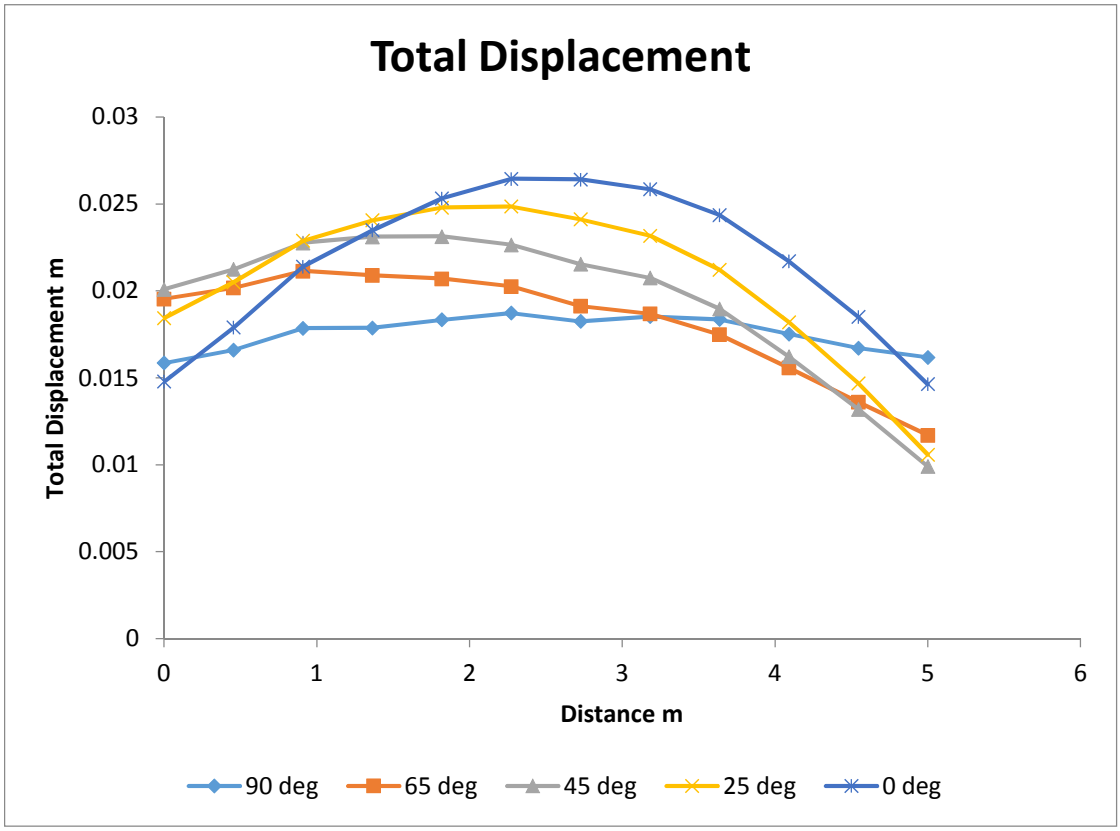

Figure 31: Displacement profile across the tunnel section 1m away from the face

normally done in practice.

Figure 31 shows the displacement profile of roof across the tunnel cross section (i.e. the displacement from side wall to side wall) 1m away from the tunnel face. The graph compares the displacement variation for the stress orientations changing from 0 to 90 degree. It is evident from the graph that for stress parallel and stress perpendicular case the displacement profile is symmetrical, the stress parallel is showing a much steeper curve than that of stress perpendicular orientation. Tunnels driven at an angle to the high stress suffers an asymmetrical displacement, as shown in the graph. This type of deformation called “guttering” is well documented in literature (Coggan et al. (2012); Clifford (2004)).

8.2.2 Lithology with 2m thick weak mudstone roof

Previous sections showed the effect of stress rotation on plastic deformation, longitudinal displacement profile and asymmetrical deformation across the tunnel for 3m mudstone. The analysis clearly shows that the stress orientation is having a significant impact on the plastic zone, thus increasing the demand for support requirements for stability. Plastic zones in all the cases completely engulf the tunnel face.

In this section, analysis is repeated by reducing the immediate weak mudstone thickness to 2m keeping all other parameters intact. The trend is consistent with the previous analysis. Plastic zones for stress perpendicular case is much larger than that of stress parallel case. For stress parallel case, unlike the previous case, the yielded elements extend into the stronger mudstone strata.

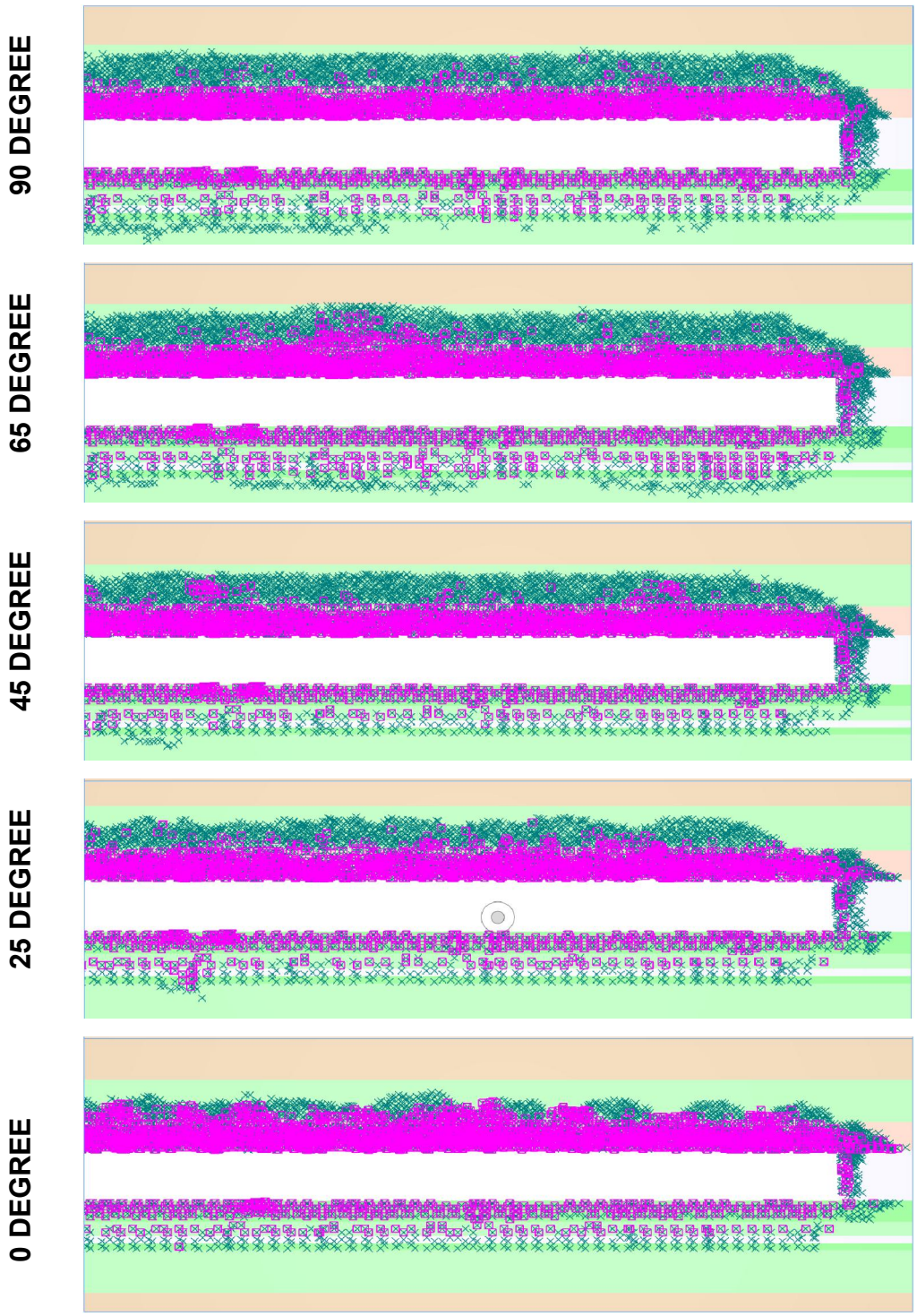

Figure 32: : Yield pattern for stress orientation varying from 90 to 0 degree for 2m thick weak mudstone layer on roof

The longitudinal displacement profile of 2m mudstone layer in Figure 33 follows the same trend like in 3m mudstone. Stress parallel condition shows a large displacement at the tunnel face and the rate of increase diminishes quickly when compared to stress perpendicular case. Even though there is no significant difference between absolute displacements at the end, the stress perpendicular condition do show a marginal increase in the displacements compared to stress parallel one. It is also visible that all the displacements already happened within a distance of approximately two times the width of the tunnel and after this the tunnel comes into a stable state. It implies that lining installed at a distance two tunnel widths away from the face will not take any load if creep effects are neglected.

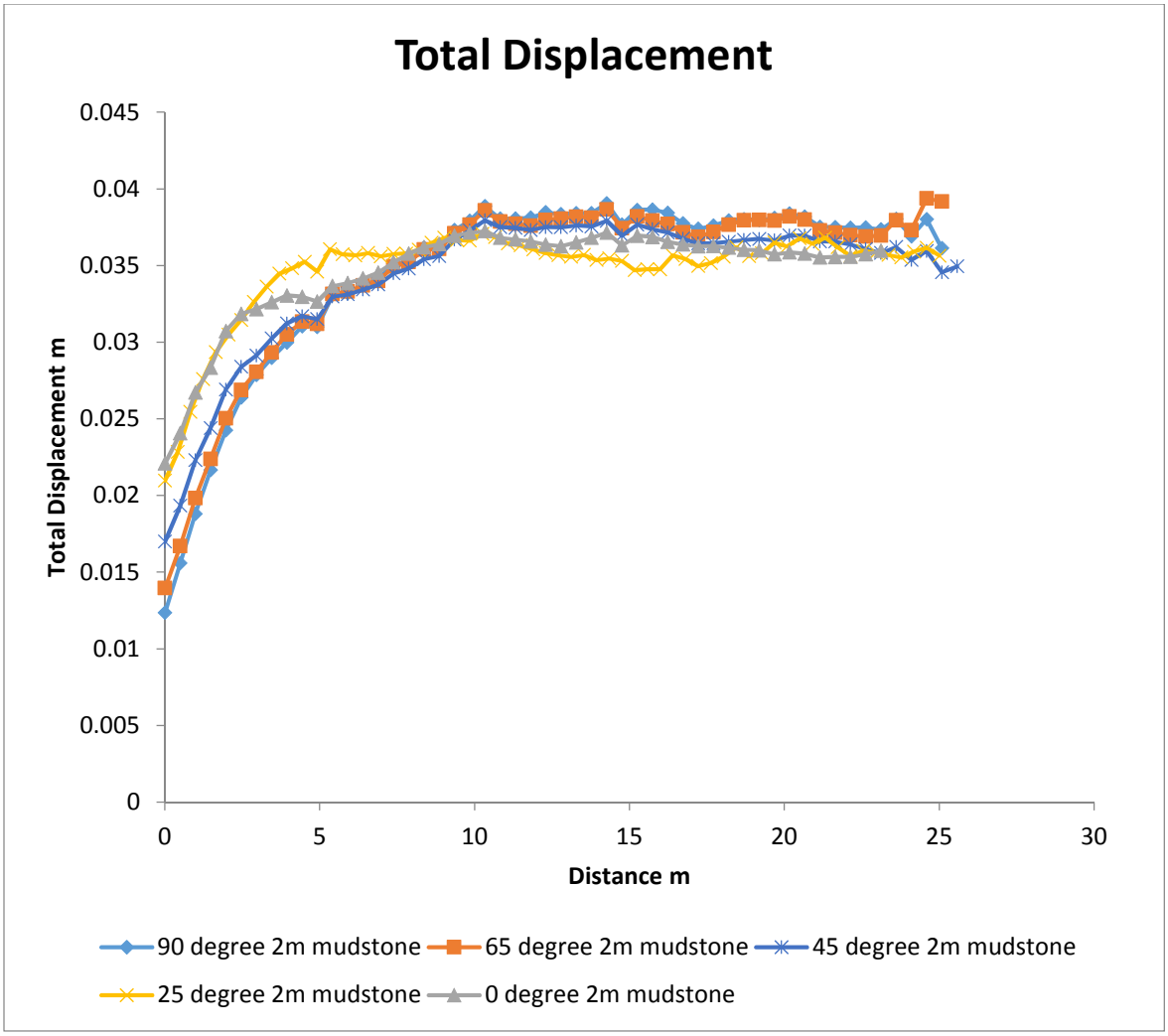

Figure 33: Longitudinal displacement profile for 2m mudstone layer on tunnel roof

Figure 34 shows the displacement across the tunnel 1m away from the tunnel face, the predictions are quite similar to what was predicted for 3m thick mudstone. Asymmetrical behaviour can be observed for stress at an angle and for stress parallel and perpendicular case the behaviour is symmetrical.

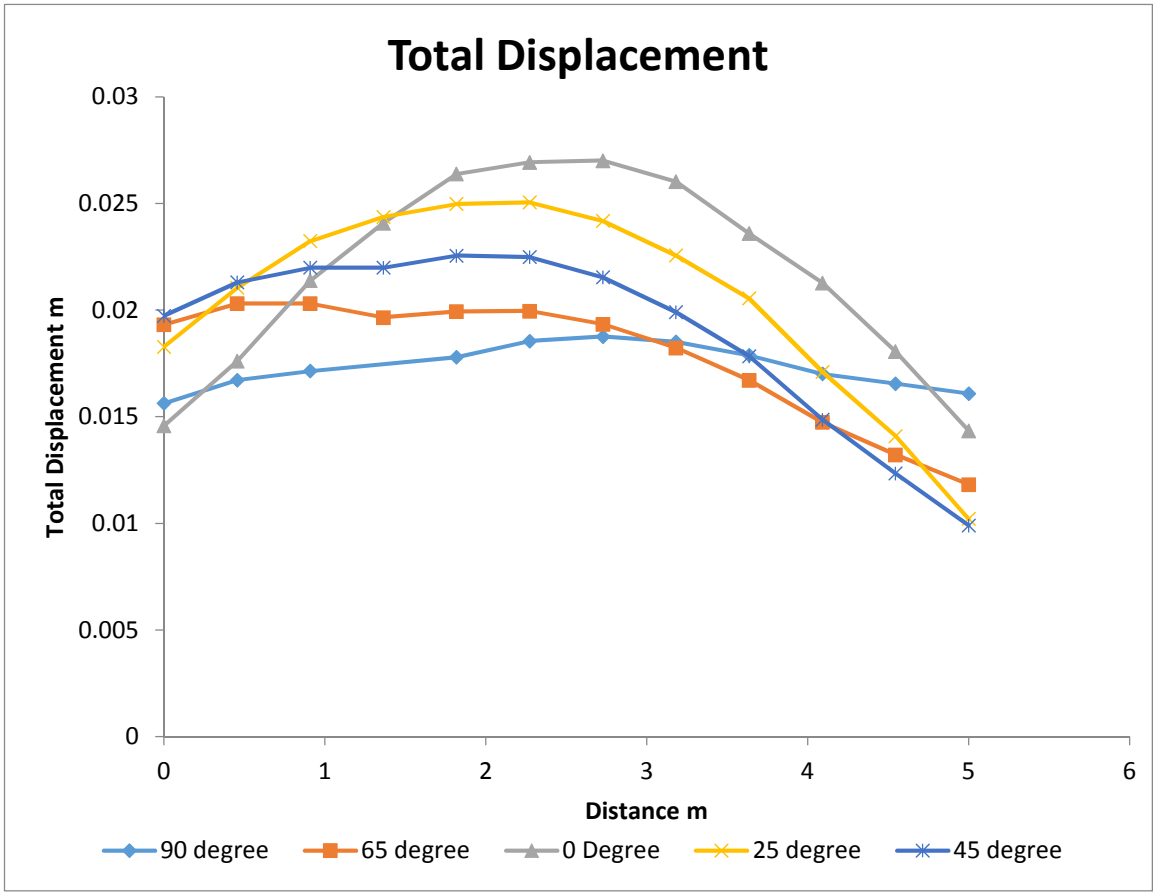

Figure 34: 2m mudstone 1m away from tunnel face

8.2.3 Lithology with 1m thick weak mudstone roof

In this section the thickness of weak mudstone roof is again reduced to 1m and the model was analysed for differing stress orientations. Since the thickness of weak strata is further reduced a reduction in damage zone is expected. The analysis confirms that there is overall reduction in the absolute displacements than from section 8.2.1 and section 8.2.2. The predicted yield along the tunnel centre line is illustrated in Figure 35.

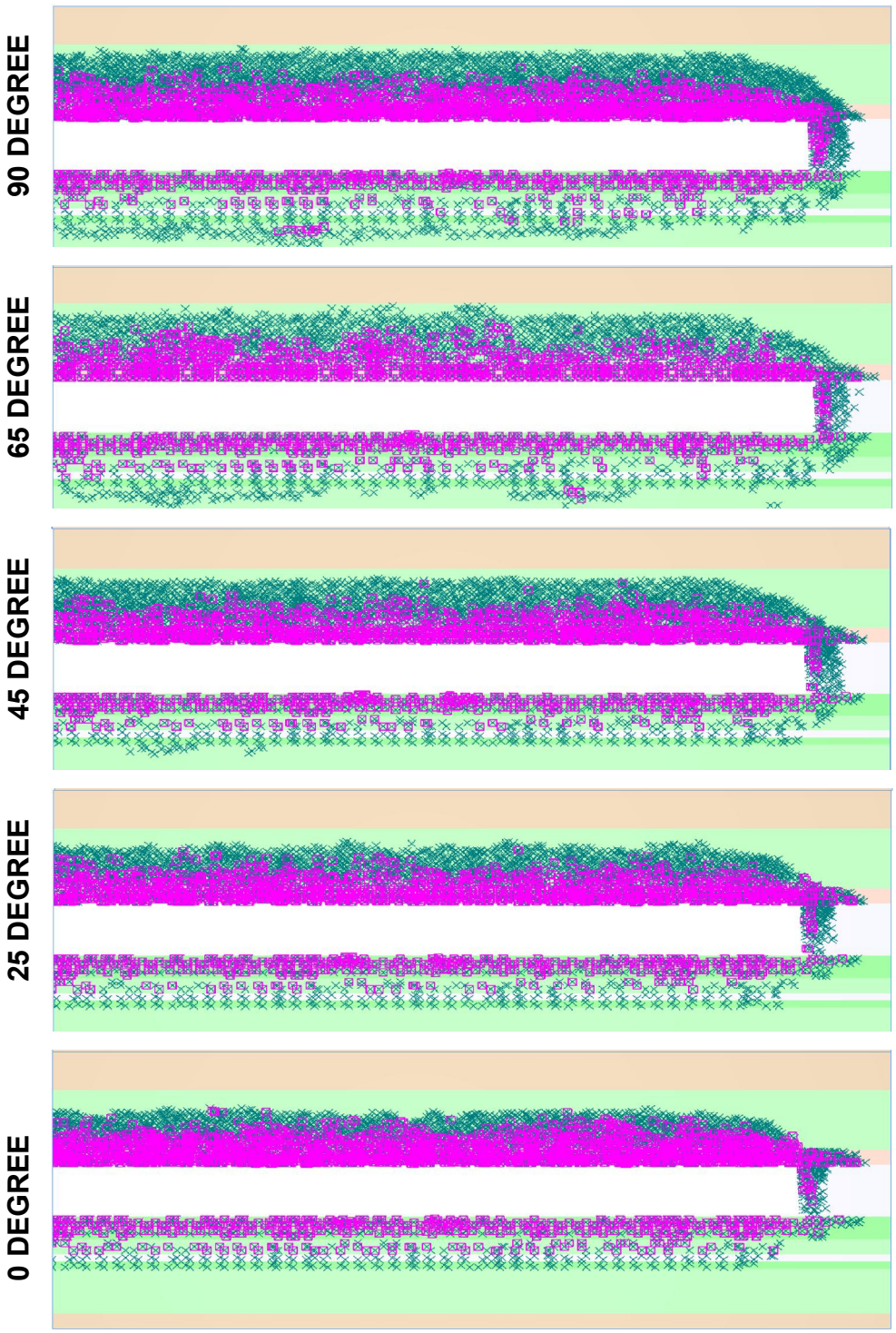

Figure 35: Yield pattern for stress orientation varying from 90 to 0 degree for 1m thick weak mudstone layer on roof

The magnitude of displacements are lower when compared to 3m and 2m thick mudstone which is shown in Figure 36. The initial displacements at the tunnel face is larger in case of stress parallel. Displacement profile is showing a tendency to reach plane strain conditions slightly earlier when compared to other cases. The curve is flatter well before reaching even twice the diameter of the tunnel, demanding early application of the supporting system.

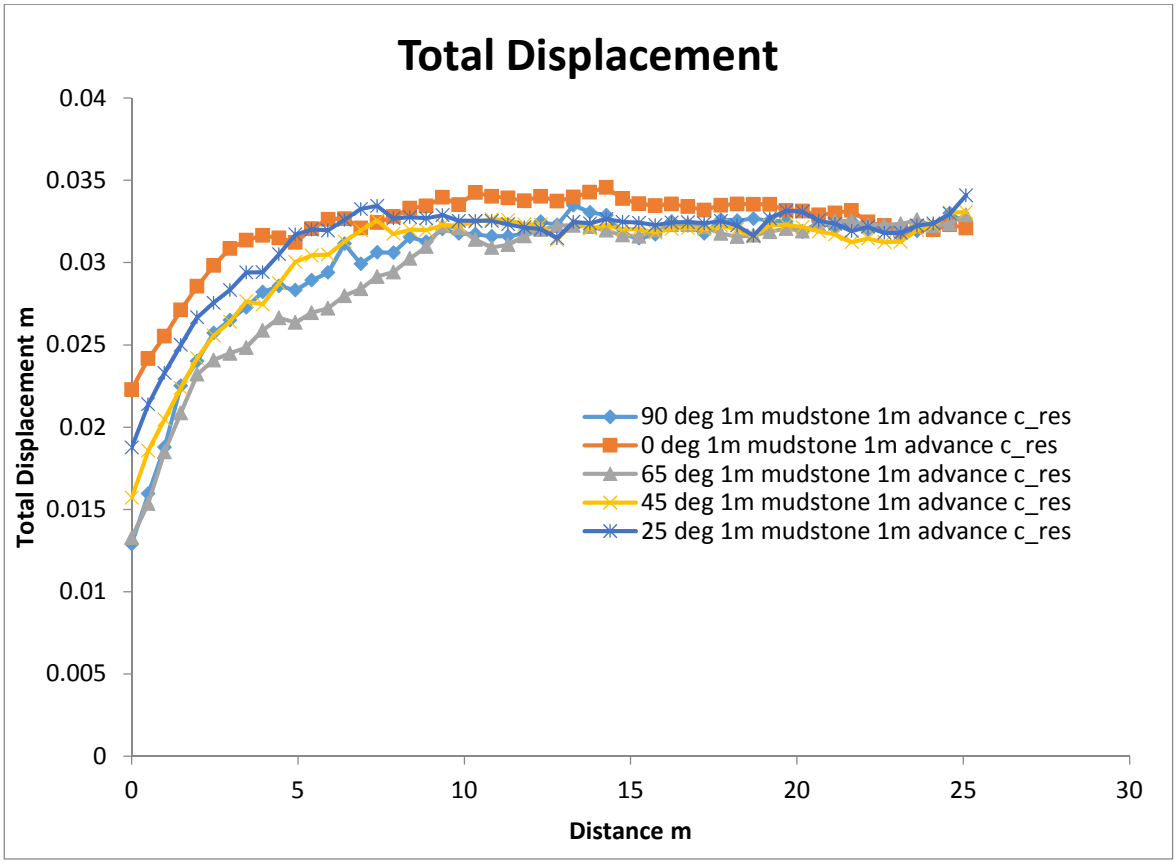

Figure 36: Longitudinal displacement profile of 1m thick mudstone coal mine roadway

Figure 37 shows the displacement profile across the tunnel, which highlights the same behaviour pattern for 3m and 2m thick models. As expected asymmetrical displacement profiles are visible for stress at an angle.

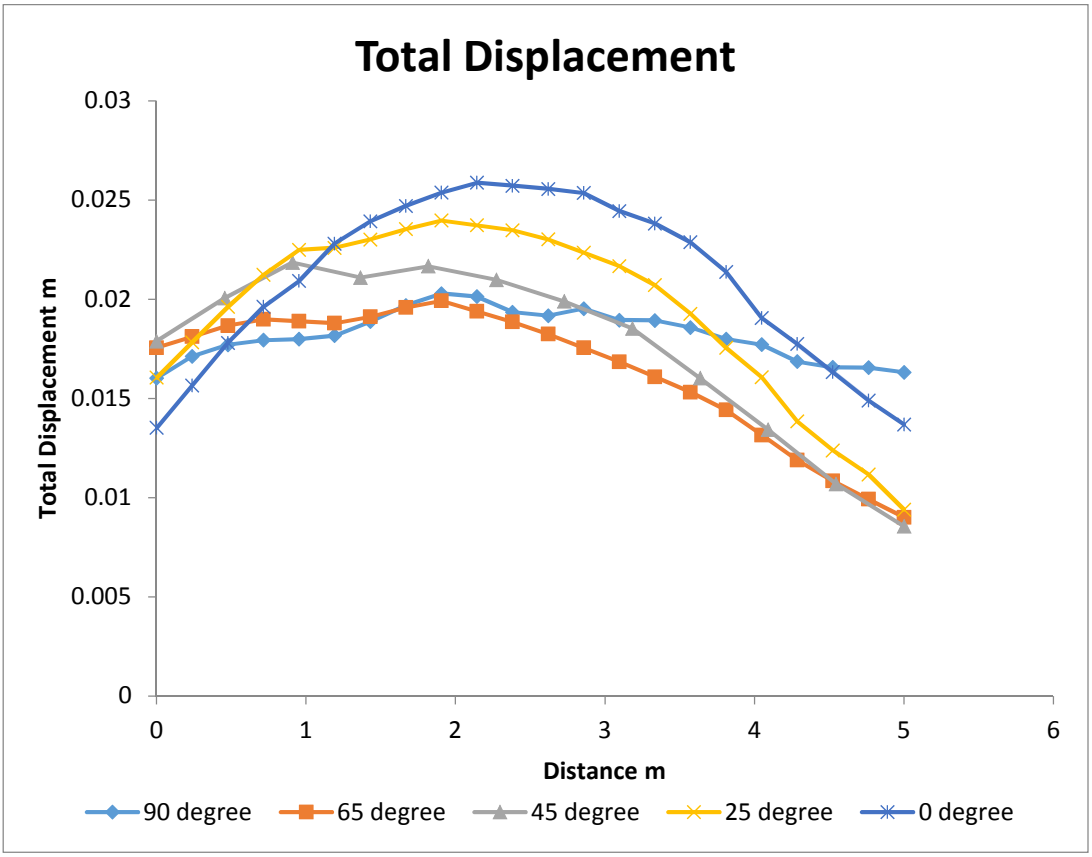

Figure 37: Displacement across the tunnel 1m away from the tunnel face

8.3 Validation of Field Data

Numerical models need to be validated with field measurements to ensure that the results are realistic. If there are large variations in the result, the model needs to be recalibrated by rechecking the critical parameters and the modelling assumptions. The field measurement presented here is from North Selby Complex (Meyer (2002)). The roof extensometers are installed 1m away from the tunnel face and read three tunnel diameters away from the face where plane strain conditions are prevailing. Both field measurements and modelled displacements from RS^3 are showing reasonable similarity in results. It is evident from the readings that the stress perpendicular condition sustained considerable deformation when compared to the stress parallel case.

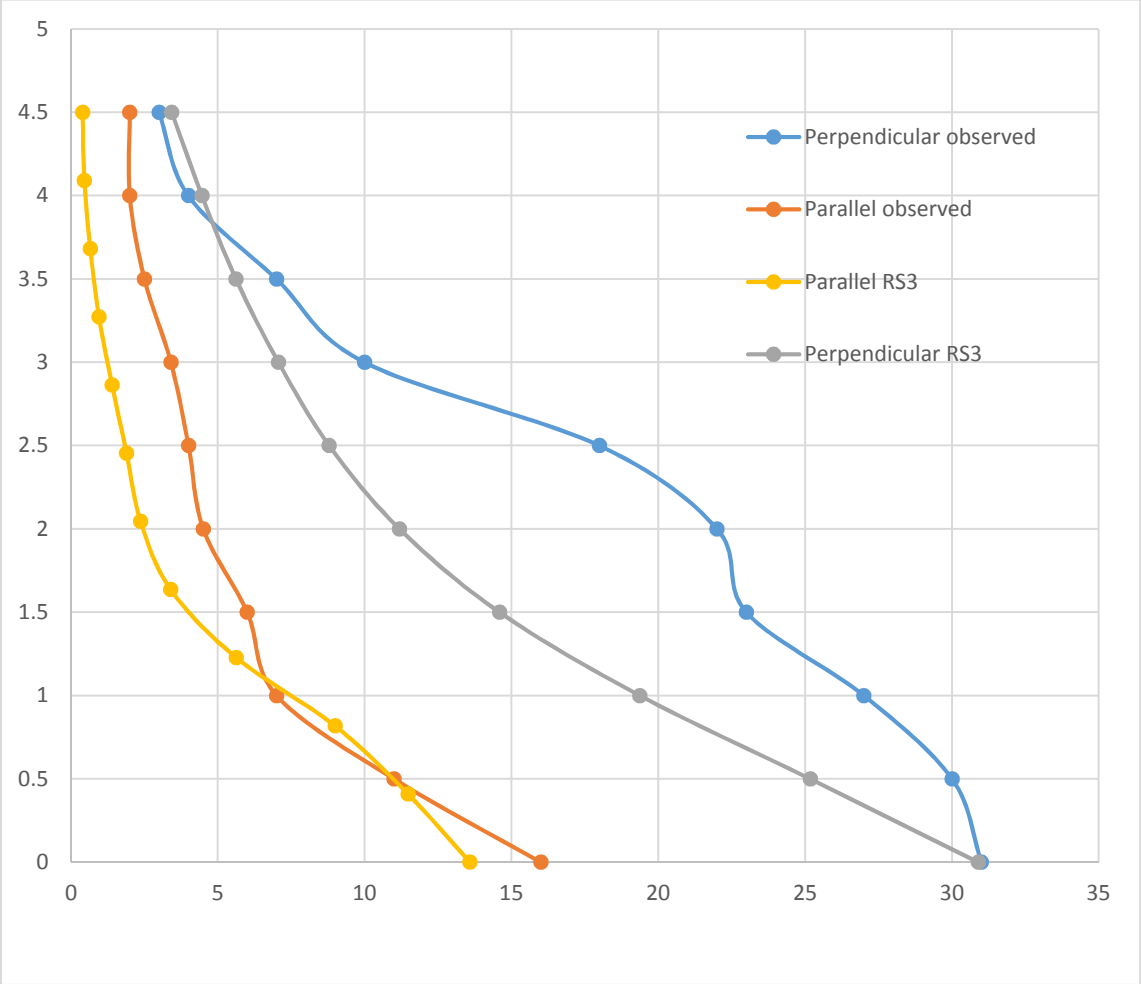

Figure 38: Modelled extensometer measurements in RS³ compared to field measurements

8.4 Impact of varying mudstone layer thickness on displacement profiles

Figure 39 and Figure 40 illustrate the longitudinal displacement profiles of different mudstone thicknesses for stress perpendicular and stress parallel situation respectively. The magnitude of displacement is highest for 3m weak mudstone followed by 2m and 1m mudstones. The trend is similar for stress perpendicular and stress parallel situation but the magnitude of displacements are higher for stress perpendicular results.

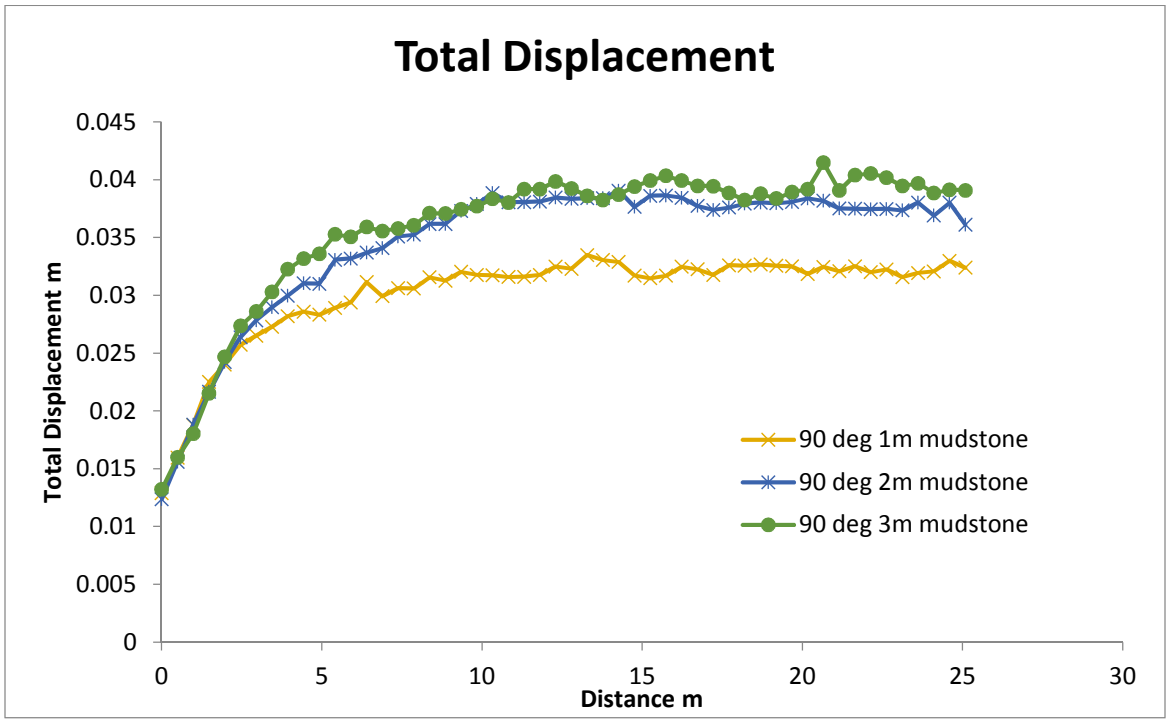

Figure 39: Longitudinal displacement profile for stress perpendicular condition for 1m, 2m and 3m mudstone

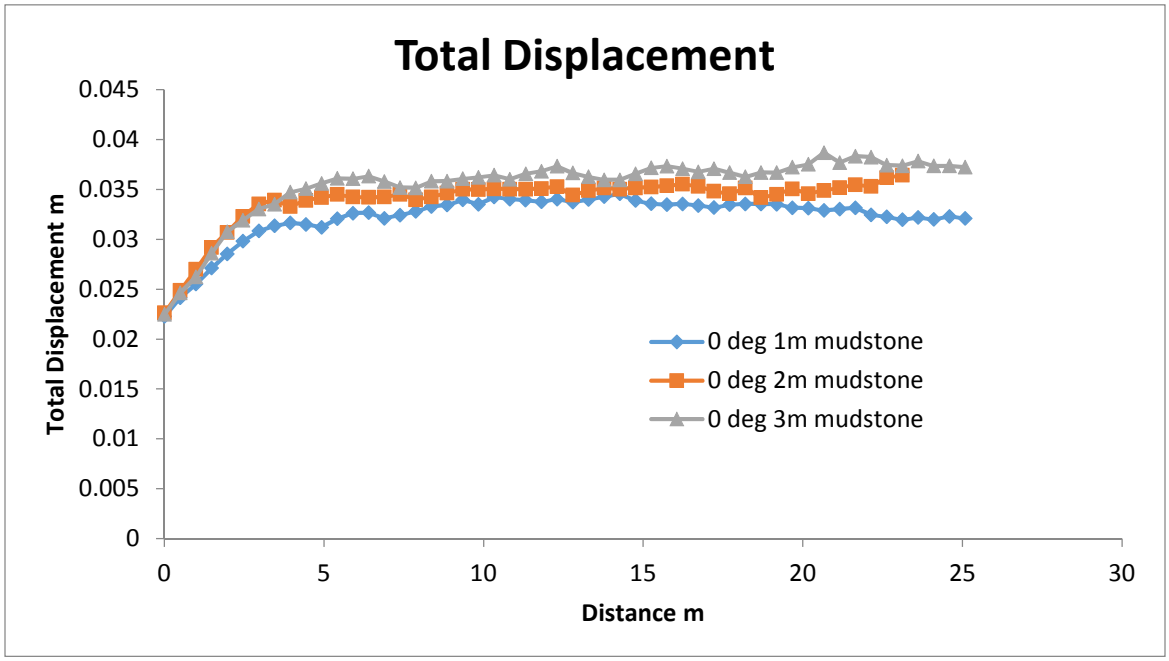

Figure 40: Longitudinal displacement profile for stress parallel condition for 1m, 2m and 3m mudstone

8.5 Bolt forces

Figures 41 to 49 display the forces acting on the bolt in plane strain condition on stress parallel, stress perpendicular and stress at an angle of 65^{o}, for 1m, 2m and 3m weak layer of mudstone respectively. Each bar chart represents 7 number of bolts across the tunnel and is colour coded for yielded and non-yielded part. Point at which the bolt forces reached 0.1MN from top, is shown and is connected using a linear plot across the bar chart.

Moving from stress perpendicular to stress parallel condition clearly shows a decrease in yielding and bolt forces. An asymmetrical distribution of bolt forces was expected for stresses at an angle, but it was not very evident from the chart, it may be due to normalisation of stresses and displacements at plane strain conditions. Moving from mudstone thickness of 1m to 3m clearly shows increase in modelled yielding and forces on the roof bolts.

For 1m mudstone stress parallel case there is practically no yielding on the bolts whereas in stress perpendicular case almost a third of the bolt has yielded. There is no yielding of the bolt at both extreme ends showing very low forces at the corner bolts. For 2m and 3m mudstone more than two thirds of the bolt portion yielded, bolts at corners were also experiencing significantly large forces.

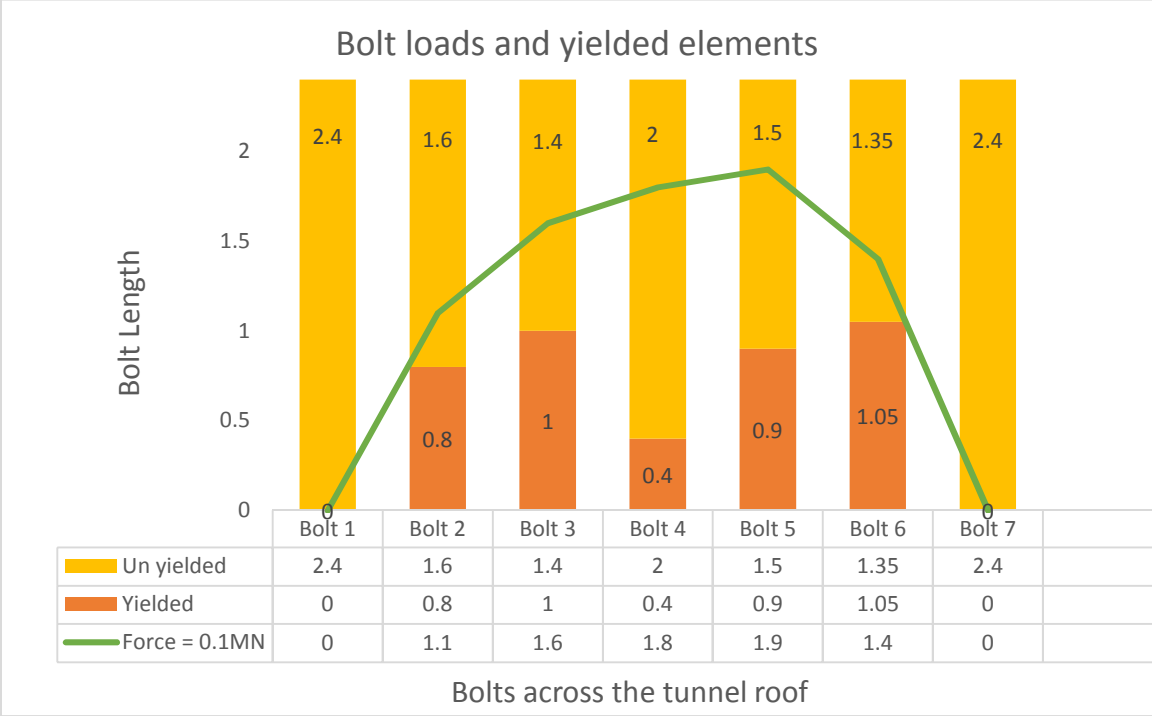

Figure 41: Bolts loads and yielded elements for 1m mudstone stress perpendicular case across the tunnel on plain strain condition

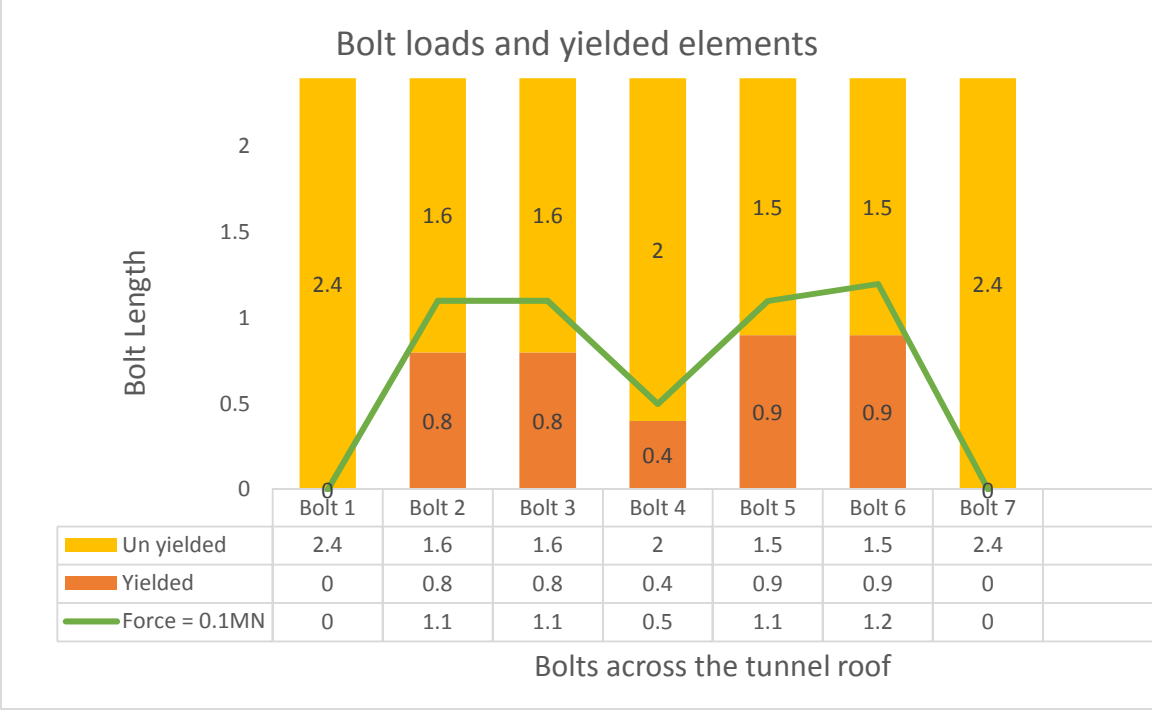

Figure 42: Bolts loads and yielded elements for 1m mudstone stress at 65 degreesacross the tunnel on plain strain condition

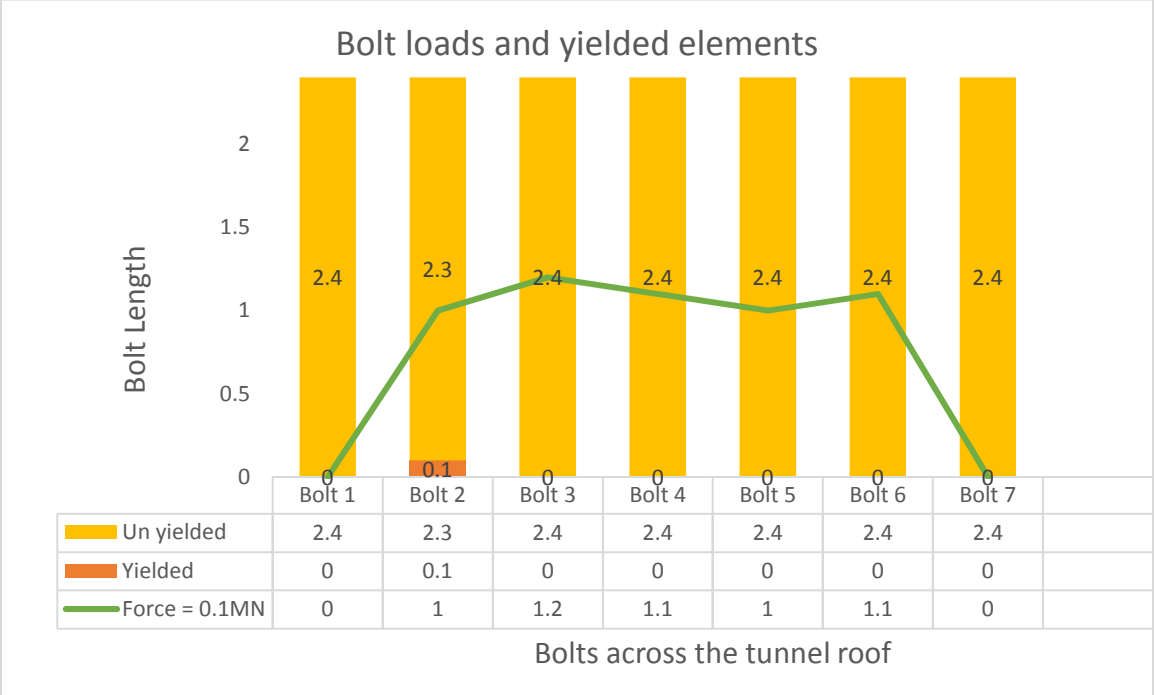

Figure 43: Bolts loads and yielded elements for 1m mudstone stress parallel case across the tunnel on plain strain condition

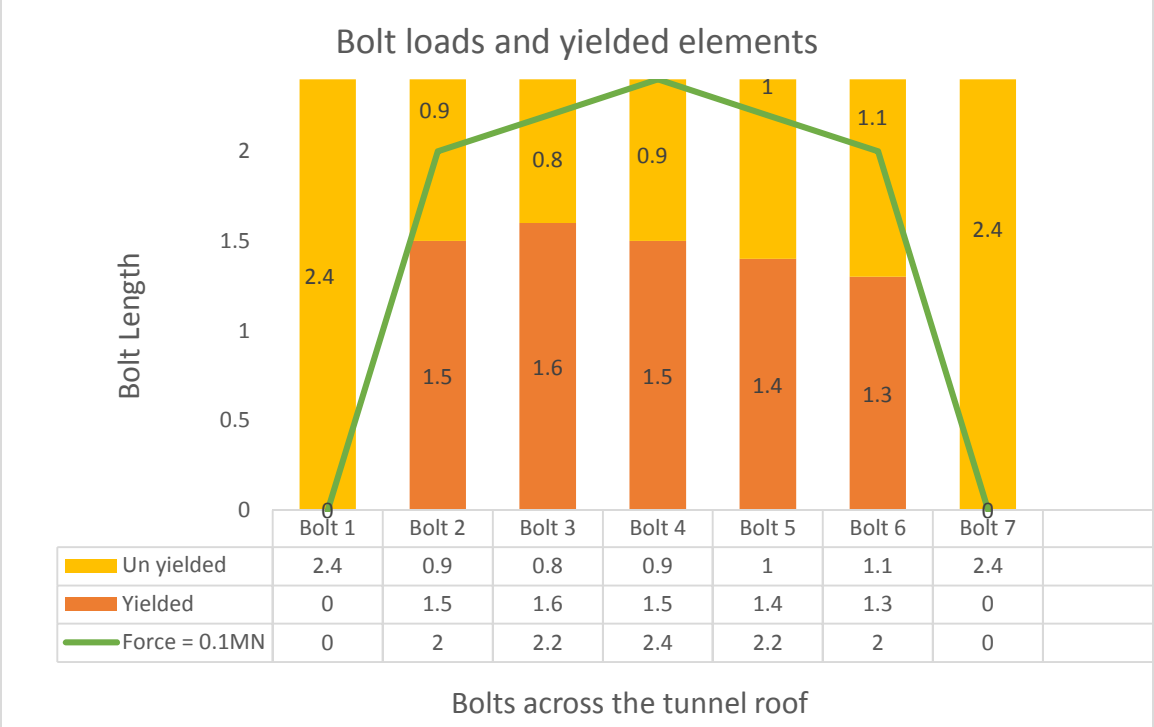

Figure 44: Bolts loads and yielded elements for 2m mudstone stress perpendicular case across the tunnel on plain strain condition

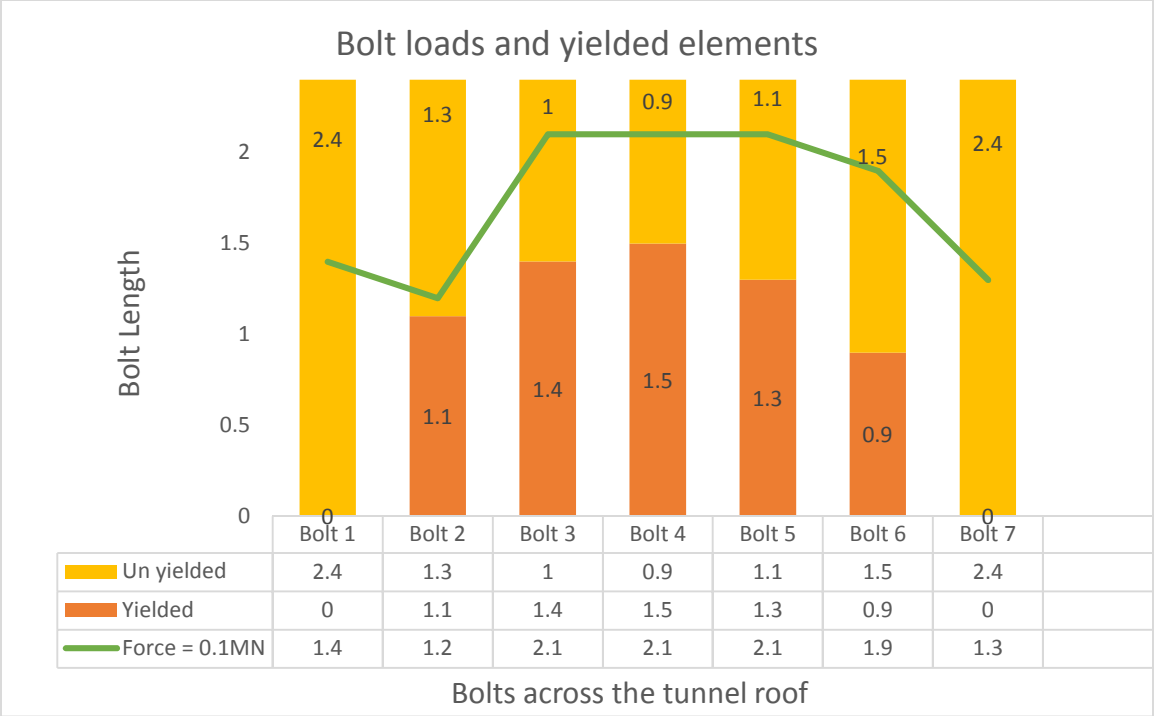

Figure 45: Bolts loads and yielded elements for 2m mudstone stress at 65degree across the tunnel on plain strain condition

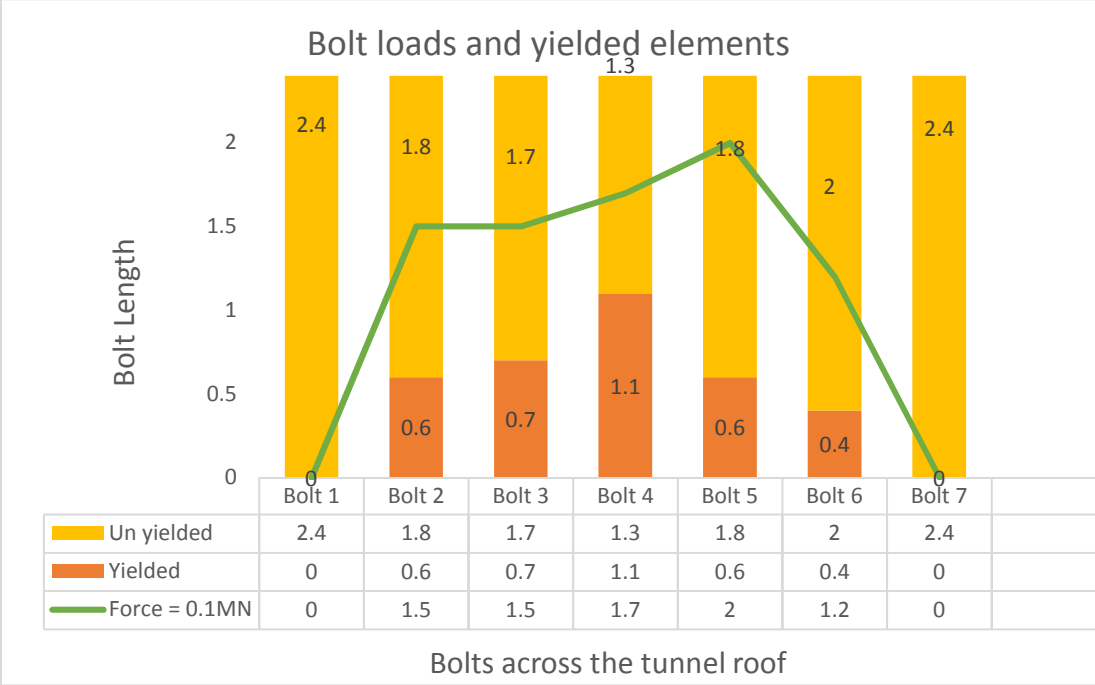

Figure 46: Bolts loads and yielded elements for 2m mudstone stress parallel condition across the tunnel on plain strain condition

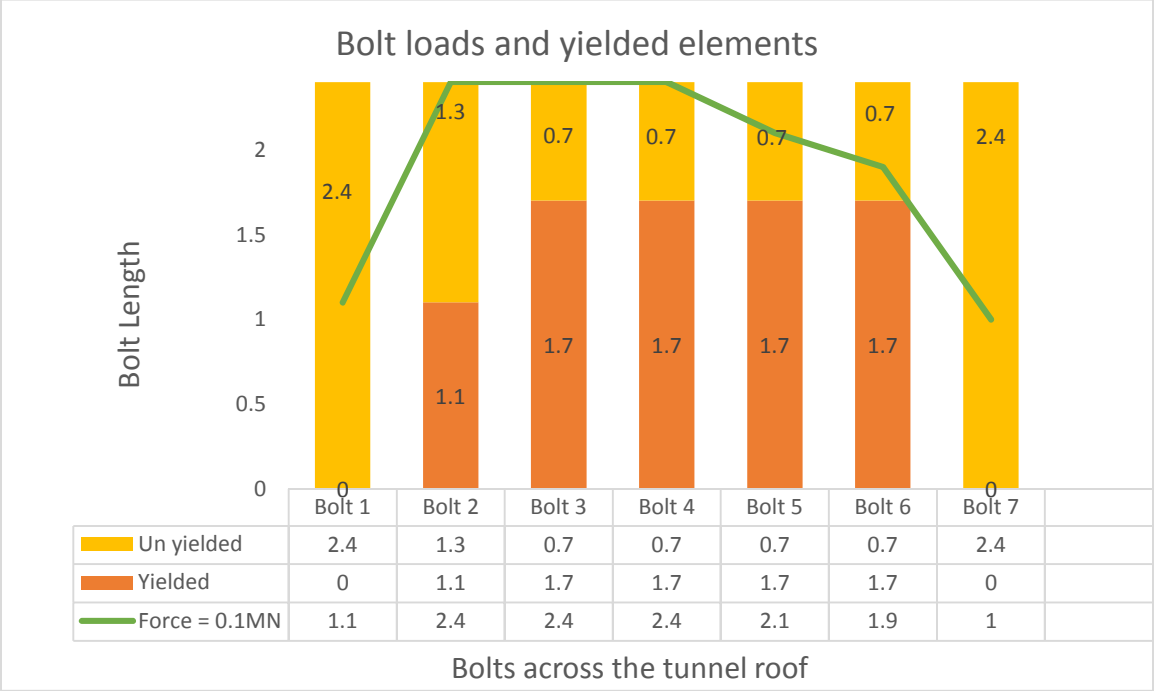

Figure 47: Bolts loads and yielded elements for 3m mudstone stress perpendicular case across the tunnel on plain strain condition

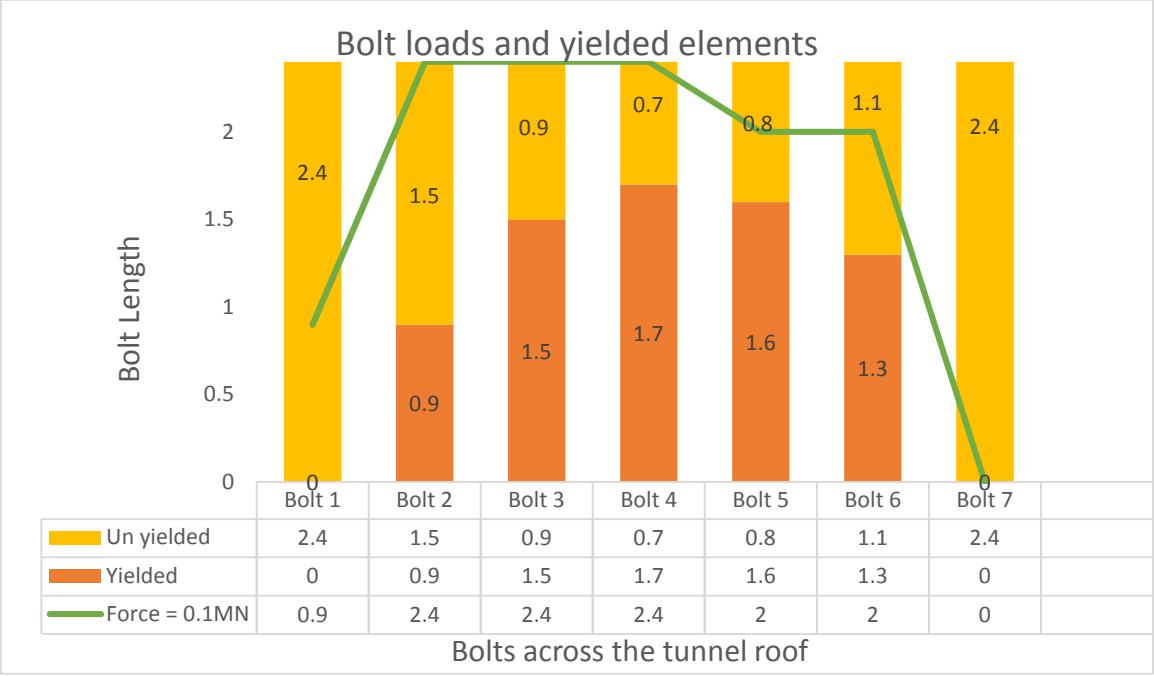

Figure 48: Bolts loads and yielded elements for 3m mudstone stress at 65 degrees across the tunnel on plain strain condition

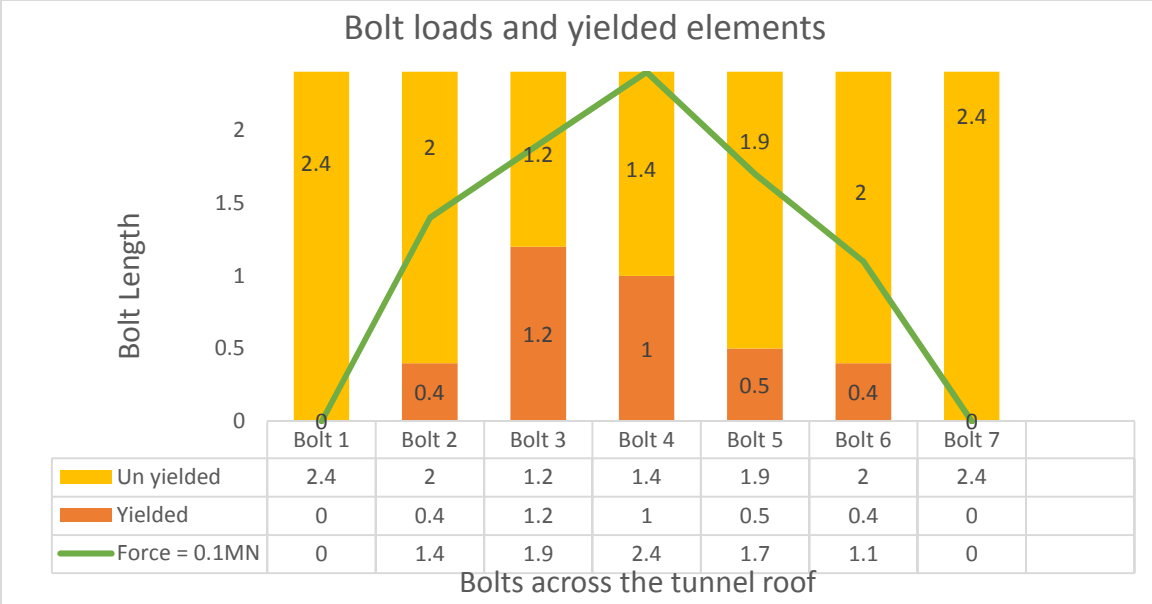

Figure 49: Bolts loads and yielded elements for 3m mudstone stress parallel case across the tunnel on plain strain condition

8.6 Conclusion

The chapter analysed and presented the results of modelled damage due to varying horizontal stress orientations. The results were in agreement with field observations. To summarise, in general an increase in stress damage and yield zones, could be observed moving from stress parallel to stress perpendicular condition. The same is the case for longitudinal displacement profile; higher magnitudes of relative displacements could be observed for stress perpendicular case. The analysis conducted shows that there is no significant variation in absolute displacements when moving from stress parallel to stress perpendicular condition, but the displacements already occurred at the tunnel face significantly varies for stress parallel and stress perpendicular condition.

Bolting load experienced for stress perpendicular condition is larger than stress parallel since the relative displacements occurring for stress perpendicular is much larger in magnitude. The trend is similar for 3m, 2m and 1m weak immediate roof layer mudstone. The spread of plastic zones and magnitude of displacements are comparatively lager for 3m weak layer of mudstone and smallest for 1m mudstone layer.

9 Three dimensional modelling of coal mine roadway junctions

Previous chapters investigated the effects of stress orientations on coal mine roadways driven in a linear path. This chapter looks at the effects of stress orientations at roadway junctions. The model created is consistent with the parameters used in chapter 6. At the tunnel end the roadway is turned at an angle of 90 degrees for 5 metres.

Analysis is run for horizontal stresses at angles 90degrees, 65 degrees, 45 degrees, 25 degrees and 0 degree to the tunnel direction. A cohesion weakening model is adopted as before which was proved to be effective in predicting the displacements in the field.

9.1 Results of the analysis

As explained before five models for varying stress angle were created and yield zones at point A as shown in the following figures were observed. The direction of maximum principal stress is shown with an arrow mark. The same legend is followed for all the results hence it is shown only on Figure 50.

The plane of observation shown in the figures are cut parallel and at the same level of tunnel roof. Two observation points A and B at the corner is selected and the variation in yield zones at this point of observation is discussed for the five stress orientations. Actual tunnel location in the plan is highlighted in a blue colour.

From the figures it is evident that stress perpendicular situation is creating maximum damage with its yield zone engulfing the whole tunnel alignment near its corner shown in Figure 50. Point “A” shows that, the damage is maximum for stress perpendicular progressively reducing to a minimum in stress parallel case. At the same time the inner corner Point “B” damage is much more in case of stress at an angle with maximum damage occurring for stress at 65 degrees. In all the cases the inner most corner which is opposite to point “B” is sustaining heavy damage for atleast a depth of 6m.

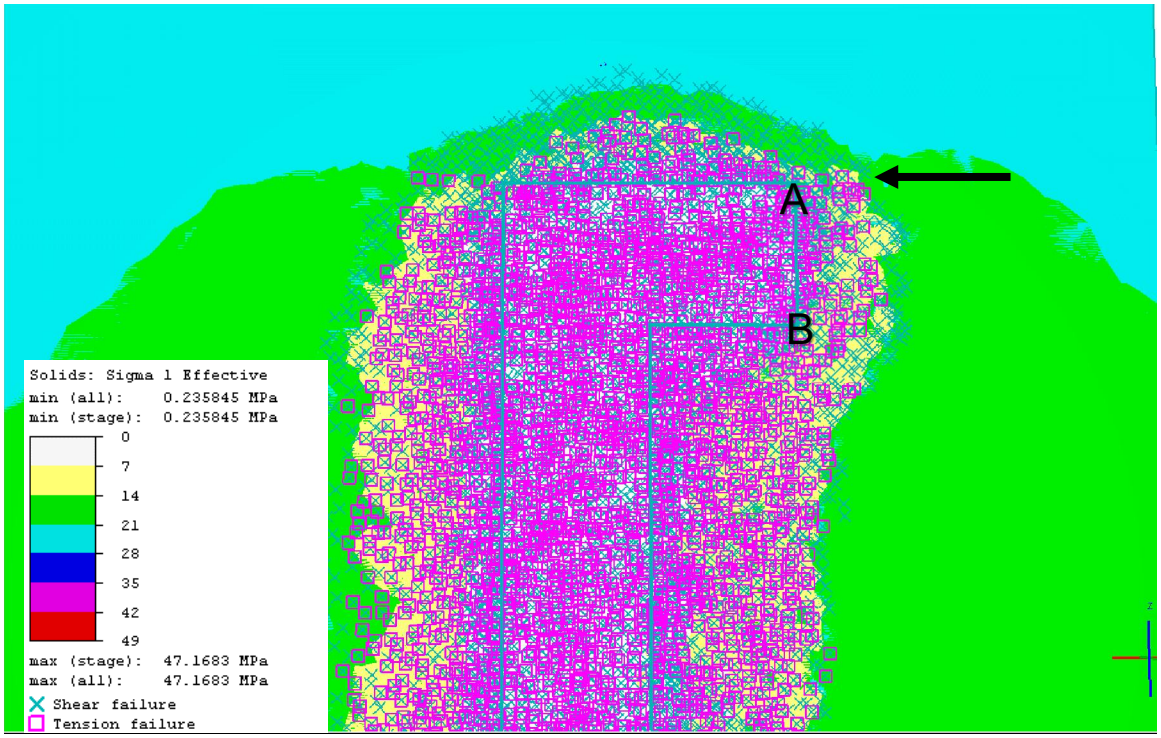

Figure 50: Yielded elements and stress redistribution for tunnel driven at 90 degrees to maximum principal stress.

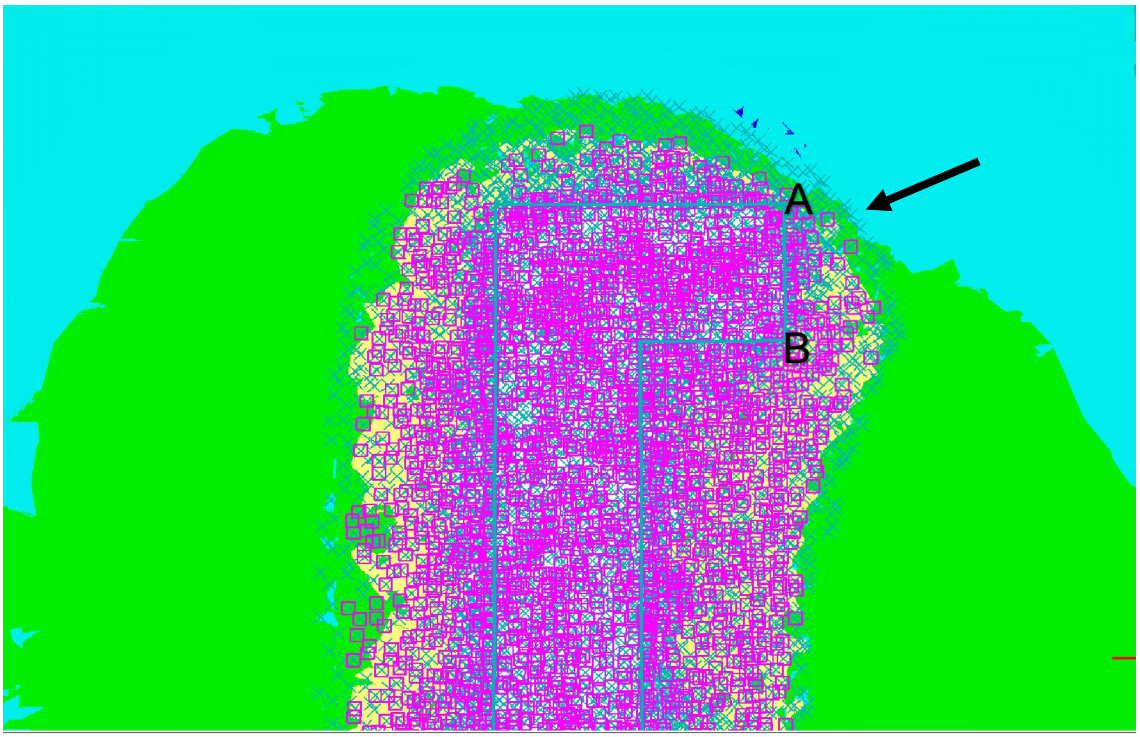

Figure 51: Yielded elements and stress redistribution for tunnel driven at 65 degrees to maximum principal stress

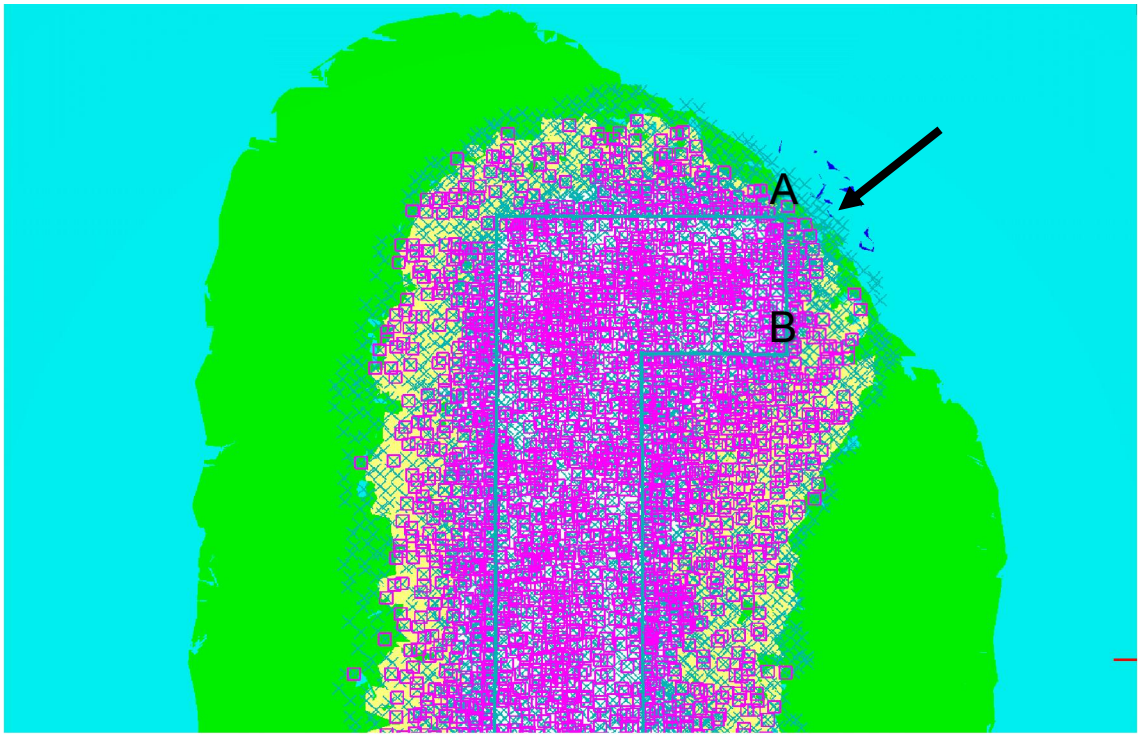

Figure 53: yielded elements and stress redistribution for tunnel driven at 45 degrees

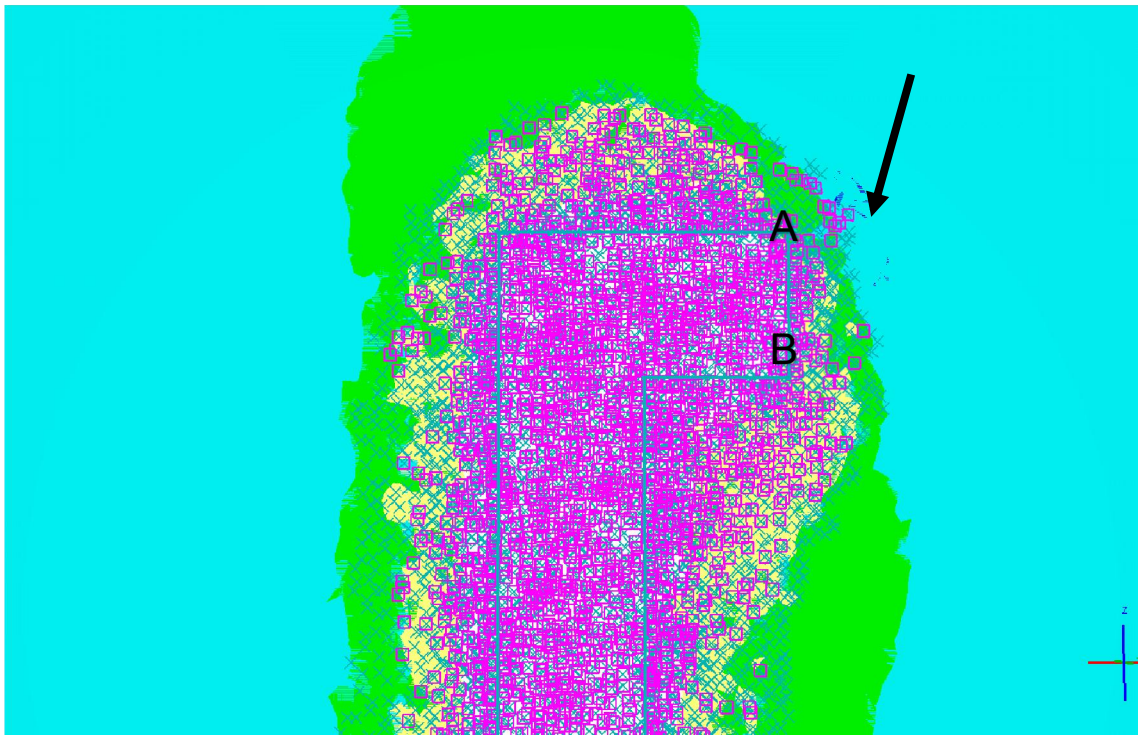

Figure 52 : Yielded elements and stress redistribution for tunnel driven at 25 degrees to maximum principal stress

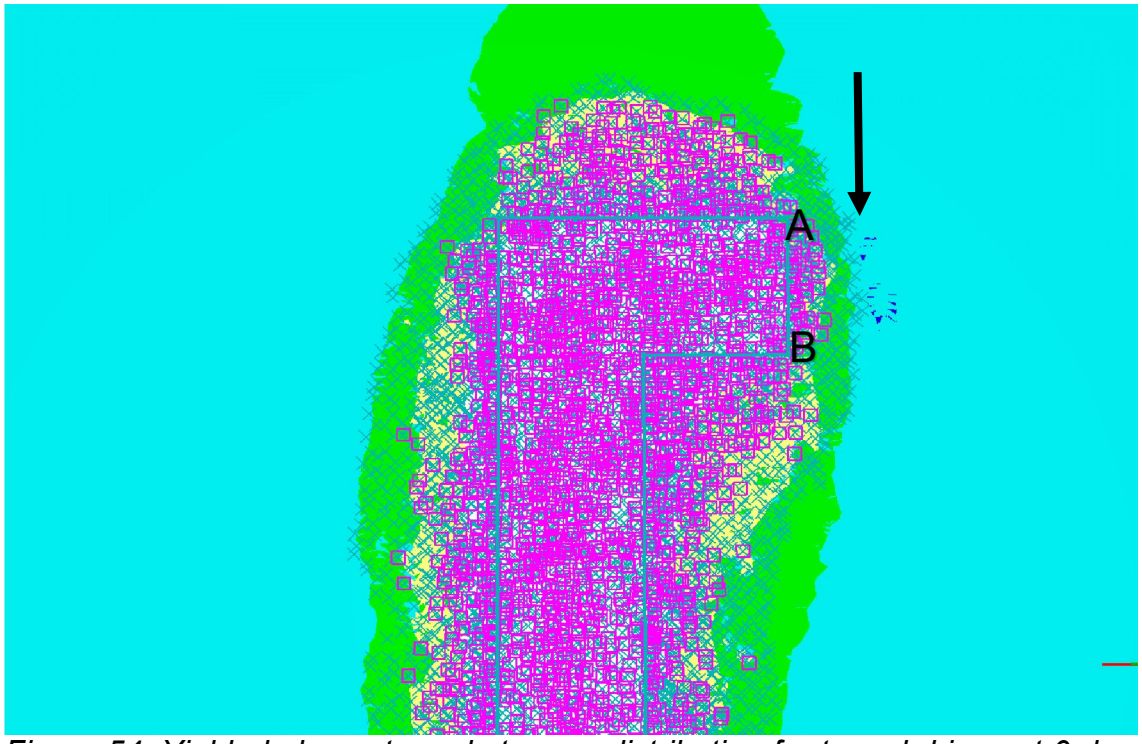

Figure 54: Yielded elements and stress redistribution for tunnel driven at 0 degrees to maximum principal stress.

9.2 Conclusion

Modelling undertaken for a coal mine roadway junction shows that the damage resulting from the stress perpendicular case is much more severe than all other conditions. Also the inner corner of the junction is sustaining heavy damage which demands extensive support requirements. Observation of the point B in the figures shows that stress at an angle is causing maximum damage than stress parallel or perpendicular condition.

10 Development of a Room and pillar mine

Previous chapters discussed applications of RS^3 as a modelling tool to predict the stress damage and displacements around coal mine roadways. In Chapter 9 a coal mine roadway junction was modelled, it proved that RS^3 could be used successfully in predicting the stress damage of more complicated models. In this chapter an attempt is made to model a full scale room and pillar panel and compare and validate it with field data.

10.1 Model description

The data used for modelling belongs to the Venkateshkhani underground mine (VK7 incline) of the Singareni Collieries Company Ltd (SCCL) in Kothagudem, India. The VK7 incline is more than five decades old. Three coal seems are present at VK-7 incline with varying thickness of 9.5m to 11.5m, 5.5 to 10.5 and 2.6m to 4m are present in Top, King and bottom seams. The King seam of this mine is extensively developed on bord and pillar, the depth of the seam varies from 330m to 415m. Average thickness of the seam is 5.5m (Singh et al. (2011)).

The King seam is at a gradient 1 in 7.5 and the strike of the seam is N22^{o}W- S22^{o}E. The top and bottom strata mainly consists of sandstone. The uniaxial compressive strength widely varies from 9MPa to 53MPa. Overlying strata is massive but the immediate the roof consisted of a number of discontinuities.

Table 5: Details of original and modified panel 26 (after Singh et al. (2011))

Parameters	Original Panel	Modified panel
No. of pillars	12	29
Panel size	145 x 165 (average)	410 x 135m (average)
Depth of Working	385-414m	359-414m
Immediate roof (5m)	Sandstone	Sandstone
Immediate floor (5m)	Coal and Sandstone	Coal and Sandstone
Seam thickness	5.5m (average)	5.5m (average)
Pillar Size	43 x 50m centre to centre	43 x 50m centre to centre
Final Extraction height	4m (average)	4m (average

Caved goaf of top seam is located 49 to 52m above the King seam with sandstone strata in between. Panel 26 of VK-7 incline Figure 55, is depillared, using a conventional splitting and slicing maintaining a diagonal line of extraction. The size of the original panel with 12 pillar was increased after 50% of coal extraction. A diagonal extraction layout was selected at an angle of 30^{o} but later modified to 44^{o} after expansion of panel to 29 pillars. Dimensional details of original and modified panel are given in Table 5.

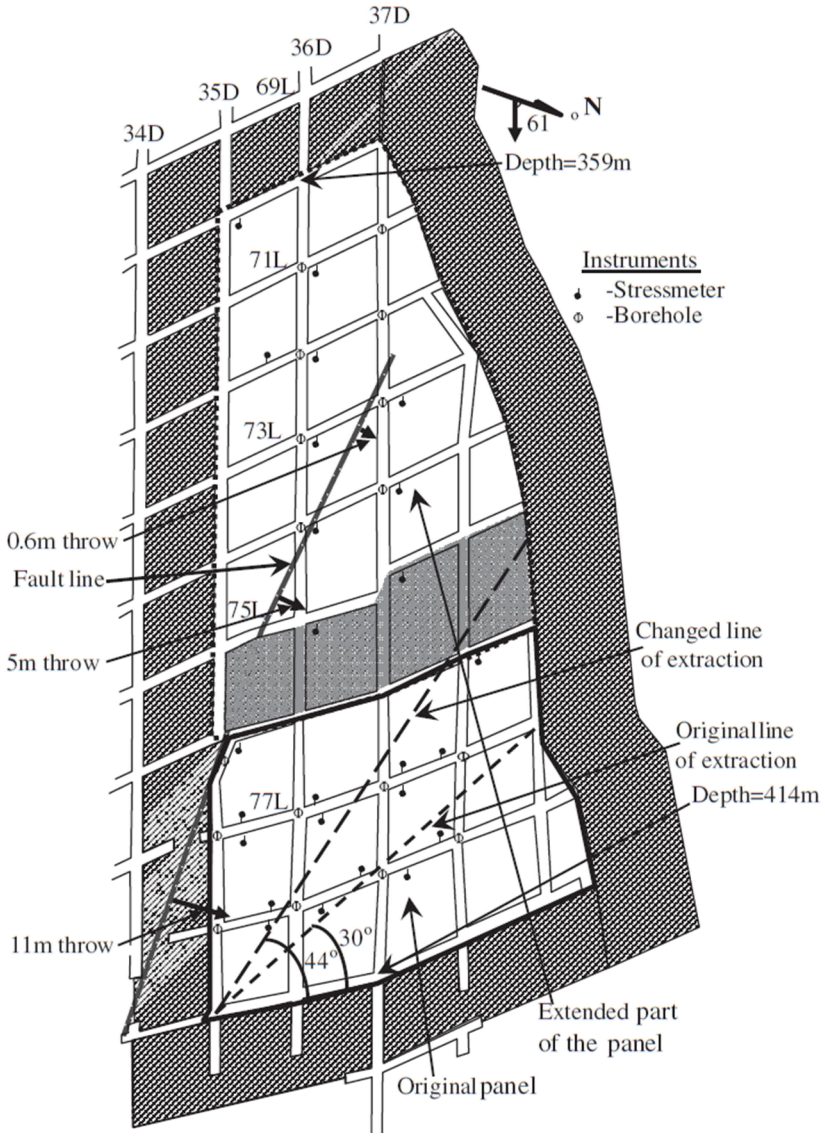

Figure 55: Original and modified panel plan on VK-7 incline Singh et al. (2011)

10.1.1 Observation of mining induced stresses on VK-7 incline

Most of the instruments for the observation got disrupted due to the high stress regime prevailing at the site. A large amount of pillar spalling and floor heaving was observed due to mine induced stresses, geological discontinuities also played a role for the deterioration of the instruments. Vibrating wire stress meter was found to be more reliable and it was installed well inside the pillar and measured remotely so that spalling of pillars will not affect the results (Singh et al. (2011)).The maximum capacity of the vibrating wire stress meters were 20MPa and the stresses exceeded this limit when the goaf was 20m away still some more measurements were available but were not reliable.

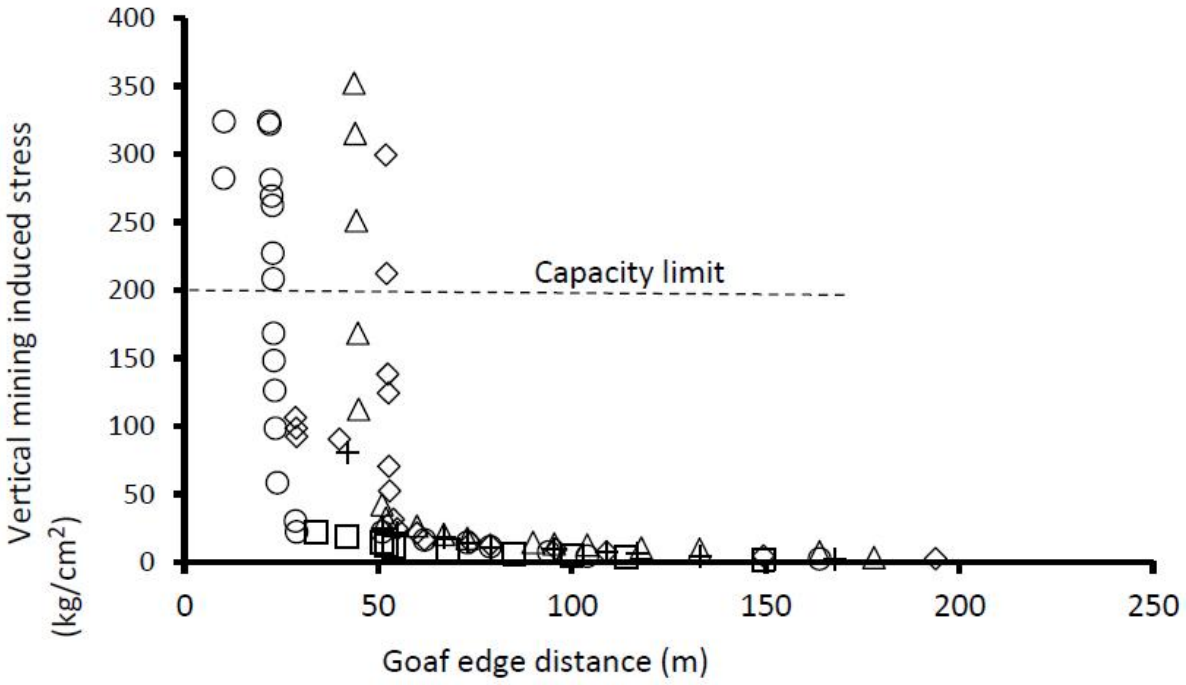

Figure 56: Field observation of mine induced stresses at VK-7 incline (after Singh et al. (2011))

10.1.2 Parameters adopted for the design

The vertical stress is derived by assuming the average depth of mine of 400m with unit density of rock 0.025MPa. The vertical stress was coming as 10MPa. There are no in-situ stress measurements available, an estimate of horizontal stresses are

made using Sheorey et al. (2001) and Zia (2011) and the value for both horizontal directions were taken as 6.4MPa. The parameters used for modelling are given in Table 6.

Table 6: Laboratory data for VK-7 incline Zia (2011)

Parameters	**Coal**	**Sandstone**
Young's Modulus	2GPa	10GPa
Poisson's ratio	0.25	0.25
Cohesion	8.66	-
Friction angle	30	-
Dilation angle	0	-

10.1.3 Modelling of mine in RS^3

For modelling in RS^3 a simplified layout of the mine is adopted having a square layout of 16 pillars of 40x40m initially. Extraction thickness of coal is assumed to be 4m as it was done in the site. Even though the coal seam thickness was upto 5.5m due to excessive floor heaving only 4m layer is extracted in the field. A diagonal depillaring method was adopted with an angle of 30^o, at field after 50% of extraction this angle was changed to 44^o but here for simplicity an angle of 30^o is maintained throughout the model.

An observation point is kept at a distance 130m diagonally away from one of the corners as shown in the Figure 57.At site the observation point is kept 4m inside the pillar so that local disturbances like spalling would not affect the measurements. In model since there is such problems so it is reasonable to assume this point at corner. The observation is made 2m below the roof level. In RS^3 the whole model is made horizontally and it is difficult to have top view as shown in Figure 57. Hence a top view is drawn using software AutoCAD in order to get the measurements to model in RS^3. A full description of model is given in Appendix C, since it may not be appropriate to give a detailed explanation in the main chapter. The inclined lines at 30^o in Figure 57 shows the mining steps adopted and in total there were 10 steps before the modelled goaf reached the observation point. The coloured zones shows the pillar extraction

done at each mining stage. The whole analysis was conducted using a coarse mesh due to computing limitations.

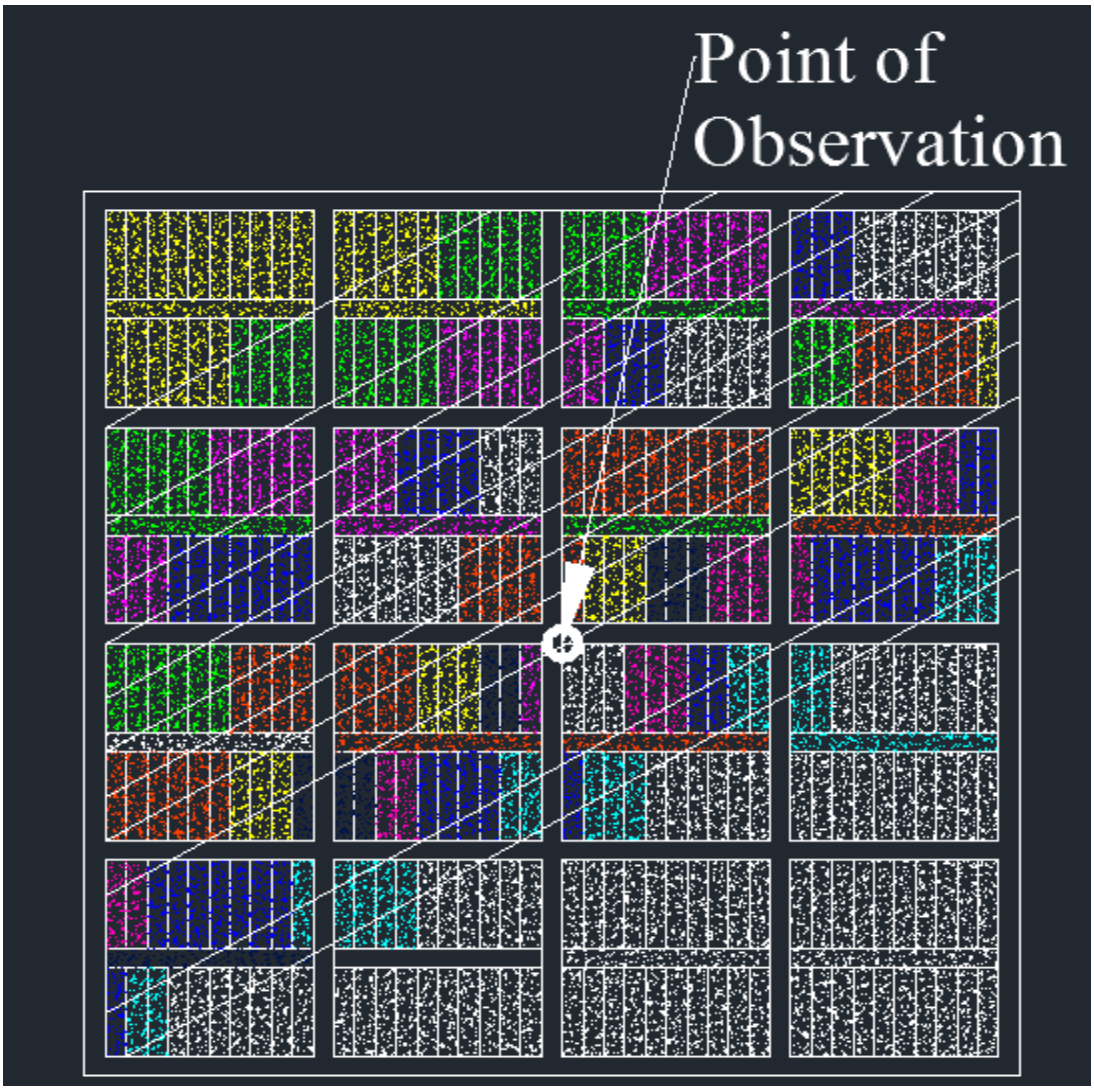

Figure 57: Mining sequence adopted in RS^3 and point of observation

10.2 Sensitivity analysis

As explained in the previous chapters, it is common practice in mine modelling to perform sensitivity analysis to calibrate the results to match field observations. Obtaining parameters is not a trivial task in a model. In this section an elastic sensitivity analysis is carried out by varying the stiffness of coal and sandstone independently.

First the analysis is carried out with varying the stiffness of the coal from 1.5 to 3GPa at 0.5GPa intervals, keeping the stiffness of sandstone the same as laboratory value of 10GPa.The Poisson's ratio is also kept as a constant as 0.25 for both coal and sandstone. The model is reanalysed by keeping the value of coal at 2GPa and varying the stiffness of the sandstone from 8GPa to 14 GPa at 2GPa intervals. The results from the analysis are presented in Figure 58 and Figure 59.

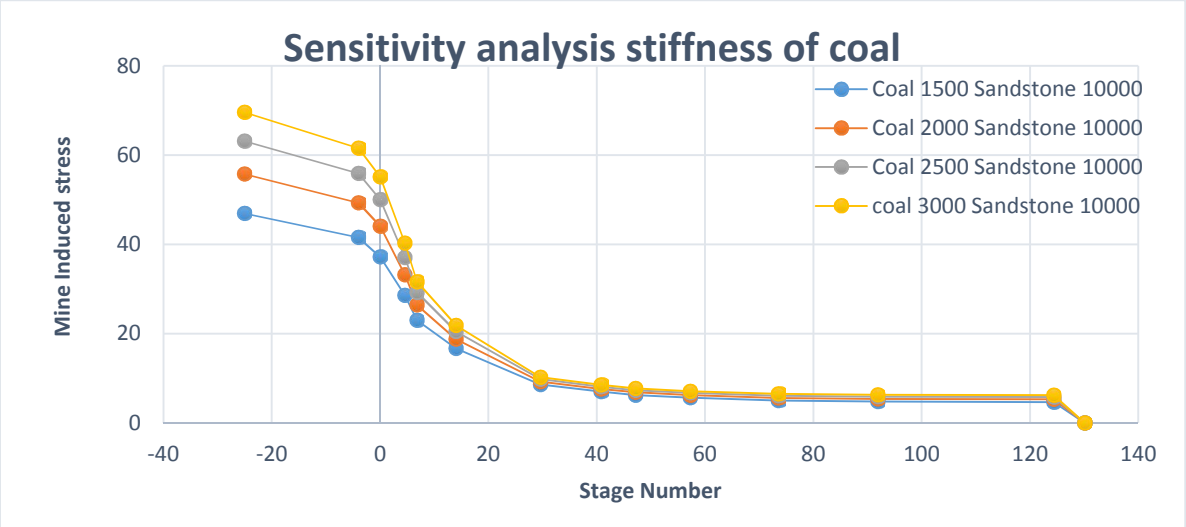

Figure 58: sensitivity analysis by varying stiffness of coal

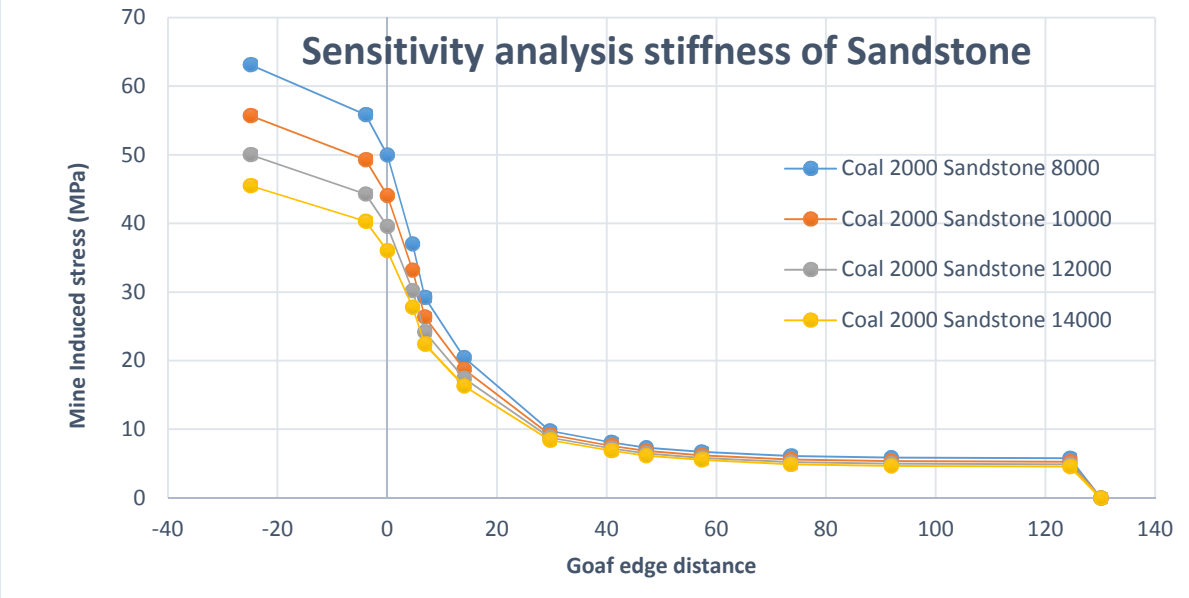

Figure 59: sensitivity analysis by varying stiffness of sandstone

10.3 Validation of field data

Based on the sensitivity analysis parameters are selected which make a best fit curve to the field measurements. Figure 60 shows the validation of numerical analysis with field data. It has to be noted that, the analysis done is elastic and it will not be realistic representation of coal strata since the stresses induced is well beyond elastic limit of the material. But the analysis could predict the stress concentrations in the model.

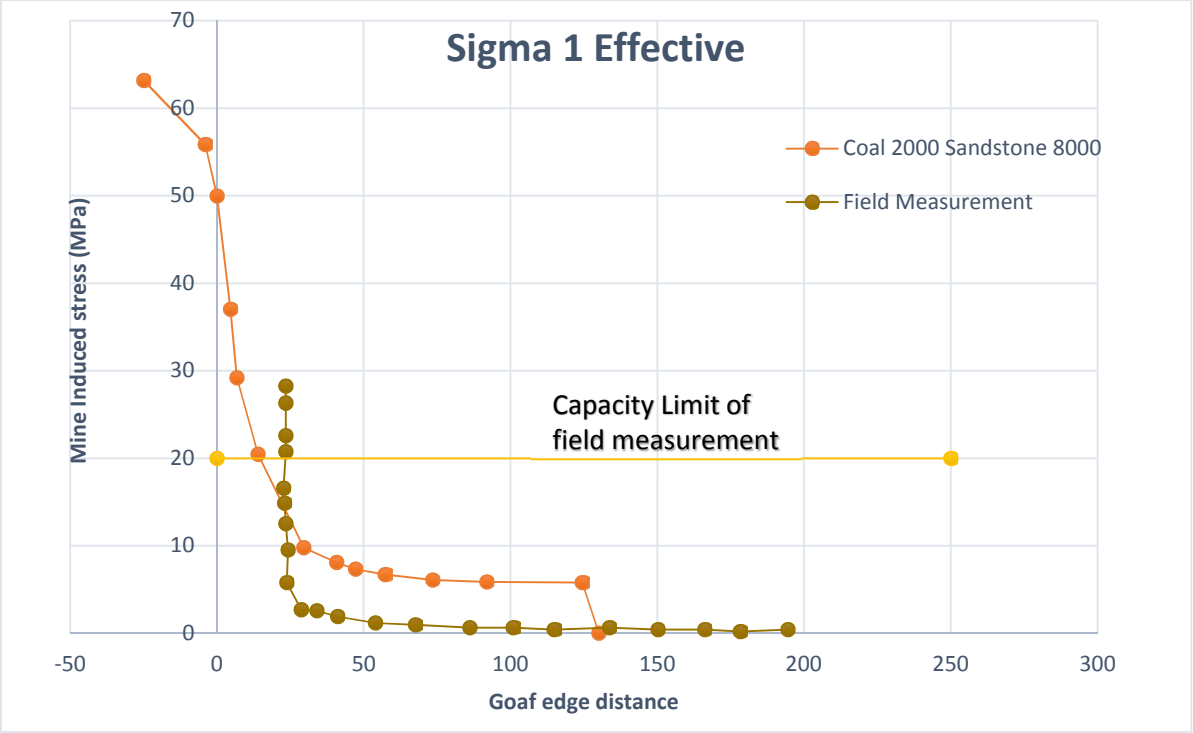

Figure 60: Validation of field data

Table 7: Model input data for RS³

	Sandstone		Coal	
	Young's modulus	Poisson's ratio	Young's modulus	Poisson's ratio
Lab data	10GPa	0.25	2GPa	0.25
RS³ input	8GPa	0.25	2GPa	0.25

The modelled output from RS³ show reasonable correlation with field measurements obtained and could be used for further analysis.

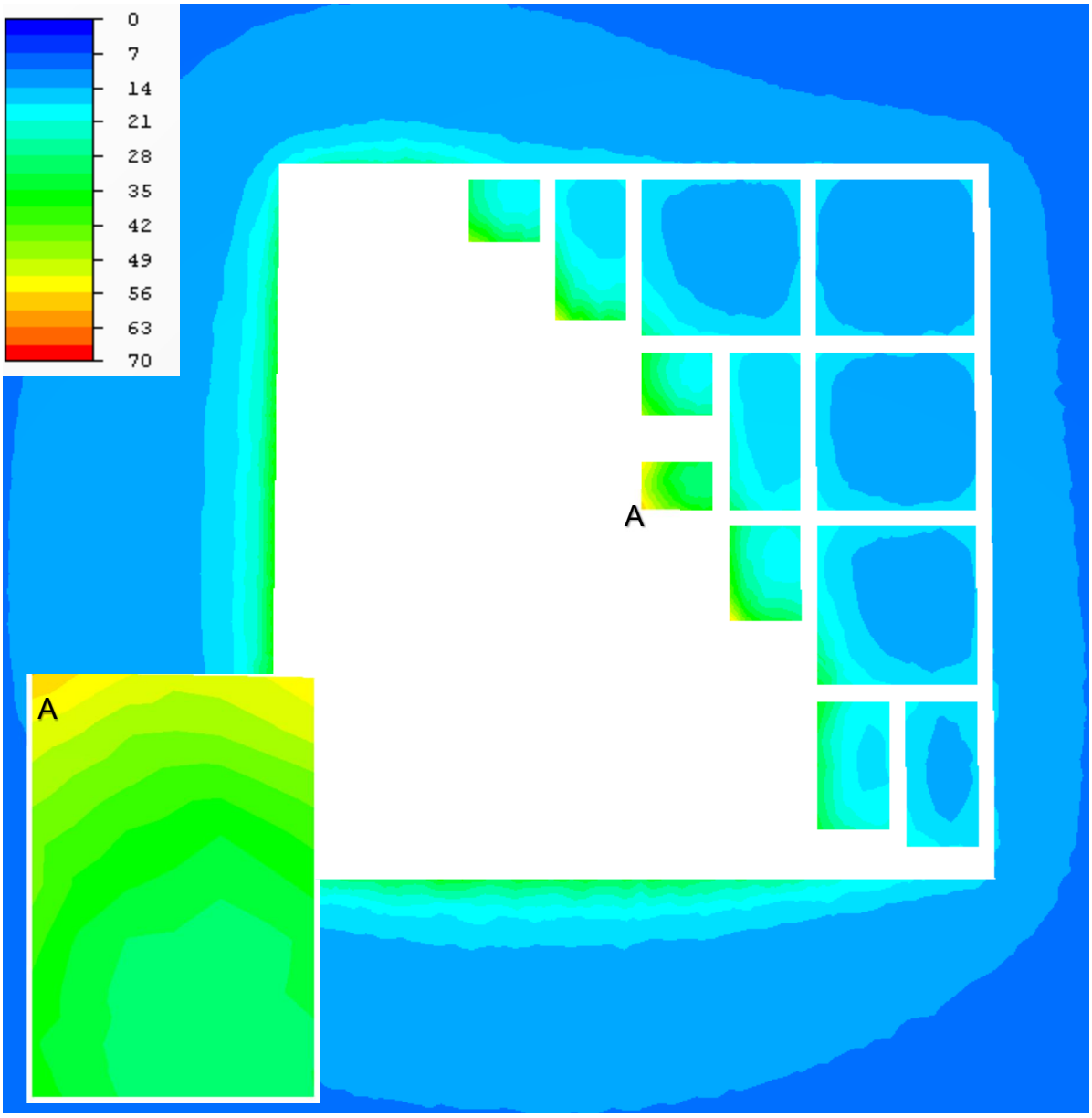

*Figure 61: Stress concentration at the observation point due to advancing goaf*In Figure 61 shows sharp gradients in stress at observation point A due to the advancing goaf at mining stage 10 is illustrated. The larger inner pillars are more or less in the in-situ stress state but the corner pillars near the goaf experiences severe stresses.

10.4 Nonlinear analysis

In Chapter 3 it was explained that a cohesion weakening model predicts the behaviour of coal mine measures more realistically. The elastic analysis carried out in the previous sections were reanalysed using a cohesion weakening model in this

section. Since the model was experiencing convergence problems plastic properties were only assigned to coal strata leaving the sandstone material set as elastic. The parameters used for the analysis is taken from Table 6.

Figure 62 illustrates the mine induced stresses due to advancing goaf on plastic model for 10th mining step. Due to convergence issues a model with lower expansion factor and coarse mesh was used.

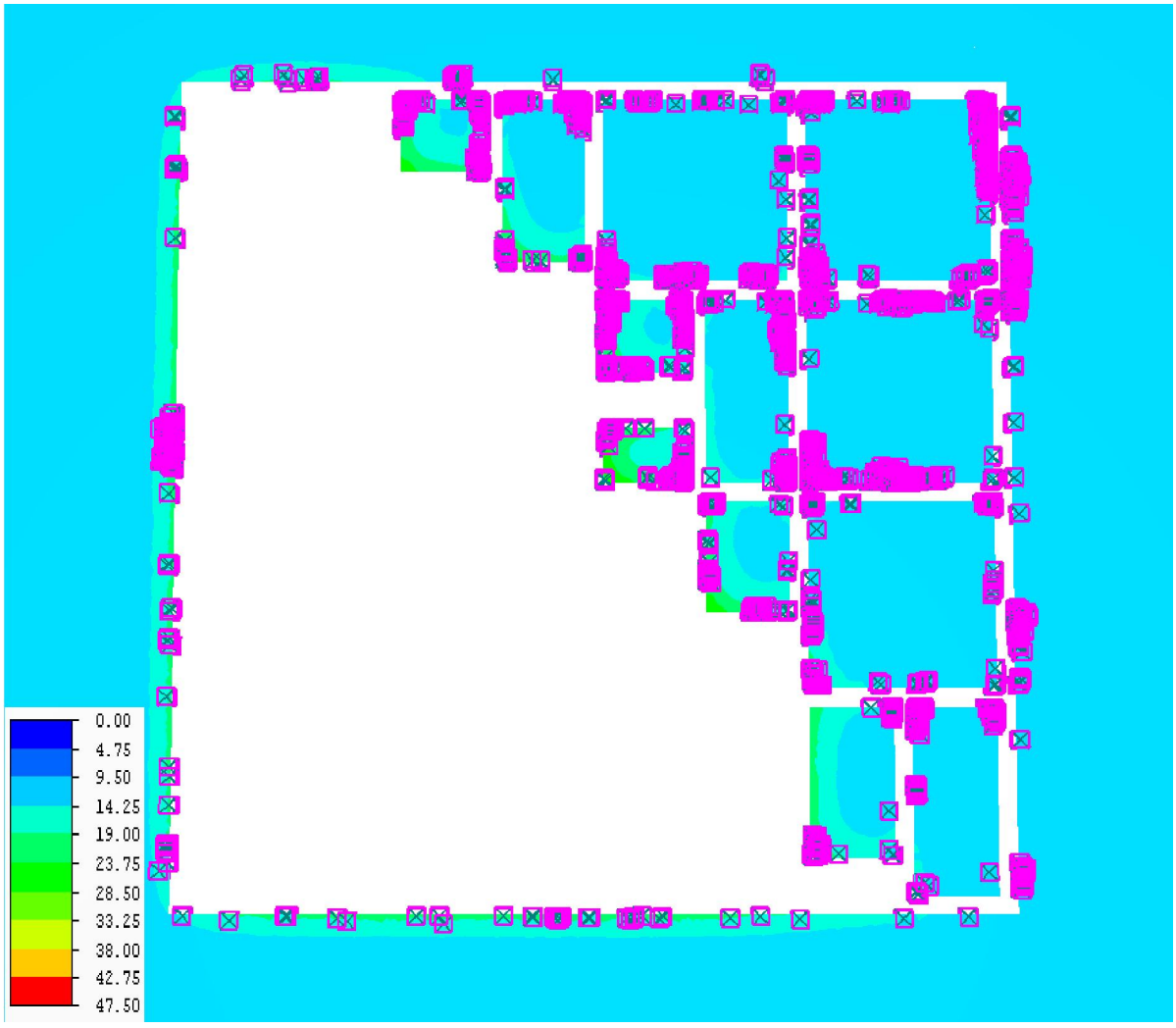

Figure 62: Plastic yielding while adopting cohesion weakening model for analysis

Plastic analysis shows are drastic reduction in stress along with associated yielding, from the Figure 64 and Figure 62 it is clear that all the corners and side walls are yielded in agreement with the field observation of spalling of side wall on the mine.

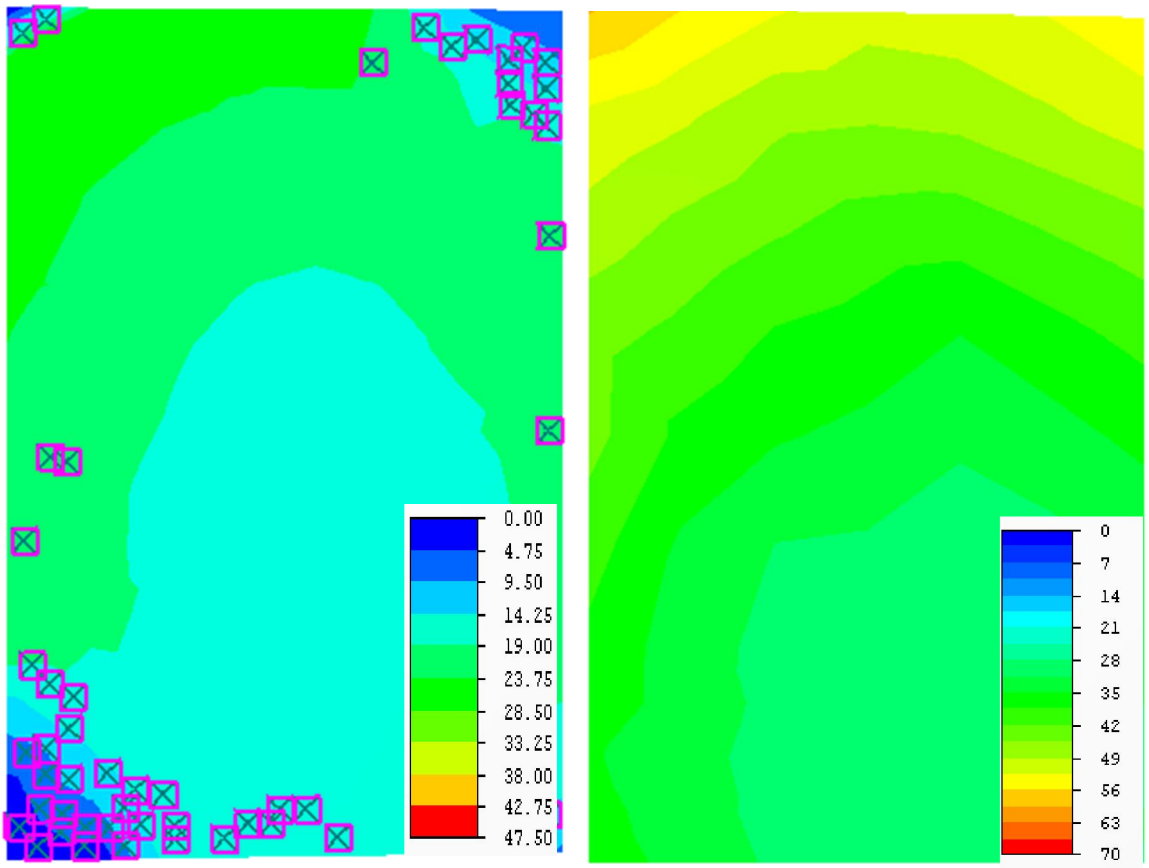

Figure 63: Comparison of Plastic and elastic analysis results for observation points

10.5 Conclusion

An attempt is made to model a simplified full scale mine panel from the case study. With the available computing capability a sequential three dimensional model was difficult to achieve. Hence a model with limited number of sequences was adopted. The mine adopts pillar extraction techniques to maximise recovery, large displacements at roof could be expected. To model without boundary effects, the outer boundary of the model should be enough far away not to influence the results. Hence a mine model is made with outer fixed boundaries far enough so that there are no significant effects on the results.

Initially an elastic model is made and a sensitivity analysis was conducted, parameters were fixed according to sensitivity analysis which best fits the mine induced stresses when compared to the field results. The model was validated against mine induced stress at field which showed very good correlation. It was

evident from the model that the existing pillar corner experience severe loading due to the advancing goaf.

A plastic analysis was conducted adopting a cohesion weakening model, the results shows significant yielding at corners. Spalling of pillar side walls was reported at site, which would be expected from the results of the model.

11 Conclusion and further study

An investigation was conducted to determine the detrimental effects of high horizontal stresses on a coal mine roadway. A full three dimensional analysis was needed to conduct the analysis since stresses at an angle to the tunnel cannot be modelled using a two dimensional software. To obtain a complete longitudinal displacement profile a three dimensional program is essential. RS^3 the new 3D FEM program from Rocscience was used for the study. RS^3 showed its capability in building a 3D sequential model and to simulate progressive failure.

Initially a simple single stage model of a coal mine roadway was created and stresses and yield patterns were analysed. This simple exercise concluded that, stress damage due to high horizontal stresses at angle are asymmetrical. The resulting stress damage is wider in the case of stress perpendicular case and for stress parallel case the damage is narrow but sharper which extends to a longer distance ahead of tunnel face.

The model was able to predict the progressive failure associated with sequential coal extraction with a continuous miner. The sequential model which had very small advance stages of 1m showed larger stress damage and displacement compared to a single stage model. The bolted sequential model predicted that stress damage on the stress perpendicular condition is much more than that of the stress parallel condition. The initial displacements at the tunnel face is larger for stress parallel case. Displacement across the tunnel for stress at an angle to the tunnel showed asymmetrical distribution. The plastic zones and displacements increased with increase in thickness of weak mudstone layer strata immediately above the tunnel roof. Examination of the bolt forces shows that the load on the bolt in the stress parallel case in much lower than that of the stress perpendicular case.

The analysis was extended for a tunnel junction turning at right angles. The stress damage showed a similar trend with the analysis carried out linear excavations. The maximum damage was found to be for the stress perpendicular condition. The stresses at an angle displayed asymmetrical yield zones at the corners of the excavation.

A case example from an Indian coal Room and pillar mine was also modelled. The mine adopted a conventional splitting and slicing method with a diagonal line for pillar extraction. The model was created using RS^3 adopting a diagonal line of depillaring at 30^o inclination. The magnification of stresses due to the advancing goaf was well captured by the model and the data is validated against field measurements. Very sharp gradients of stresses were visible at the observation point. A brittle plastic model was able to capture spalling of corners, which was also reported at field.

Overall the software was able to capture the damage due to high horizontal stress field. It was able to incorporate realistic constitutive behaviour to simulate the post peak behaviour of coal measure rocks. The model was also able to predict the progressive failure on a multistage model. The results compare favourably with previous modelling undertaken for the North Selby Coal field. However large files restricts the modeller to use the results at ease. For a large mine site, a number of revisions for the model would be expected, it may not be an easy task to rerun the model for each revision. The computing capability of the system may restrict the use of the model for complicated mine layouts.

11.1 Further Study

RS^3 has the ability to incorporate joint planes; hence a room and pillar model incorporating geological discontinuities should be modelled. A linear multistage coal mine roadway model creates a 2.6Gigabytes file and takes 18 hours of computation time. The computing power of an ordinary office desktop computer is not enough to easily handle these large files. Due to these limitations, the full scale mine model was created largely as a single stage model having limited number of steps. With the help of high performance computing a sequential multistage model of a mine with bolting sequence could be created which will give a more realistic picture of stress damage and progressive failure for the room and pillar mine.

12 References

Altounyan, P.H.K.B.D., 1999. Designing for Success. World Coal, 47-52.

Bobet, A., 2010. Numerical Methods in Geomechanics. Arabian Journal for Science & Engineering (Springer Science & Business Media BV) 35.

Bobet, A., Fakhimi, A., Johnson, S., Morris, J., Tonon, F., Yeung, M.R., 2009. Numerical models in discontinuous media: Review of advances for rock mechanics applications. Journal of geotechnical and geoenvironmental engineering 135, 1547-1561.

Brinkgreve, R.B., 2005. Selection of soil models and parameters for geotechnical engineering application, Soil Constitutive Models Evaluation, Selection, and Calibration. ASCE, pp. 69-98.

Cai, M., 2008. Influence of stress path on tunnel excavation response – Numerical tool selection and modeling strategy. Tunnelling and Underground Space Technology 23, 618-628.

Chase, F.E., Mark, C., Heasley, K.A., 2002. Deep cover pillar extraction in the US coalfields, 21st International conference on ground control in mining, Morgantown, pp. 6-8.

Clifford, B., 2004. The assessment of ground control risk and support integrity in coal mine roadways, Camborne School of Mines, University of Exeter, Cornwall, p. 349.

Coggan, J., Gao, F., Stead, D., Elmo, D., 2012. Numerical modelling of the effects of weak immediate roof lithology on coal mine roadway stability. International Journal of Coal Geology 90-91, 100-109.

Darling, P., 2011. SME mining engineering handbook, 3rd ed. Society for Mining, Metallurgy, S.l.

Gale, W.J., Blackwood, R.L., 1987. Stress distributions and rock failure around coal mine roadways. International Journal of Rock Mechanics and Mining Sciences & Geomechanics Abstracts 24, 165-173.

Hajiabdolmajid, V., Kaiser, P., 2003. Brittleness of rock and stability assessment in hard rock tunneling. Tunnelling and Underground Space Technology 18, 35-48.

Hajiabdolmajid, V., Kaiser, P., Martin, C., 2002. Modelling brittle failure of rock. International Journal of Rock Mechanics and Mining Sciences 39, 731-741.

Hammah, R., Curran, J., 2009. It is Better to be Approximately Right than Precisely Wrong: Why Simple Models Work in Mining Geomechanics, 43 rd US Rock Mechanics Symposium and 4th U.S.-Canada Rock Mechanics Symposium, Asheville, US.

Hoek, E., 2004. Estimates of rock mass strength. Discussion paper # 4, http://www.rocscience.ca/hoek/pdf/Estimates_of_rock_mass_strength.pdf, 4.

Hoek, E., Brown, E.T., 1980. Underground excavations in rock. The Institution of Mining and Metallurgy, London.

Hoek, E., Carranza-Torres, C., Corkum, B., 2002. Hoek-Brown failure criterion-2002 edition. Proceedings of NARMS-Tac, 267-273.

Hoek, E., Kaiser, P.K., Bawden, W.F., 1995. Support of underground excavations in hard rock. Balkema, Rotterdam.

Itasca, 2005. FLAC -Fast Lagrangian analysis of continua Online Manual. Itasca Consulting Group Inc 5, 3058.

Jing, L., 2003. A review of techniques, advances and outstanding issues in numerical modelling for rock mechanics and rock engineering. International Journal of Rock Mechanics and Mining Sciences 40, 283-353.

Jing, L., Hudson, J., 2002. Numerical methods in rock mechanics. International Journal of Rock Mechanics and Mining Sciences 39, 409-427.

Jing, L., Stephansson, O., 2007. Discrete Fracture Network (DFN) Method, in: Lanru, J., Ove, S. (Eds.), Developments in Geotechnical Engineering. Elsevier, pp. 365-398.

Kent, F.L., Coggan, J.S., Altounyan, P.F.R., 1998. Investigation into Factors Affecting Roadway Deformation in the Selby Coalfield. Geotechnical & Geological Engineering 16, 273-289.

Marinos, P., Hoek, E., 2000. GSI: a geologically friendly tool for rock mass strength estimation, Proc. GeoEng2000 Conference, Melbourne, pp. 1422-1442.

McCreath, D., Diederichs, M., 1994. Assessment of near-field rock mass fracturing around a potential nuclear fuel waste repository in the Canadian Shield, International journal of rock mechanics and mining sciences & geomechanics abstracts. Elsevier, pp. 457-470.

Meyer, L.H.I., 2002. Numerical Modelling Of Ground Deformation Around Underground Development Roadways, With Particular Emphasis On Three-Dimensional Modelling of The Effects of High Horizontal Stress, Camborne School of Mines. University of Exeter, p. 324.

Pan, X.D., Hudson, J.A., 1988. Plane strain analysis in modelling three-dimensional tunnel excavations. International Journal of Rock Mechanics and Mining Sciences & Geomechanics Abstracts 25, 331-337.

Pan, X.D., Reed, M.B., 1991. A coupled distinct element—finite element method for large deformation analysis of rock masses. International Journal of Rock Mechanics and Mining Sciences & Geomechanics Abstracts 28, 93-99.

Pande, G.N., Beer, G., Williams, J.R., 1990. Numerical methods in rock mechanics. Wiley, Chichester etc.

Plaxis, 2011. Material Models Manual. Plaxis BV. http://www.plaxis.nl/files/files/2D2011-3-Material-Models.pdf.

Potts, D.M., Ganendra, D., 1994. An evaluation of substepping and implicit stress point algorithms. Computer Methods in Applied Mechanics and Engineering 119, 341-354.

Reed, M.B., 1988. A viscoplastic model for soft rock. Engineering Computations Vol. 5, pp.65 - 70.

Rocscience, 2013. 3D Meshing Customization Developers Tips. Rocscience Inc., Toronto Canada, 8.

Rocscience, 2014a. Personal Communication.

Rocscience, 2014b. Phase2 Theory - Convergence Criteria. 4.

Sakurai, S., 1997. Lessons learned from field measurements in tunnelling. Tunnelling and Underground Space Technology 12, 453-460.

Sheorey, P.R., Murali Mohan, G., Sinha, A., 2001. Influence of elastic constants on the horizontal in situ stress. International Journal of Rock Mechanics and Mining Sciences 38, 1211-1216.

Singh, R., Mandal, P.K., Singh, A.K., Kumar, R., Sinha, A., 2011. Coal pillar extraction at deep cover: With special reference to Indian coalfields. International Journal of Coal Geology 86, 276-288.

Smith, I.M., Griffiths, D.V., 2004. Programming the finite element method, 4th ed. Wiley, Hoboken, NJ.

Starfield, A.M., Cundall, P.A., 1988. Towards a methodology for rock mechanics modelling. International Journal of Rock Mechanics and Mining Sciences & Geomechanics Abstracts 25, 99-106.

Su, W.H., Peng, S.S., 1987. Cutter roof and its causes. Mining Science and Technology 4, 113-132.

Terzaghi, K., Peck, R.B., Mesri, G., 1948. Soil mechanics in engineering practice, 3rd ed. Wiley, New York ; Chichester.

Vlachopoulos, N., Diederichs, M., 2014. Appropriate Uses and Practical Limitations of 2D Numerical Analysis of Tunnels and Tunnel Support Response. Geotech Geol Eng, 1-20.

Vlachopoulos, N., Diederichs, M.S., 2009. Improved Longitudinal Displacement Profiles for Convergence Confinement Analysis of Deep Tunnels. Rock Mechanics and Rock Engineering 42, 131-146.

Wiles, T., 2007. Evidence based model calibration for reliable predictions, Proceedings Fourth International Seminar on Deep and High Stress Mining (Deep Mining 07), Y. Potvin (ed), pp. 7-9.

Wilson, A.H., 1980. A method of estimating the closure and strength of lining required in drivages surrounded by a yield zone. International Journal of Rock Mechanics and Mining Sciences & Geomechanics Abstracts 17, 349-355.

Wilson, A.H., 1983. The stability of underground workings in the soft rocks of the Coal Measures. International Journal of Mining Engineering 1, 91-187.

Zdravkovic, D.M.P.L., 2001a. Finite Element Analysis in Geotechnical Engineering: Volume One - Theory. Thomas Telford, London, p. 440.

Zdravkovic, D.M.P.L., 2001b. Finite Element Analysis in Geotechnical Engineering: Volume Two - Application. Thomas Telford, London, p. 427.

Zia, S., 2011. Numerical Modelling of Room and Pillar Mining and Study of Stress Redistribution for Depillaring of a Deep Coal Seam. Master Dissertation, Camborne School of Mines, University of Exeter, 102.

Appendix A

Validation of RS^3 software using closed form solutions

In order to get familiar with the software a number of examples were done apart from the tutorial files available with the software. In this section one of the example tutorial from Phase^2 is done using RS^3, and the results are compared. Parameters used are given in Table 8, failure criteria used was Hoek Brown and a perfectly plastic model was adopted hence residual parameters are kept same as peak parameters.

Table 8: Parameters used for modelling in Phase^2 and RS^3

Parameter	Value
Young's Modulus (MPa)	6143.7
Poisson's ratio	0.3
σ_{ci} (MPa)	50
m_b	1.67677
S	0.003866
a	0.505734

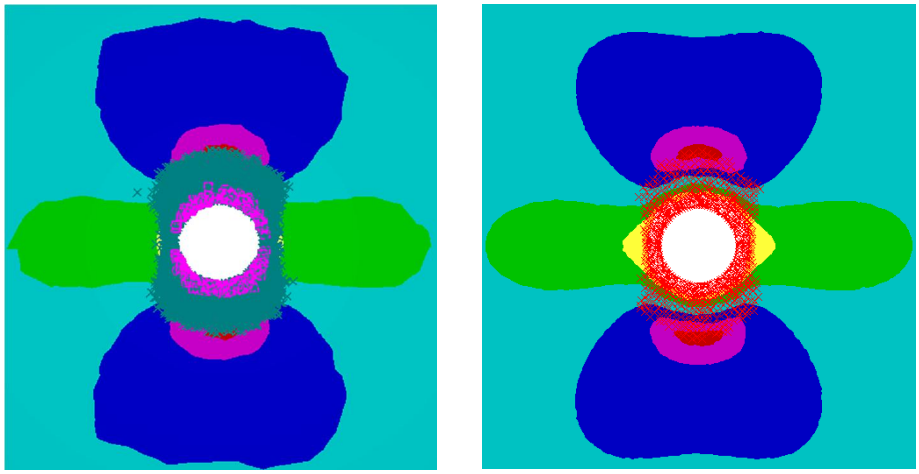

(a) Modelled output from RS^3 (b)Modelled output from Phase^2

Figure 64: Comparison of maximum principal stress distribution and plastic zones output from Phase^2 and RS^3

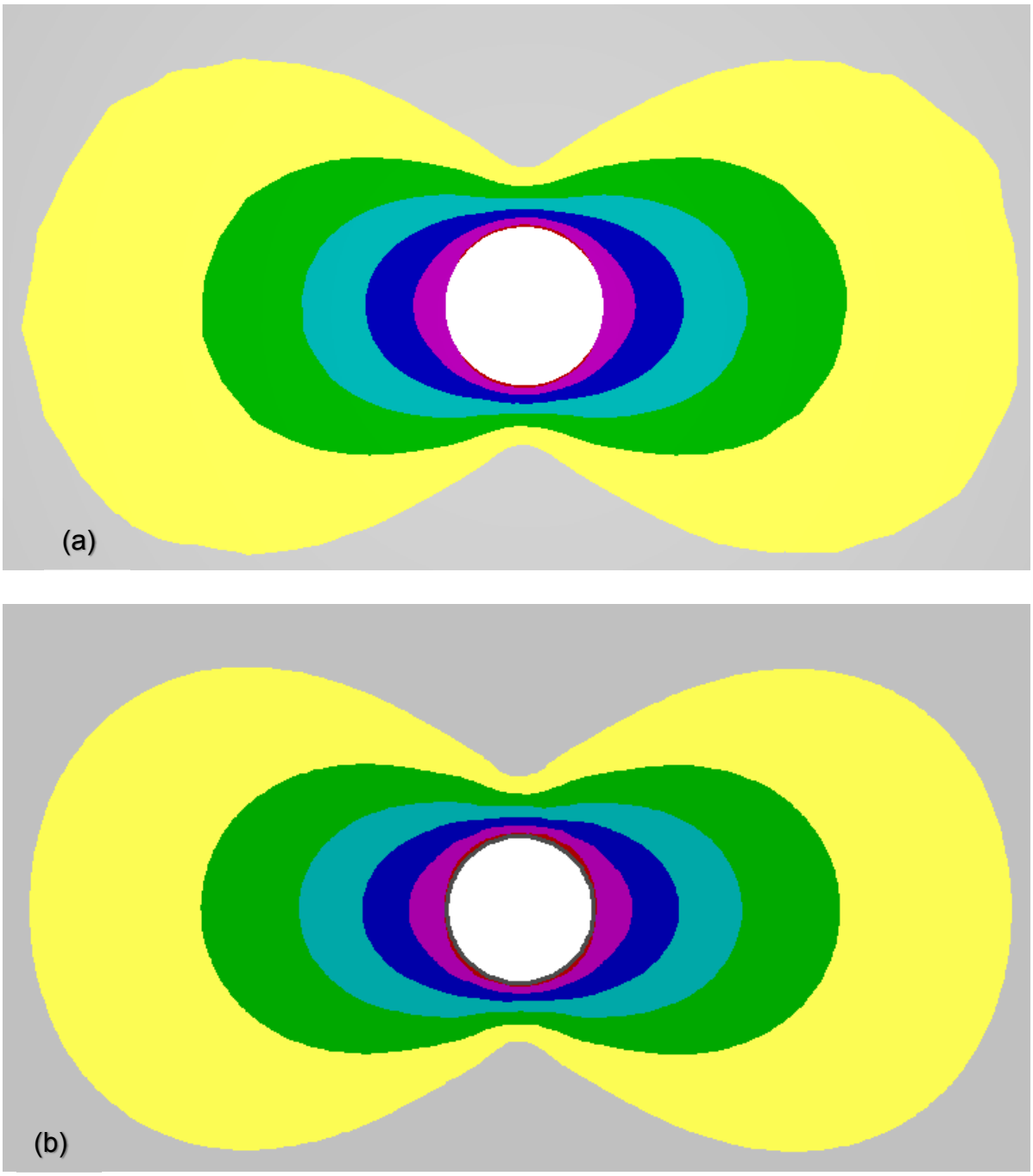

Figure 65: Modelled results for displacements from (a) RS[3] (b) Phase[2]

The results of the analysis showed similar results for Phase[2] and RS[3] modelling. The results gave more confidence to proceed with more complicated models.

Appendix B

Modelling of effects rate of tunnel advance using RS^3

Excavation rates have a significant impact on the development of plastic zones, a single stage excavation will be showing a lesser yield zone and displacements than that of a multistage excavation, this is because in a multistage excavation, the tunnel is passing through an already stress damaged zone. Models with different advancement rates will show different longitudinal displacement profile (Vlachopoulos and Diederichs, 2009). In his paper (Vlachopoulos and Diederichs, 2009) clearly illustrated difference in longitudinal displacement profile in a single stage excavation, tunnel with advance rates of twice the diameter (2D), 1D, 0.4D and 0.2D. It explains the importance of having an advance rate of approximately 0.2D to simulate a continuous mining process as it is done using a continuous miner or a TBM.

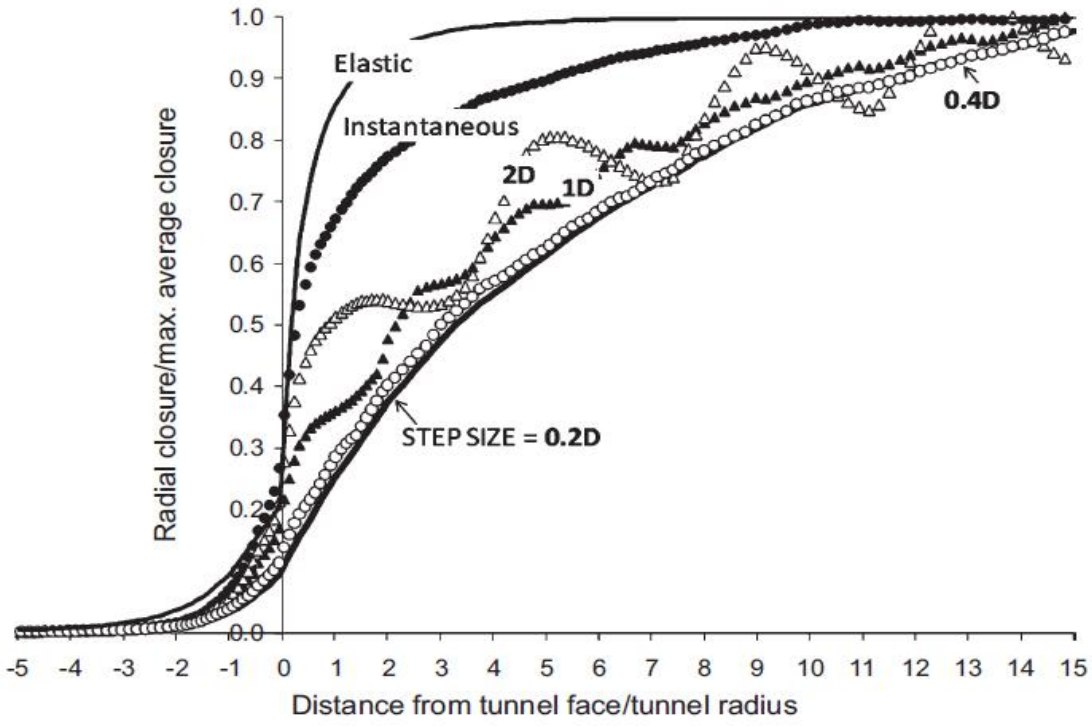

Figure 66: Difference in longitudinal displacement profile on varying excavation step size (Vlachopoulos and Diederichs, 2009)

The parameters used for the modelling are given in Figure 66. The same model is replicated in Phase^2 and in RS^3 and the longitudinal displacement profile (LDP) is compared. LDP is drawn only from tunnel face.

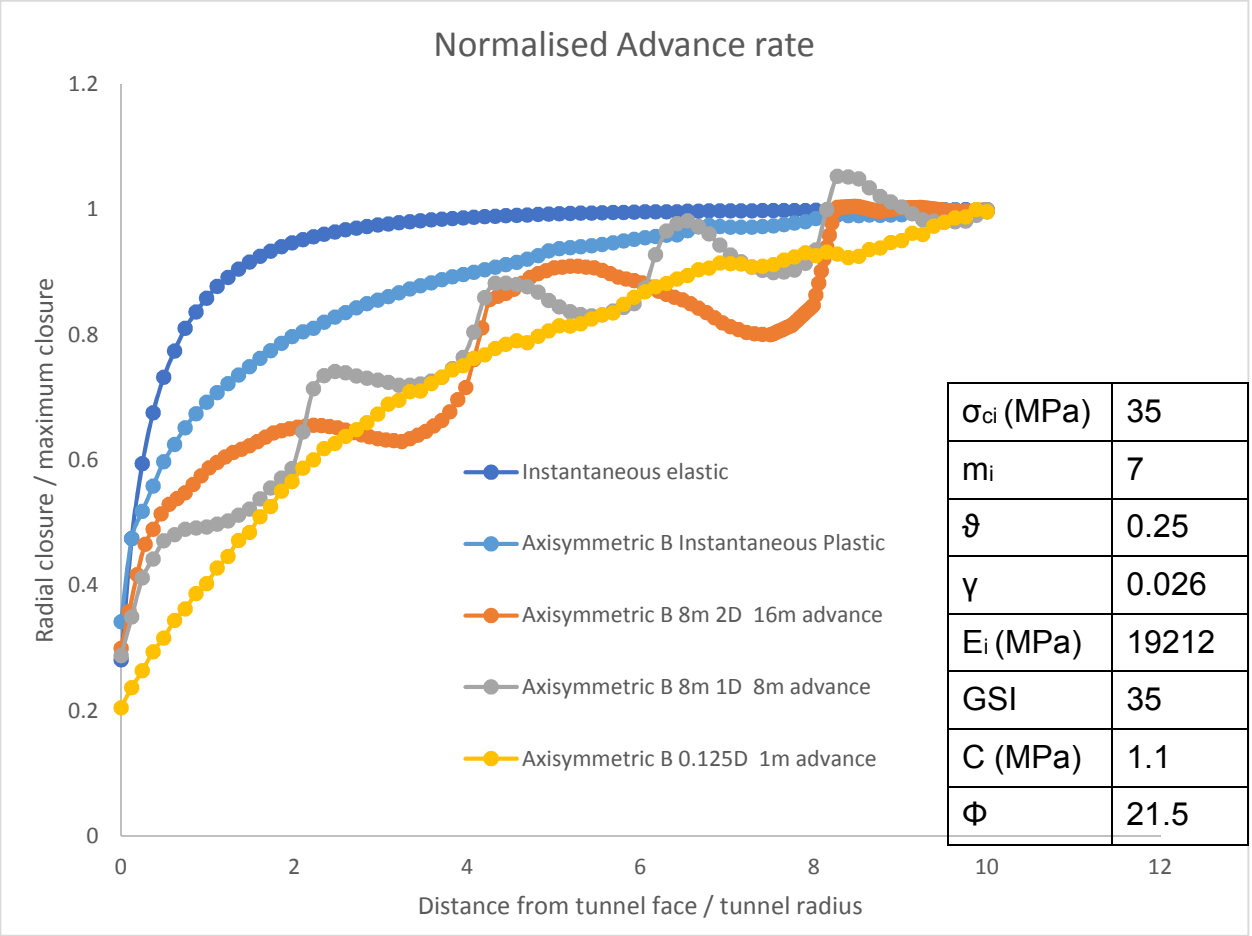

σ_{ci} (MPa)	35
m_i	7
ϑ	0.25
γ	0.026
E_i (MPa)	19212
GSI	35
C (MPa)	1.1
Φ	21.5

Figure 67: Modelled longitudinal displacement profile in Phase^2

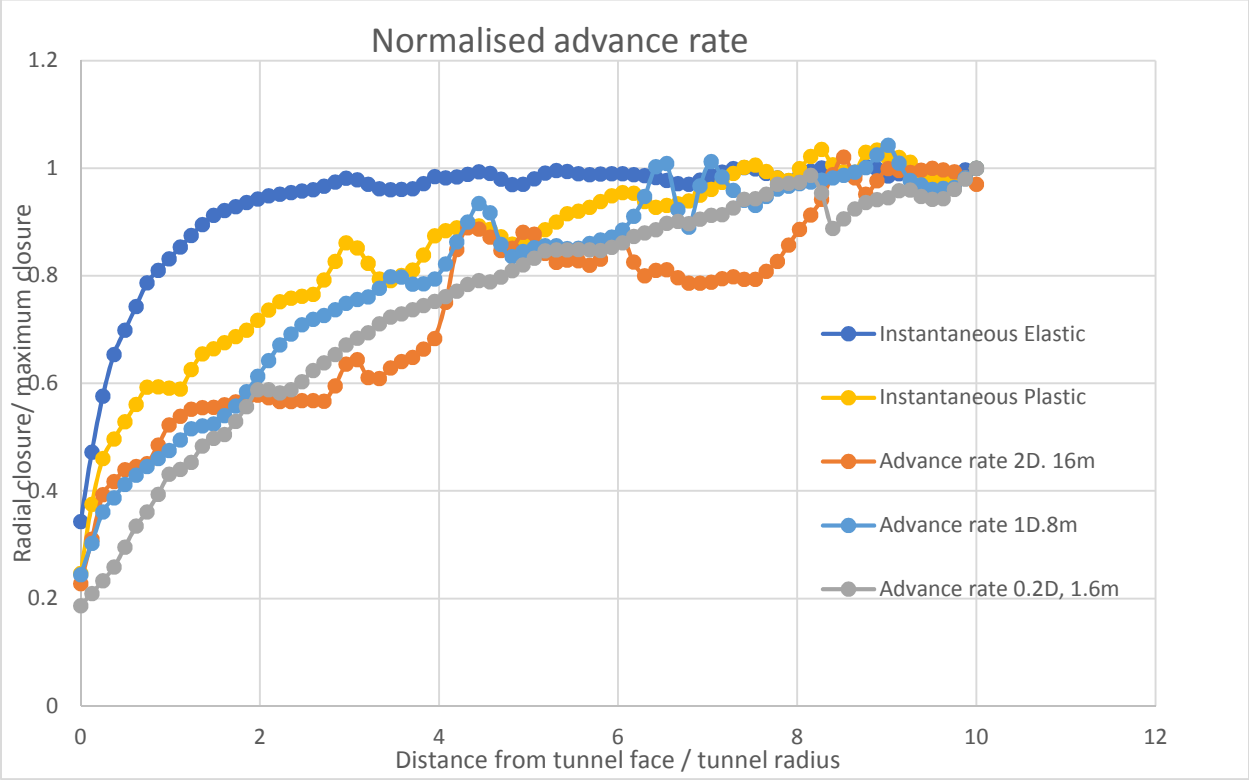

Figure 68: Modelled longitudinal displacement profile in RS³

Figure 68 and Figure 67 show a smooth displacement profile for elastic instantaneous analysis and for 0.2D advance rate as in agreement with (Vlachopoulos and Diederichs, 2009). Other advance rates are showing wavy nature of LDP. A larger expansion factor and finer mesh is needed is RS³ to obtain smoother graphs similar to Phase².

The capability of RS³ to produce full LDP is demonstrated using above example, being a full three dimensional FEM it will be able to produce full LDP's of any complex geometries which is not possible using axisymmetric 2D analysis.

Appendix C

Building of Room and pillar mine model geometry in RS^3

In this section, the sequence followed to generate a model room and pillar mine in RS^3 is explained. RS^3 allows to create the model geometry in three different ways - horizontal, vertical and inclined. Vertical is best suited for modelling vertical geometries like shafts and inclined is create geometries that are at an angle to horizontal. The most suitable way of modelling a horizontal tabular geometry is by using the horizontal option. Modelling a mine with diagonal depillaring is not a straightforward task in RS^3.

In the 2D model view where the software allows to model front/back view of the model is only visible, hence how the mine advances in each stage has to be pre-calculated and should be given as input to the sequence designer in RS^3. Hence an AutoCAD drawing was prepared and mesurments for sequencing for diagonal depillaring are taken from it. The first stage for the model is in-situ stress state. The second stage is to mine all the roadways which are at 40m intervals leaving pillars of 40m x 40m.For this all the cross roadways are seperated by 4m slices and on stage 2 all the cross roadways are excavated manually. Diagonal depillaring started from third stage onwards and the details of measuremnts are tabulated in Table 9.The heading number of the row shows the corresponding opening region in Figure 69.

The measurements from Table 9 was entered in the sequence designer adopting custom sequence. An example input for the region 1 as implemented in sequence designer in RS^3 is shown in Figure 70. Due to complete recovery of pillar, the overlying strata is supposed to cave in, hence the input boudary restraints play a critical role. Modelling with a low expansion factor showed a significant reduction in principal stresses since the external boundary restraints affect the stresses. To avoid this external restraint effect the outer boudaries are kept at a distance of atleast 300m away from the mine.Modelling showed the restraints with a very large expansion factor has given a substantial increase in magnitude of the maximum stress than with very low expansion factors.

Table 9: Input measurements for diagonal depillaring of room and pillar mine

	1	2	3	4	5	6	7	8	9	10	11	12
Stage 3	0-68	0-88	0-28									
Stage 4	68-108	88-136	28-68	0-24	0-44							
Stage 5	108-132	-	68-100	24-60	44-88	0-16						
Stage 6	132-148	136-180	100-112	60-76	-	16-44						
Stage 7	148-164		112-128	76-88	-	44-56	0-12	0-44				
Stage 8	164-180		128-148	88-116	88-136	56-72	12-28	-				
Stage 9			148-172	116-136	136-180	72-96	28-64	44-136	0-28			
Stage 10			172-180	136-156		96-108	64-76		28-40			
Stage 11				156-160		108-120	76-84		40-56			
Stage 12				160-168		120-140	84-88 104-116		56-64	0-12	0-44	
Stage 13				168-180		140-164	116-124		64-80 92-96	12-40	-	0-8
Stage 14						164-180	124-144		80-88 96-108	40-64	44-88	8-16

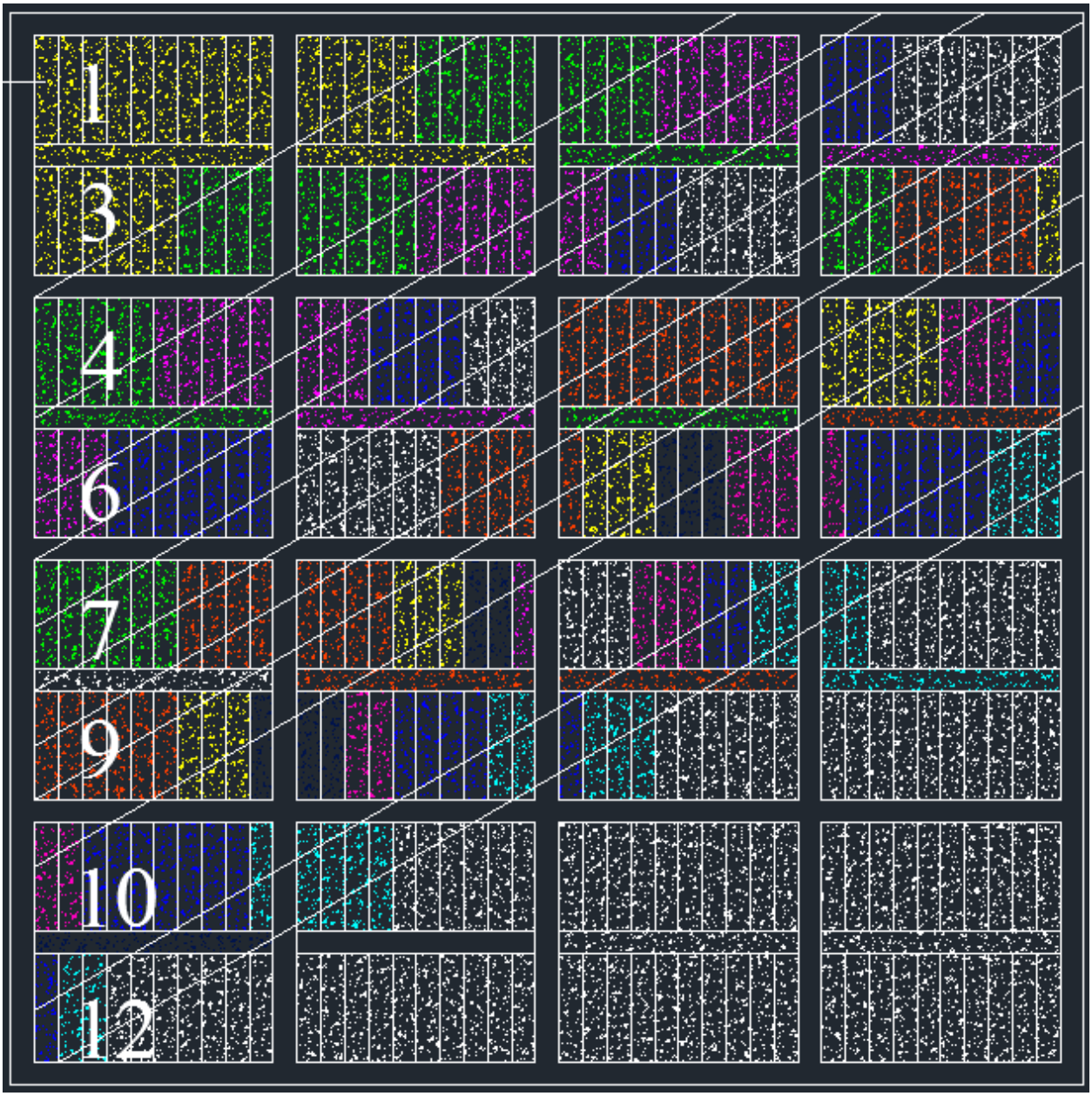

Figure 69: AutoCAD drawing prepared for input measurements in RS^3, color coding is given for easy identification of different stages

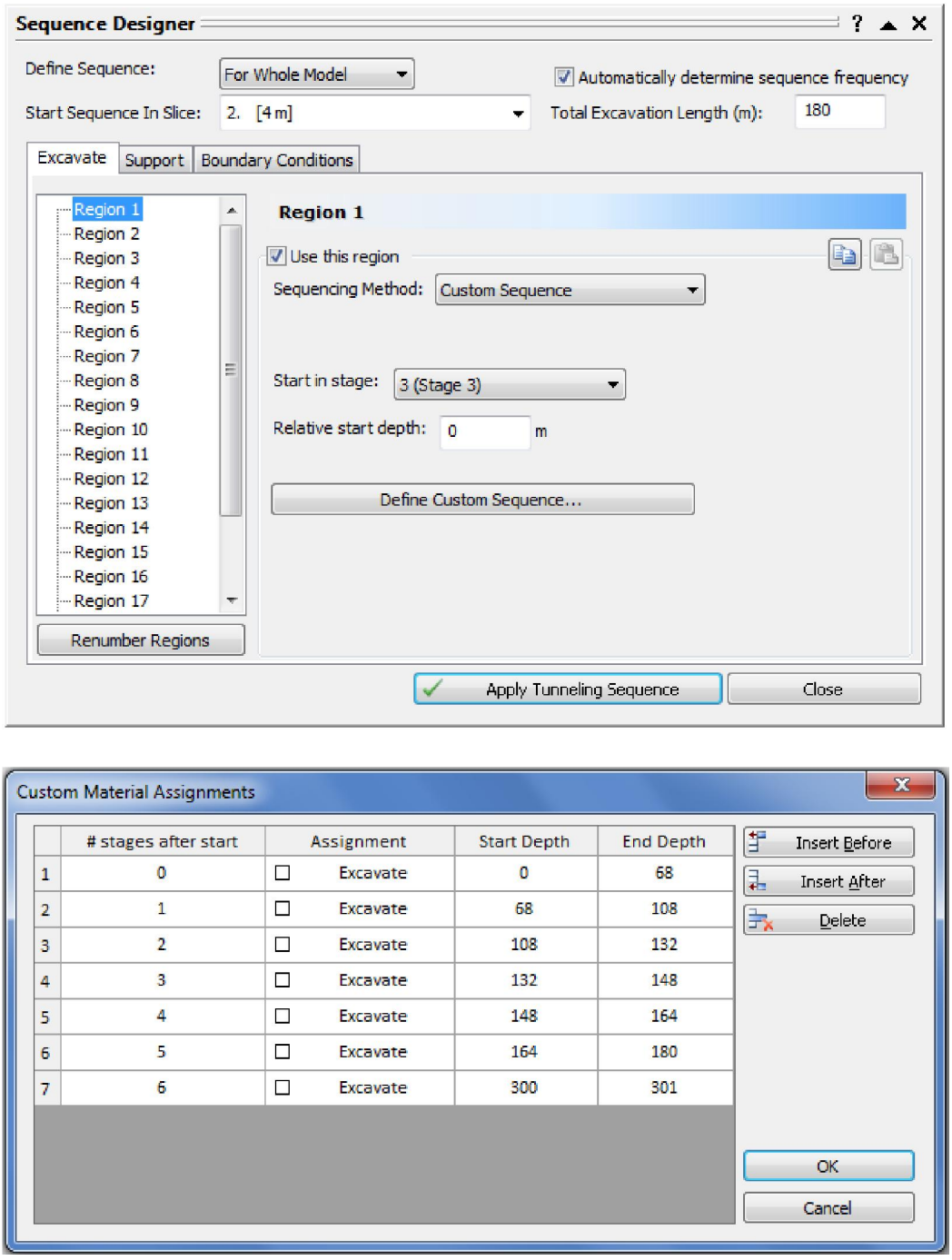

Figure 70: Custom sequence designer in RS³ showing the implementation of stage wise diagonal depillaring.

The remaining procedures like assigning material properties, field stress conditions, assigning restraints are similar to that of any model. Care has taken in the meshing to avoid bad elements having high aspect ratios. This was again a trial and error procedure which was repeated till a model having zero bad elements was produced.

Contents on the accompanying DVD

The total analysis for this dissertation generated more than 80Gigabytes of data. It is obviously impossible to contain all the documents in the DVD. Hence most important model results are included. A brief explanation of the contents in the folders available in the DVD is explained in the following table.

Folder Name	Content
Simple Single Stage	Initial model for 1m thick mudstone is included. Results from the models is presented in chapter 6.
Single Vs Multistage excavation	Models for a single stage excavation and multistage excavation which forms the basis of chapter 7 is included. Since multistage excavation generated 2.61GB file, only the results from stage 105 is included. Full analysis can be recreated using the given .rs3compute file associated with it.
Cohesion Weakening Multistage CMR	Multistage model results for stress perpendicular case for 1m, 2m and 3m mudstone. Since the size of each file is 2.61GB, only the results for the final stage of stress perpendicular case out of 105 stages is included. Results are presented in Chapter 8. Cases for other stress orientation can be recreated by changing the field stress angles.
Junction model	Full modelling results for chapter 9 is included
Room and Pillar mine	Elastic model used for the validation of the field data is included. Plastic analysis using cohesion weakening model is also included.
Axisymmetric	Results used in Appendix B is presented.
Final Report	Final report in .docx and .pdf file format is included.